



uOttawa

# **MBBR Produced Solids: Particle Characteristics, Settling Behaviour and Investigation of Influencing Factors**

**Raheleh Arabgol**

*Thesis submitted in partial fulfillment of the requirements for the degree of  
Doctor of Philosophy in Environmental Engineering*

Ottawa-Carleton Institute for Civil Engineering  
Department of Civil Engineering  
Faculty of Engineering

© Raheleh Arabgol, Ottawa, Canada, 2021

# Preface

This dissertation is an original work performed by Raheleh Arabgol. This research was conducted under the supervision of Dr. Robert Delatolla and Dr. Peter Vanrolleghem. Three manuscripts were prepared for publication in peer-reviewed journals. Versions of these manuscripts are located in chapters 3 to 5 of the dissertation. References for each manuscript and author contributions are presented below:

- Chapter 3 includes a version of Publication 1:

Arabgol, R., Vanrolleghem, P. A., Piculell, M., and Delatolla, R. (2020). *The impact of biofilm thickness-restraint and carrier type on attached growth system performance, solids characteristics and settleability*. Environmental Science: Water Research & Technology, 6(10), 2843–2855. (Published)

Raheleh Arabgol performed the experiment, data collection, data analyses, interpreted the result, wrote and revised the manuscript.

Maria Piculell contributed to the interpretation of the results and revision of the manuscript.

Peter Vanrolleghem (supervisor) contributed to the experimental design, directed the research, contributed to the interpretation of the results and revision of the manuscript.

Robert Delatolla (supervisor) developed the research question, designed and planned the study, directed the research, contributed to interpreting the results, and revised the manuscript.

- Chapter 4 includes a version of Publication 2:

A version of the following manuscript has been submitted to the journal of Biosystems Engineering in 2021.

Arabgol, R., Vanrolleghem, P. A., and Delatolla, R., *MBBR effluent particles: Influence of carrier geometrical properties and levels of biofilm thickness restraint on biofilm properties, effluent particle size distribution, settling velocity distribution and settling behaviour.*

Raheleh Arabgol performed the experiment, collected and analyzed the data, interpreted the results, and wrote the manuscript.

Peter Vanrolleghem (supervisor) contributed to the experimental design, directed the research, contributed to the interpretation of the results and revision of the manuscript.

Robert Delatolla (supervisor) developed the research question, designed and planned the study, directed the research, contributed to interpreting the results, and revised the manuscript.

- Chapter 5 includes a version of Publication 3:

A version of the following manuscript is in preparation for submission to the journal of Environmental Sciences.

Arabgol, R., Vanrolleghem, P. A., and Delatolla, R., *Particle characteristics and settling behaviour of MBBR produced solids along with removal performance and biofilm responses to various carbonaceous loading rates.*

Raheleh Arabgol started-up and performed the experiment, collected and analyzed the data, interpreted the results, and wrote the manuscript.

Peter Vanrolleghem (supervisor) contributed to the experimental design, directed the research, contributed to the interpretation of the results and revision of the manuscript.

Robert Delatolla (supervisor) developed the research question, designed and planned the study, directed the research, contributed to interpreting the results, and revised the manuscript.

I am aware of the University of Ottawa Academic Regulations; I certify that I have obtained written permission from each co-author to include the above materials in my thesis. The above material describes work completed during my full-time registration as a graduate student at the University of Ottawa.

## **Abstract**

The separation of solids from biological wastewater treatment is an important step in the treatment process, as it has a significant impact on effluent water quality. The moving bed biofilm reactor (MBBR) technology is a proven upgrade or replacement wastewater treatment system for carbon and nitrogen removal. However, a challenge of this technology is the characteristics of the effluent solids that results in their poor settlement; with settling being the common method of solids removal. The main objective of this research is to understand and expand the current knowledge on the settling characteristics of MBBR produced solids and the parameters that influence them. In particular, in this dissertation, the impacts are studied of carrier types, biofilm thickness restraint design of carriers, and varying carbonaceous loading rates on MBBR performance, biofilm morphology, biofilm thickness, biofilm mass, biofilm density, biofilm detachment rate, solids production, particle size distribution (PSD) and particle settling velocity distribution (PSVD).

With this aim, three MBBR reactors housing three different carrier types were operated with varying loading rates. In order to investigate the effect of carrier geometrical properties on the MBBR system, the conventional, cylindrically-shaped, flat AnoxK™ K5 carrier with protected voids was compared to two newly-designed, saddle-shaped Z-carriers with the fully exposed surface area. Moreover, the AnoxK™ Z-200 carrier was compared to the AnoxK™ Z-400 carrier to evaluate the biofilm thickness restraint design of these carriers, where the Z-200 carrier is designed for greater biofilm thickness-restraint. The Z-200 carrier is designed to limit the biofilm thickness to the level of 200  $\mu\text{m}$  as opposed to 400  $\mu\text{m}$  for the Z-400 carrier. Finally, to investigate the effects of varying carbonaceous loading rates on system removal performance, biofilm characteristics and solids characteristics, further analyses were performed at three different loading

rates of 1.5 to 2.5 and 6.0 g-sBOD/m<sup>2</sup>·d in steady-state conditions. The PSD and the PSVD analyses were combined to relate these two properties. A settling velocity distribution analytical method, the ViCAs, was applied in combination with microscopy imaging and micro-flow imaging to investigate the relation of PSD and settling behaviour of MBBR produced particles.

The obtained results have indicated that the carrier type significantly impacted the MBBR performance, biofilm, and particle characteristics. As such, the K5 carrier MBBR system demonstrated a statistically significantly higher carbonaceous removal rate and efficiency ( $3.8 \pm 0.3$  g-sBOD/m<sup>2</sup>·d and  $59.9 \pm 3.0\%$  sBOD removal), higher biofilm thickness ( $281.1 \pm 8.7$  μm), higher biofilm mass per carrier ( $43.9 \pm 1.0$  mg), lower biofilm density ( $65.0 \pm 1.5$  kg/m<sup>3</sup>), lower biofilm detachment rate ( $1.7 \pm 0.7$  g-TSS/ m<sup>2</sup>·d) and hence lower solids production ( $0.7 \pm 0.3$  g-TSS/d) compared to the two Z-carriers. The Z-carriers' different shape exposes the biofilm to additional shear stress, which could explain why the Z-carriers have thinner and denser biofilm, resulting in higher solids production and lower system performance in comparison with K5. Moreover, the carrier type was also observed to impact the particle characteristics significantly. PSD analysis demonstrated a higher percentage of small particles in the Z-carrier system effluent and hence a significantly lower solids settling efficiency. Therefore, the solids produced in the K5 reactor have shown enhanced settling behaviour, consisting of larger particles with faster settling velocities compared to Z-carriers.

This dissertation also investigated the effects of restraint biofilm thickness on MBBR performance by comparing the Z-200 biofilm thickness-restraint carrier to the Z-400 carrier. No significant difference was observed in removal efficiency, biofilm morphology, biofilm density, biofilm detachment rate, and solids production between the Z-200 to the Z-400 carriers. The PSD and the PSVD analyses did not illustrate any significant difference in the particles' settling

behaviour for these two biofilm thickness restraint carriers, indicating that the biofilm thickness-restraint carrier design was not a controlling factor in the settling potential of MBBR produced solids.

Finally, this research studied the effect of varying loading rates and demonstrated a positive, strong linear correlation between the measured sBOD loading rate and the removal rate, indicating first-order BOD removal kinetics. The biofilm thickness, biofilm density and biofilm mass decreased when the surface area loading rate (SALR) was increased from 2.5 to 6.0 g-sBOD/m<sup>2</sup>·d. The solids retention time (SRT) was also shown to decrease by increasing the SALR, where the lowest SRT ( $1.7 \pm 0.1$  days) was observed at the highest SALR, with the highest cell viability ( $81.8 \pm 1.7\%$ ). Significantly higher biofilm detachment rate and yield were observed at SALR 2.5, with the thickest biofilm and a higher percentage of dead cells. Consequently, a higher fraction of larger and rapidly settling particles was observed at SALR of 2.5 g-sBOD/m<sup>2</sup>·d, which leads to a significantly better settling behaviour of the MBBR effluent solids.

This study expands the current knowledge of MBBR-produced particle characteristics and settling behaviour. A comprehensive understanding of the MBBR system performance and the potential influencing factors on the MBBR produced solids, particle characteristics, and their settleability will lead to optimized MBBR design for future pilot- and full-scale applications of the MBBR.

## **Acknowledgements**

First and foremost, I would like to express my sincere gratitude to my supervisors, Dr. Robert Delatolla and Dr. Peter A. Vanrolleghem, for their outstanding knowledge, guidance, patience and inspiration throughout the research. Their encouragement and emotional support had brought me through difficult times of this journey, especially when experiments were not turning out right. I would also like to thank Dr. Maria Piculell for her collaboration on my research and her valuable feedback and suggestions.

I acknowledge and thank Dr. Yves Dionne for giving me the opportunity to conduct my experiment at the Gatineau wastewater treatment plant and also the personnel of the treatment plant for their cooperation and supports.

I would also like to extend my sincere gratitude to all my past and present colleges, the technical staff at the Department of Civil Engineering at the University of Ottawa and the University of Laval, for their support, contributions, and creating such a friendly working environment.

Last but not least, a heartfelt thanks to my family, my mother and my sisters, for their unconditional love and support that helped me overcome many challenging moments, although they were far away. Finally, special thanks go to all my nearest and dearest friends who became like my family and accompanied me through hard times and kept me inspired.

# Table of Content

<b>Preface.....</b>	<b>ii</b>
<b>Abstract.....</b>	<b>v</b>
<b>Acknowledgements .....</b>	<b>viii</b>
<b>Table of Content.....</b>	<b>ix</b>
<b>List of Figures.....</b>	<b>xiii</b>
<b>List of Tables .....</b>	<b>xvi</b>
<b>List of Acronyms .....</b>	<b>xvii</b>
<b>Chapter 1 – Introduction .....</b>	<b>1</b>
1.1 Background .....	1
1.2 Research objectives .....	5
1.3 Thesis organization .....	6
1.4 References .....	8
<b>Chapter 2 – Literature review .....</b>	<b>14</b>
2.1 Biological wastewater treatment .....	14
2.1.1 Suspended growth systems – Activated sludge .....	15
2.1.2 Attached growth systems – Biofilm reactors .....	17
2.2 Biofilm development and detachment.....	18
2.3 MBBR technology.....	21
2.3.1 Effect of carrier type on MBBR system performance .....	23
2.3.2 Effect of SALR on MBBR system performance .....	26
2.3.3 Effect of biofilm characteristics on MBBR system performance .....	29
2.4 MBBR solids characteristics .....	30
2.4.1 Effect of carrier type on MBBR solids characteristics .....	31
2.4.2 Effect of SALR on MBBR solids characteristics .....	33
2.4.3 Effect of biofilm characteristics on MBBR solids characteristics .....	34
2.5 Solids characteristics and settling behaviour .....	35
2.5.1 Particle settling velocity.....	37
2.6 References .....	42
<b>Chapter 3 – The Impact of Biofilm Thickness-Restraint and Carrier Type on Attached Growth System Performance, Solids Characteristics and Settleability.....</b>	<b>51</b>

3.1	Context .....	51
3.2	Abstract .....	51
3.3	Introduction .....	52
3.4	Materials and methods .....	57
3.4.1	Experimental setup.....	57
3.4.2	Carrier characteristics .....	58
3.4.3	Wastewater characteristics.....	59
3.4.4	Biofilm inoculation and start-up .....	60
3.4.5	Reactor operation .....	61
3.4.6	Constituent analytical methods .....	62
3.4.7	Solids analysis.....	62
3.4.8	Biofilm thickness analysis .....	63
3.4.9	Particle size distribution analysis of solids .....	64
3.4.10	Statistical analyses .....	65
3.5	Results and discussion.....	65
3.5.1	Reactor carbonaceous and ammonia removal performance .....	65
3.5.2	Biofilm thickness .....	69
3.5.3	Solids concentration, production, detachment .....	72
3.5.4	Solids characteristics and settleability .....	74
3.6	Conclusion.....	78
3.7	References .....	79
<b>Chapter 4 – MBBR effluent particles: Influence of carrier geometrical properties and levels of biofilm thickness restraint on biofilm properties, effluent particle size distribution, settling velocity distribution and settling behaviour .....</b>		<b>85</b>
4.1	Context .....	85
4.2	Abstract .....	85
4.3	Introduction .....	86
4.4	Materials and methods .....	89
4.4.1	Experimental setup and operation.....	89
4.4.2	Constituent analysis .....	90
4.4.3	Biofilm characteristics analysis .....	90

4.4.4	Biofilm Morphology .....	91
4.4.5	Particle settling velocity distribution (PSVD) .....	91
4.4.6	Particle size distribution (PSD).....	92
4.4.7	Statistical analysis.....	93
4.5	Results and discussion.....	94
4.5.1	System performance.....	94
4.5.2	Biofilm characteristics (Thickness/mass/ density).....	96
4.5.3	Biofilm morphology.....	99
4.5.4	Solids analysis.....	100
4.5.5	Particle settling velocity distribution (PSVD) .....	102
4.5.6	Particle size distribution (PSD).....	104
4.6	Conclusion.....	107
4.7	References .....	108
<b>Chapter 5 – Particle Characteristics and Settling Behaviour of MBBR Produced Solids along with Removal Performance and Biofilm Responses to Various Carbonaceous Loading Rates.....</b>		<b>114</b>
5.1	Context .....	114
5.2	Abstract .....	114
5.3	Introduction .....	115
5.4	Materials and methods .....	118
5.4.1	Experimental setup and reactor operation.....	118
5.4.2	Constituent analysis .....	119
5.4.3	Biofilm characteristics .....	120
5.4.4	Cell viability and microbial activity .....	121
5.4.5	Solids analysis.....	122
5.4.6	Particle settling velocity distribution (PSVD) .....	122
5.4.7	Particle size distribution (PSD).....	124
5.4.8	Statistical analyses .....	125
5.5	Results and discussion.....	125
5.5.1	Reactor kinetics.....	125
5.5.2	Biofilm characteristics (thickness, mass, density) .....	129

5.5.3	Biofilm morphology.....	132
5.5.4	Biomass characteristics - Cell Viability.....	133
5.5.5	Solids analysis.....	135
5.5.6	Solids characteristics and settleability .....	137
5.6	Conclusion.....	141
5.7	References .....	141
<b>Chapter 6 – Discussion and Conclusion.....</b>		<b>148</b>
6.1	The impacts of Carrier types .....	148
6.2	The impacts of biofilm thickness-restraint.....	151
6.3	The impacts of varying SALR .....	153
6.4	Novel contribution, practical implication, and future direction .....	155
<b>Appendix A- Statistical analysis .....</b>		<b>157</b>
<b>Appendix B – Biofilm thickness measurement.....</b>		<b>163</b>

## List of Figures

<b>Figure 2-1:</b> Substrate concentration gradients through the depth of biofilm, i.e. yellow line illustrates the oxygen concentration gradient through the biofilm, creating aerobic and anaerobic zones (Piculell, 2016).....	19
<b>Figure 2-2:</b> Three steps of biofilm formation .....	20
<b>Figure 2-3:</b> Effective surface area ( $m^2/m^3$ ) or grid height to control the biofilm thickness of AnoxKaldnes® (Bassin and Dezotti, 2018).....	25
<b>Figure 2-4:</b> Effect of SALR and surface overflow rates ( $v_i$ ) on solids removal efficiency (Ivanovic and Leiknes, 2012).....	34
<b>Figure 2-5:</b> Settling regimes (Ekama et al., 1997).....	36
<b>Figure 2-6:</b> The forces acting on a particle .....	38
<b>Figure 2-7:</b> Variation of $C_d$ with particle geometry (Droste and Gehr, 2018).....	39
<b>Figure 3-1:</b> Experimental setup.....	57
<b>Figure 3-2:</b> (a) top view occupied area of biofilm in one void of the K5 carriers, and (b) cross-sectional images of biofilm thickness in a compartment of Z-carries .....	64
<b>Figure 3-3:</b> SARR versus SALR across a range of loading rates for various carriers with respect to (a) sBOD (b) sCOD, and (c) TAN removal.....	67
<b>Figure 3-4:</b> SARR and percent removal at SALR of $6 \pm 0.8$ g-sBOD/ $m^2 \cdot d$ for (a) sBOD (b) sCOD and (c) TAN removal .....	68
<b>Figure 3-5:</b> Biofilm thickness of various carriers, average and 95% confidence interval.....	70
<b>Figure 3-6:</b> Stereomicroscopy images of carriers showing biofilm thickness measurements, (a) top view of K5 carrier, (b) top view of Z-200 carrier and side view of cut Z-200 carrier, and (c) top view of Z-400 carrier and side view of cut Z-400 carrier.....	72
<b>Figure 3-7:</b> Impact of various carrier types on unsettled effluent particle distribution at SALR of $6.0 \pm 0.8$ g-sBOD/ $m^2 \cdot d$ , (a) particle size distribution of particles between 2–400 $\mu m$ , and (b) total volume percentages of particles smaller and larger than 400 $\mu m$ .....	75
<b>Figure 3-8:</b> Impact of various carrier types on effluent particle distribution at SALR of $6.0 \pm 0.8$ g-sBOD/ $m^2 \cdot d$ after 4 hours of settling, (a) particle size distribution of particles between 2–400 $\mu m$ , and (b) total volume percentages of particles smaller and larger than 400 $\mu m$ .....	75
<b>Figure 4-1:</b> Biofilm thickness, density and biomass for different reactors.....	97
<b>Figure 4-2:</b> VPSEM images of biofilm at 60 $\times$ magnification with a small insert image, at the upper right of each image, at higher magnification of 600 $\times$ for (a) K5, (b) Z-200, and (c) Z-400 carriers .....	100
<b>Figure 4-3:</b> TSS concentration, solids production and detachment rate for different reactors..	101

<b>Figure 4-4:</b> (a) Particle settling velocity distribution curves for influent and effluent of MBBRs with different types of carriers and (b) the percentage of particles with a velocity faster than 0.5 m/hr .....	103
<b>Figure 4-5:</b> Accumulative particle size distribution for particles collected (a) in the first 2 minutes, (b) between the 15–30 minutes, and (c) between 2–4hours (=240 minutes) of settling for different reactors effluents. ....	105
<b>Figure 4-6:</b> D <sub>50</sub> measured over different time intervals for different carrier types.....	105
<b>Figure 4-7:</b> Particle size distribution curves for different carriers before (in black colour) and after (in blue colour) 4 hours of settling.....	106
<b>Figure 4-8:</b> Microscopy images of settled and unsettled particles over the time for K5, Z-200 and Z-400 effluent .....	107
<b>Figure 5-1:</b> The ViCAs experimental setup.....	124
<b>Figure 5-2:</b> SARRs across three different experimental SALRs with respect to (a) sBOD (b) sCOD and (c) TAN removal, with 95% confidence band of the best-fit regression line .....	126
<b>Figure 5-3:</b> Biofilm thickness, density and biomass in the reactors for different experimental phases.....	131
<b>Figure 5-4:</b> VPSEM images acquired for assessment of biofilm morphology at (a) SALR of 1.5 g-sBOD/m <sup>2</sup> ·d, (b) SALR of 2.5 g-sBOD/m <sup>2</sup> ·d and c) SALR of 6.0 g-sBOD/m <sup>2</sup> ·d (the small middle left images are stereoscope images that illustrate a quarter of carrier at each condition) .....	133
<b>Figure 5-5:</b> Biofilm volume and viable cell removal rates across the three different loading rates with 95% confidence band of the best fit regression line (showing a linear correlation between SALR and RR).....	135
<b>Figure 5-6:</b> (a) TSS and solids production, (b) yield and detachment rate and (c) VSS:TSS ratio of the effluent solids and percent coverage of viable cells in the biofilm at three different SALRs .....	136
<b>Figure 5-7:</b> Particle settling velocity distribution curves for influent and effluent at three different experimental SALRs.....	138
<b>Figure 5-8:</b> Percent mass of particles with a velocity greater than 0.5 m/hr .....	139
<b>Figure 5-9:</b> Accumulative particle size distribution at different settling intervals related to ViCAs column (a) settled particle between time 0 to 2 minutes, (b) settled particle between time 15 to 30 minutes, and (c) settled particle between time 120 to 240 minutes. ....	140
<b>Figure A-1:</b> Residual Plot for sBOD SARR for different carrier types across SALR.....	157
<b>Figure A-2:</b> Residual Plot for TAN SARR for different carrier types across SALR. ....	158
<b>Figure A-3:</b> Residual Plot for sBOD BVRR and VCRR across SALR.....	159

**Figure B-1:** Thickness measurements for different type of carriers (a) each replication and (b) the average of all three taken carriers with 95% CI..... 163

**Figure B-2:** Thickness measurements for K5 carrier at different SALRs for (a) each replication and (b) the average of all three taken carriers with 95% CI ..... 163

## List of Tables

<b>Table 2-1:</b> Effect of various SALR ranges on removal efficiency, used in previous researches.	28
<b>Table 2-2:</b> The comparison of various methods used to measure the settling velocity distribution (Aiguier et al., 1996; Tyack and Hedges, 1996; Lucas-Aiguier et al., 1998; Hasler, 2007; Berrouard, 2010).....	41
<b>Table 3-1:</b> Reactor properties at SALR of $6 \pm 0.8$ g-sBOD/m <sup>2</sup> ·d.....	58
<b>Table 3-2:</b> Characteristics of raw wastewater entering the Gatineau WRRF and the clarified feed wastewater entering the on-site MBBR reactors .....	59
<b>Table 3-3:</b> Effluent solids concentration, production and detachment rates in MBBR reactors (n=10).....	73
<b>Table 4-1:</b> Influent and effluent wastewater characteristics (n ≈ 10) along with operational conditions for the three reactors.....	95
<b>Table 5-1:</b> Reactor properties for different experimental loading rates.....	119
<b>Table 5-2:</b> Experimental conditions, Influent and effluent wastewater characteristics at the three tested experimental loading rates.....	127
<b>Table 5-3:</b> Average and 95% confidence interval values of the percentage of cell viability in the biofilm, biofilm volume (BVRR) and the viable cell sBOD removal rate (VCRR).....	134
<b>Table A-1:</b> ANOVA for liner regression between sBOD removal rate and loading rate .....	157
<b>Table A-2:</b> ANOVA for liner regression between TAN removal rate and loading rate .....	158
<b>Table A-3:</b> ANOVA results, Liner regression analysis of biofilm volume (BVRR) and the viable cell sBOD removal rate (VCRR) across the loading rate .....	159
<b>Table A-4:</b> Statistical significance ( <i>p</i> -values) of measured parameters to designate the difference of system performance, biofilm characteristics and solids characteristics for different carriers	160
<b>Table A-5:</b> Statistical significance ( <i>p</i> -values) of measured parameters to designate the difference of system performance, biofilm characteristics and solids characteristics at different SALR ...	161
<b>Table A-6:</b> Statistical significance analysis ( <i>p</i> -values) for ViCAs tests .....	162

## List of Acronyms

BOD	Biochemical oxygen demand
CAS	Conventional activated sludge
cBOD	Carbonaceous biological oxygen demand
CLSM	Confocal laser scanning microscopy
COD	Chemical oxygen demand
DO	Dissolved oxygen
DPA	Dynamic particle analyzer
EBA	Exposed biofilm area
ECD	Equivalent circular diameter
EPS	Extracellular polymeric substances
HDPE	High-density polyethylene
HRT	Hydraulic retention time
IFTS	Institut de filtration et des techniques separatives
MBBR	Moving bed biofilm reactors
MTBL	Mass transfer boundary layer
PE	Polyethylene
PP	Polypropylene
PSA	Protected surface area
PSD	Particle size distribution
PSVD	Particle settling velocity distribution
RAS	Return activated sludge
RBC	Rotating biological contactor
SALR	Surface area loading rate
SARR	Surface area removal rate
sBOD	Soluble biochemical oxygen demand
sCOD	Soluble chemical oxygen demand
SRT	Solids retention time
TAN	Total ammonia nitrogen
TRC	Total residual chlorine
TSS	Total suspended solids
UFT	Umwelt and fluid technique
ViCAs	Vitesse de chute en assainissement (French acronym)
VICTOR	Vitesse de chute des polluants des rejets urbains
VPSEM	Variable pressure scanning electron microscope
VSS	Volatile suspended solids
WRRF	Water resource recovery facility
WSER	Wastewater systems effluent regulations
WWTP	Wastewater treatment plants

# Chapter 1 – Introduction

## 1.1 Background

Increasing awareness of the detrimental impacts of improper discharge into aquatic environments has resulted in the implementation of new regulations and increasingly stringent wastewater discharge standards in Canada and around the world (Di Trapani et al., 2010; Gazette, 2012; Dias et al., 2018). Therefore, water resource recovery facilities (WRRFs) are required to reduce the concentration of deleterious substances – such as carbonaceous biochemical oxygen demand (cBOD), total suspended solids (TSS), total residual chlorine and unionized ammonia as nitrogen ( $\text{NH}_3\text{-N}$ ) (Gazette, 2012) – prior to discharge into surface water bodies. Biological wastewater treatment processes are the most common means to remove carbonaceous material and nitrogen from the wastewater. In biological processes, microorganisms degrade and transform the soluble or particulate harmful substances into new products, including biologically produced particles (Metcalf & Eddy, 2014). Therefore, separation of the biologically produced solids from the treated wastewater is crucial to achieving a complete biological treatment, which requires an understanding of these particle characteristics (WEF, 2009; Wang, 2012; Metcalf & Eddy, 2014).

The moving bed biofilm reactor (MBBR) technology is an attached growth biological treatment system, which has received considerable attention as a standalone and add-on technology for upgrading or replacing passive and conventional wastewater treatment systems in the last two decades (Ødegaard et al., 1994; Delatolla and Babarutsi, 2005; Delatolla et al., 2010; Young et al., 2016; Ødegaard, 2016; Bassin and Dezotti, 2018; Ahmed et al., 2019). The basic principle of the MBBR systems is the use of freely moving plastic carriers in the reactor as a substratum for bacterial growth and biofilm formation without being washed out (Ødegaard et al., 1994, 2000b; Bassin and Dezotti, 2018). Therefore, a large quantity of biomass with higher solids retention time

(SRT) is maintained in a small footprint, which leads to lower production of biomass in the process. High load tolerance, no need for backwashing, high treatment efficiency, and low vulnerability to cold temperature are some other advantages of the MBBR technology (Ødegaard, 2004; Loupasaki and Diamadopoulos, 2013; Young et al., 2016; Ramli and Abdul Hamid, 2017; Bassin and Dezotti, 2018; Mannacharaju et al., 2018; Tian and Delatolla, 2019). Although minimizing the quantity of solids and the subsequent sludge production can be considered an advantage of MBBR systems (Dias et al., 2018; McQuarrie, 2010; Ødegaard, 2004), MBBR effluent solids concentrations have been shown to not allow sufficient bio-flocculation, which hinders their removal via settling (Ødegaard et al., 2010; Metcalf & Eddy, 2014). Therefore, several studies have highlighted the necessity of using intense solids separation techniques to remove MBBR effluent suspended solids such as filtration, lamella settling, and enhanced sedimentation with pre-coagulation (Ødegaard et al., 2010; Ivanovic and Leiknes, 2012; Bassin and Dezotti, 2018). Poor settling characteristics of the biologically produced MBBR solids is a potential drawback and remains a key challenge of this technology (Ødegaard et al., 2010; Karizmeh, 2012; Ivanovic and Leiknes, 2012; Bassin and Dezotti, 2018). This problem highlights the importance of studying the parameters that affect MBBR-produced particle characteristics and the particle settling behaviour to further optimize MBBR design.

MBBR produced solids refer to biofilm detached from the substratum due to erosion, abrasion, and sometimes sloughing (Wuertz et al., 2003; Metcalf & Eddy, 2014). The biofilm growth, and subsequently, the detachment of biofilm control the biofilm thickness, the quantity of biomass in the reactor, the suspended solids in the bulk liquid phase, and the biofilm growth itself depends on the operational conditions (Rittmann, 2007). As one of the important operational parameters, the substrate loading rate can influence reactor performance (Aygün et al., 2008; Javid

et al., 2013), the biofilm detachment rate, and hence, the solids production. Increasing the substrate loading rate increases the solids production with more undesirable particles in the effluent, which may negatively affect the settling performance (Ødegaard, 2000; Ivanovic et al., 2006; Aygun et al., 2008; Javid et al., 2013; Karizmeh et al., 2014). Despite the importance of particle characteristics in solid-liquid separation units, there is still a fundamental lack of understanding of MBBR effluent particle characteristics and their potential dependence with the biofilm characteristics and operational conditions.

It is known that carriers play an important role in the MBBR systems. Many carriers have been developed to increase the protected surface area (PSA) of the carriers to improve the MBBR removal performance (Piculell, 2016; Bassin and Dezotti, 2018; Morgan-Sagastume, 2018). Previous studies have investigated the performance of carbonaceous-removal and nitrifying MBBR reactors using a variety of carriers. These studies mainly focused on the effects of the surface area loading rate (SALR), hydraulic retention time (HRT), volumetric filling degree of the carriers, dissolved oxygen (DO) concentration and temperature on carbon and ammonia removal (Barwal and Chaudhary 2014; Young et al. 2016; Chaali et al. 2018). Studies have indicated that the MBBR removal performance is only influenced by the carrier's surface area, regardless of the size and shape of the carriers (Ødegaard et al., 1994, 2000a; Rusten et al., 1998; Di Trapani et al., 2008; Levstek and Plazl, 2009). On the other hand, it has been demonstrated that the carrier geometry (such as size and shape) can also affect mixing and aeration requirements and therefore leads to different hydraulic characteristics, level of turbulence, and shear forces in the reactor (Kruszelnicka et al., 2018). Exposure to varying degrees of shear force in the reactor may affect the thickness of the biofilm, the morphology and the quantity of attached biomass, along with the detachment rate. The relationship between carrier design and biofilm characteristics, such as

biofilm thickness and density, along with solids characteristics, is yet to be understood in its full complexity. Therefore, there is currently a gap of knowledge as to how the design of various carriers affects the overall system performance of the MBBR technology, in addition to the biofilm characteristics, effluent solids characteristics and settling behaviour of the particles in the effluent of these systems.

MBBR carrier development has generally focused on enlarging the PSA (Bassin and Dezotti, 2018; Morgan-Sagastume, 2018). Indeed, higher PSA is expected to improve the MBBR performance based on the same volume of carriers per reactor (Ødegaard et al., 2000b; Barwal and Chaudhary, 2014; Piculell, 2016). However, it is not only the theoretical carrier's surface area but the active biofilm surface area that affects MBBR performance. Hence, researchers have defined exposed biofilm area (EBA), as the biofilm area exposed to the bulk liquid, for a more reliable and predictive MBBR design (Piculell, 2016). In most MBBR carriers, which are generally cylindrically-shaped with voids, the EBA considerably decreases by increasing the biofilm thickness, especially once the carriers are clogged with biofilm. The reduction of EBA might eventually impact the MBBR system performance (Forrest et al., 2016; Piculell et al., 2016). This negative impact of uncontrolled biofilm growth on the MBBR removal performance depends on the magnitude of the difference between the EBA and the designed PSA of the carriers (Martín-Pascual et al., 2012; Bassin et al., 2016). Moreover, different carrier types are more or less sensitive to clogging based on their geometric configuration, because the flow velocity inside the carrier voids is affected by the geometry of the carriers and hence may influence the biofilm thickness (Kruszelnicka et al., 2018). As such, conventional porous carriers with long and narrow voids are more prone to thicker biofilm and clogging due to the low turbulence inside the voids. In comparison, exposed carrier bodies facilitate biofilm detachment and are less prone to uncontrolled

biofilm growth (Forrest et al., 2016). Therefore, limiting the biofilm thickness has been identified by other studies to be a potential key factor to avoid carrier clogging and ensure more stable system performance (Piculell, 2016). In this regard, recently, a new type of carrier has been designed in order to restrain biofilm thickness. The newly designed AnoxK™ Z-series of carriers are configured to be able to control and maintain biofilm thickness up to a maximum predefined level and to keep the EBA unchanged. Thus far, only a few studies have been performed on the biofilm thickness-restraint Z-carriers, and these mostly focused on nitrifying MBBR systems and the effect of biofilm thickness restraining on nitrogen removal and calcium scaling effects. Therefore, there is a knowledge gap in the potential usage of biofilm thickness-restraint carriers in carbonaceous biological processes and their impacts on kinetics, as well as biofilm characteristics, particle characteristics and their settling behaviour. Moreover, understanding the impact of controlled biofilm thickness on the detachment mechanisms of biological mass from the carriers, and hence, the effluent suspended solids concentration and settleability, may lead to optimized design of the MBBR system and subsequent downstream solids separation units.

## **1.2 Research objectives**

The main objective of this research is to determine the influence of carrier type, restrained biofilm thickness, and varying SALR on the performance of the MBBR technology, on the biofilm properties, on the characteristics of the MBBR produced solids, and on the settling behaviour of the effluent solids. In particular, the specific objectives of this research are to:

1. Investigate the effect of carrier type (role of physical and geometrical properties) on MBBR technology performance, solids characteristics, biofilm properties and biomass characteristics (comparison of new, emerging thickness-restraint carriers with a conventional carrier).

2. Investigate the effect of limiting the biofilm thickness, using newly designed thickness-restraint Z-carriers, on MBBR technology performance, solids characteristics, biofilm properties and biomass characteristics.
3. Investigate the effect of varying carbonaceous SALR on MBBR technology performance, solids characteristics (including solids production, particle size distribution and particle settling velocity distribution), and biofilm and biomass characteristics.
4. Investigate the benefits of applying the ViCAs settling velocity distribution analytical method ("Vitesse de Chute en Assainissement", a French acronym for settling velocity in wastewater) combined with microscopy imaging to relate particle size distribution to settling behaviour of MBBR produced particles.

The related analyses of this study were conducted at the macro, meso, and micro scales (quantifying the removal kinetics, solids characteristics, biofilm properties, and biomass characteristics, along with their interdependence) to expand the current knowledge of MBBR-produced particle characteristics and settling behaviour. A comprehensive understanding of MBBR system performance and the potential influencing factors on MBBR produces solids, particle characteristics, and their settleability will lead to optimized MBBR design.

### **1.3 Thesis Organization**

The dissertation is written in the form of a manuscript-based thesis composed of six chapters: Chapter 1 describes the background information of this research, research objectives, and the list of publications developed in the scope of this research. Chapter 2 provides an overview of biological treatment technologies and a literature review relevant to this research's objectives and the work presented in the subsequent chapters.

Chapter 3 is a published research article entitled "*The impact of biofilm thickness-restraint and carrier type on attached growth system performance, solids characteristics and settleability*". This article has been published in the peer-reviewed journal of *Environmental Science: Water Research & Technology* in 2020. The overall system performance of the carbon removal MBBR system for three different types of carriers was investigated in this study (objective #1). In addition, the biofilm characteristics, solids characteristics, and particle size distribution of the suspended solids produced in the MBBR reactor filled with newly designed thickness-restraint Z-carriers were also investigated at a consistent loading rate (objectives #2).

Chapter 4 is a research article entitled "*MBBR effluent particles: Influence of carrier geometrical properties and levels of biofilm thickness restraint on biofilm properties, effluent particle size distribution, settling velocity distribution and settling behaviour*". This article has been submitted to the journal of *Biosystems Engineering* in 2021. This study completes chapter 3 and includes the assessment of solids characteristics and the particle settling behaviour (Objective #4).

Chapter 5 is a version of the manuscript under revision to be prepared for submission to the *Journal of Environmental Sciences*, entitled: "*Particle characteristics and settling behaviour of MBBR produced solids along with removal performance and biofilm responses to various carbonaceous loading rates*". This publication investigates the effect of varying SALR on system performance, biofilm characteristics (morphology, thickness, mass, and density), biomass activity, solids characteristics and particle settling behaviour (Objective #3).

Chapter 6 presents the conclusion and discussion of the findings of this research in addition to some recommendations for future research.

## 1.4 References

- Ahmed, W., Tian, X., and Delatolla, R. (2019). “Nitrifying moving bed biofilm reactor: Performance at low temperatures and response to cold-shock.” *Chemosphere*, 229, 295–302.
- Aygun, A., Nas, B., and Berktaş, A. (2008). “Influence of high organic loading rates on COD removal and sludge production in moving bed biofilm reactor.” *Environmental Engineering Science*, 25(9), 1311–1316.
- Barwal, A., and Chaudhary, R. (2014). “To study the performance of biocarriers in moving bed biofilm reactor (MBBR) technology and kinetics of biofilm for retrofitting the existing aerobic treatment systems: A review.” *Reviews in Environmental Science and Biotechnology*, 13(3), 285–299.
- Bassin, J. P., and Dezotti, M. (2018). “Moving Bed Biofilm Reactor (MBBR).” *Advanced Biological Processes for Wastewater Treatment*, Springer, Cham, 37–75.
- Bassin, J. P., Dias, I. N., Cao, S. M. S., Senra, E., Laranjeira, Y., and Dezotti, M. (2016). “Effect of increasing organic loading rates on the performance of moving-bed biofilm reactors filled with different support media: Assessing the activity of suspended and attached biomass fractions.” *Process Safety and Environmental Protection*, 100, 131–141.
- Chaali, M., Naghdi, M., Brar, S. K., and Avalos-Ramirez, A. (2018). “A review on the advances in nitrifying biofilm reactors and their removal rates in wastewater treatment.” *Journal of Chemical Technology and Biotechnology*, 93(11), 3113–3124.
- Delatolla, R. A., and Babarutsi, S. (2005). “Parameters affecting hydraulic behavior of aerated lagoons.” *Journal of Environmental Engineering*, 131(10), 1404–1413.

- Delatolla, R., Tufenkji, N., Comeau, Y., Gadbois, A., Lamarre, D., and Berk, D. (2010). “Investigation of laboratory-scale and pilot-scale attached growth ammonia removal kinetics at cold temperature and low influent carbon.” *Water Quality Research Journal of Canada*, 45(4), 427–436.
- Dias, R. A., Martins, R. C., Castro, L. M., and Quinta-Ferreira, R. M. (2018). “Biosolids production and COD removal in activated sludge and moving bed biofilm reactors.” *WASTES – Solutions, Treatments and Opportunities II*, Taylor & Francis Group, London, 271–276.
- Forrest, D., Delatolla, R., and Kennedy, K. (2016). “Carrier effects on tertiary nitrifying moving bed biofilm reactor: An examination of performance, biofilm and biologically produced solids.” *Environmental Technology*, 37(6), 662–671.
- Gazette, C. (2012). “Wastewater systems effluent regulations, Part II.” 145(15), 1632–1812.
- Ivanovic, I., and Leiknes, T. O. (2012). “Particle separation in moving bed biofilm reactor: Applications and opportunities.” *Separation Science and Technology*, 47(5), 647–653.
- Ivanovic, I., Leiknes, T., and Ødegaard, H. (2006). “Influence of loading rates on production and characteristics of retentate from a biofilm membrane bioreactor (BF-MBR).” *Desalination*, 199(1–3), 490–492.
- Javid, A. H., Hassani, A. H., Ghanbari, B., and Yaghmaeian, K. (2013). “Feasibility of utilizing moving bed biofilm reactor to upgrade and retrofit municipal wastewater treatment plants.” *International Journal of Environmental Research*, 7(4), 963–972.
- Karizmeh, M. S. (2012). “Investigation of biologically-produced solids in moving bed bioreactor (MBBR) treatment systems.” M.Sc. thesis, University of Ottawa, Canada.

- Karizmeh, M. S., Delatolla, R., and Narbaitz, R. M. (2014). “Investigation of settleability of biologically produced solids and biofilm morphology in moving bed bioreactors (MBBRs).” *Bioprocess and Biosystems Engineering*, 37(9), 1839–1848.
- Kruszelnicka, I., Kramarczyk, D. G., Poszwa, P., and Stręk, T. (2018). “Influence of MBBR carriers’ geometry on its flow characteristics.” *Chemical Engineering and Processing - Process Intensification*, 130(June), 134–139.
- Levstek, M., and Plazl, I. (2009). “Influence of carrier type on nitrification in the moving-bed biofilm process.” *Water Science and Technology*, 59(5), 875–882.
- Loupasaki, E., and Diamadopoulou, E. (2013). “Attached growth systems for wastewater treatment in small and rural communities: A review.” *Journal of Chemical Technology and Biotechnology*, 88(2), 190–204.
- Mannacharaju, M., Natarajan, P., Villalan, A. K., Jothieswari, M., Somasundaram, S., and Ganesan, S. (2018). “An innovative approach to minimize excess sludge production in sewage treatment using integrated bioreactors.” *Journal of Environmental Sciences*, Elsevier B.V., 67, 67–77.
- Martín-Pascual, J., López-López, C., Cerdá, A., González-López, J., Hontoria, E., and Poyatos, J. M. (2012). “Comparative kinetic study of carrier type in a moving bed system applied to organic matter removal in urban wastewater treatment.” *Water, Air, and Soil Pollution*, 223(4), 1699–1712.
- Metcalf & Eddy. (2014). *Wastewater Engineering: Treatment and Resource Recovery*. McGraw-Hill, New York.

- Morgan-Sagastume, F. (2018). "Biofilm development, activity and the modification of carrier material surface properties in moving-bed biofilm reactors (MBBRs) for wastewater treatment." *Critical Reviews in Environmental Science and Technology*, 48(5), 439–470.
- Ødegaard, H. (2000). "Advanced compact wastewater treatment based on coagulation and moving bed biofilm processes." *Water Science and Technology*, 42(12), 33–48.
- Ødegaard, H. (2016). "A road-map for energy-neutral wastewater treatment plants of the future based on compact technologies (including MBBR)." *Frontiers of Environmental Science & Engineering*, 10(4), 2.
- Ødegaard, H., Cimbritz, M., Christensson, M., and Dahl, C. P. (2010). "Separation of biomass from moving bed biofilm reactors (MBBRs)." *Proceedings of the Water Environment Federation*, 2010(7), 212–233.
- Ødegaard, H., Gisvold, B., Helness, H., Sjøvold, F., and Zuliang, L. (2000a). "High rate biological/chemical treatment based on the moving bed biofilm process combined with coagulation." *Chemical Water and Wastewater Treatment VI*, 245–255.
- Ødegaard, H., Gisvold, B., and Strickland, J. (2000b). "The influence of carrier size and shape in the moving bed biofilm process." *Water Science and Technology*, 41(4–5), 383–391.
- Ødegaard, H., Rusten, B., and Westrum, T. (1994). "A new moving bed biofilm reactor: applications and results." *Water Science and Technology*, 29(10–11), 157–165.
- Ødegaard, H. (2004). "Sludge minimization technologies - An overview." *Water Science and Technology*, 49(10), 31–40.
- Piculell, M. (2016). "New dimensions of moving bed biofilm carriers influence of biofilm

- thickness and control possibilities.” Ph.D. thesis, Lund University, Sweden.
- Piculell, M., Welander, P., Jönsson, K., and Welander, T. (2016). “Evaluating the effect of biofilm thickness on nitrification in moving bed biofilm reactors.” *Environmental Technology*, 37(6), 732–743.
- Ramli, N. A., and Abdul Hamid, M. F. (2017). “A review on two different systems in municipal sewage treatment plant.” *2017 IEEE Conference on Energy Conversion*, 207–211.
- Rittmann, B. E. (2007). “Where are we with biofilms now? Where are we going?” *Water Science and Technology*, 55(8–9), 1–7.
- Rusten, B., McCoy, M., Proctor, R., and Siljudalen, J. G. (1998). “The innovative moving bed biofilm reactor/solids contact reaeration process for secondary treatment of municipal wastewater.” *Water Environment Research*, 70(5), 1083–1089.
- Tian, X., and Delatolla, R. (2019). “Meso and micro-scale effects of loading and air scouring on nitrifying bio-cord biofilm.” *Environmental Science Water Research & Technology*, 5, 1183–1190.
- Di Trapani, D., Mannina, G., Torregrossa, M., and Viviani, G. (2008). “Hybrid moving bed biofilm reactors: A pilot plant experiment.” *Water Science and Technology*, 57(10), 1539–1545.
- Di Trapani, D., Mannina, G., Torregrossa, M., and Viviani, G. (2010). “Quantification of kinetic parameters for heterotrophic bacteria via respirometry in a hybrid reactor.” *Water Science and Technology*, 61(7), 1757–1766.
- Wang, J. (2012). “Fundamentals of biological processes for wastewater treatment.” *Biological Sludge Minimization and Biomaterials/Bioenergy Recovery Technologies*, John Wiley &

Sons, Inc., Hoboken, NJ, USA, 1–80.

Wuertz, S., Bishop, P. L., and Wilderer, P. A. (2003). *Biofilms in Wastewater Treatment: An Interdisciplinary Approach*. IWA publishing.

WEF. (2009). *Design of Municipal Wastewater Treatment Plants: WEF Manual of Practice No. 8*. McGraw-Hill, New York.

WEF. (2011). *Moving Bed Biofilm Reactors. WEF Manual of Practice No. 35*, McGraw Hill, Alexandria, Virginia, USA.

Young, B., Delatolla, R., Ren, B., Kennedy, K., Laflamme, E., and Stintzi, A. (2016). “Pilot-scale tertiary MBBR nitrification at 1°C: Characterization of ammonia removal rate, solids settleability and biofilm characteristics.” *Environmental Technology*, 37(16), 2124–2132.

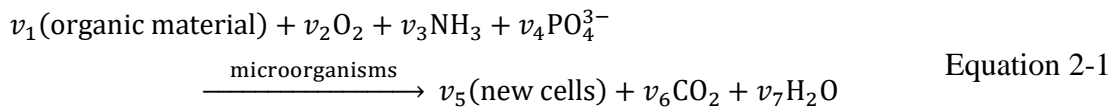
## Chapter 2 – Literature review

### 2.1 Biological wastewater treatment

The municipal water resource recovery facilities (WRRF) are aimed to remove contaminants from the wastewater prior to discharge into the surface water resources. The wastewater systems effluent regulations (WSER) under the Canadian Fisheries Act (2012) has regulated the discharge concentration of four constituents: total suspended solids (TSS) and carbonaceous biological oxygen demand (cBOD) not to exceed 25 mg/L, total residual chlorine (TRC) to be equal or less than 0.02 mg/L and unionized ammonia as nitrogen (NH<sub>3</sub>-N) to be lower than 1.25 mg/L at 15 ± 1 °C (Gazette, 2012). However, new provisions of the Fisheries Act “allow the federal government to establish an equivalent agreement if provisions under the laws of province are found to be equivalent in effect to provisions of the federal regulations” (Gazette, 2018). Consequently, the Canada-Quebec equivalency agreement was entered (on August 23, 2018) to reduce regulatory duplication and increase regulatory clarity for the management of wastewater systems in Quebec. Based on this, Quebec’s regulations and authorizations are enforced for the effluent quality in the province of Quebec, in which the standards for TSS and cBOD are deemed equivalent to WSER (Gazette, 2018).

The harmful constituents present in wastewater can be removed by physical, chemical, or biological treatment processes to meet the effluent discharge standards. Biological wastewater treatment is the most common and currently the most cost-effective method to remove organic matter and nitrogen from the wastewater. In order to biologically remove carbonaceous material or nutrients from the wastewater, a variety of different microorganisms are used to oxidize (or convert) the dissolved and particulate carbonaceous organic matter or nutrients into simple end-products and additional biomass (Equation 2-1). Primarily, bacteria are responsible for the

oxidation of organic compounds. Moreover, fungi, algae, protozoans, and higher organisms also have essential roles in transforming soluble and colloidal organic pollutants into carbon dioxide and water as well as biomass. Although the biological wastewater treatment processes can remove the constituents by biological activities, the separation of biologically produced cells from the treated wastewater is required to accomplish the biological treatment (WEF, 2009; Wang, 2012; Metcalf & Eddy, 2014). Since the biomass has a slightly greater specific gravity than water, it can be removed from the liquid by gravity sedimentation before discharge into a natural watercourse (Wang, 2012).



Where  $v_i$  are the stoichiometric coefficients, and *new cells* are the biomass produced as a result of the oxidation of the organic matter in the presence of nutrients (Metcalf & Eddy, 2014).

Typically, the biological treatment system can be divided into two main categories according to the state of the growth of the microorganisms: suspended growth and attached growth systems (Metcalf & Eddy, 2014).

### 2.1.1 Suspended growth systems – Activated sludge

In a suspended growth system, the microorganisms required for biological treatment grow freely and maintain in suspension in the bulk liquid by mechanical mixing or aeration. The wastewater is treated by contact with these suspended microorganisms. Then the flocculated bacteria is removed from the treated wastewater by a proper solid-liquid separation method at the end. Lagoons and conventional activated sludge (CAS) are two examples of widely used suspended growth systems worldwide (WEF, 2009; Metcalf & Eddy, 2014). Although lagoon

operation is cost-effective and straightforward as they require minimal maintenance, large areas and land availability are required due to their long retention time. As such, lagoons are susceptible to either a limited or a lack of nitrification in cold temperature conditions (Gazette, 2012; Young, 2017).

Activated sludge, the second example of widely used suspended growth systems, was developed in England in the early 1900s, and it is still the most common process used for both municipal and industrial wastewater treatment (WEF, 2009; Metcalf & Eddy, 2014). A typical configuration of activated sludge consists of an aeration tank followed by a sedimentation tank with solids recycled from the settler to the aeration tank. The aeration tank provides a suitable environment with enough contact time for a mixture of various microorganisms to aerobically metabolize the biodegradable contaminants in the wastewater. The suspended biomass is settled and thickened in a clarifier and is returned to the aeration tank because it contains active microorganisms required for continual treatment. However, a portion of the thickened solids should be removed periodically to avoid the excess biomass in the effluent flow (Wang, 2012; Metcalf & Eddy, 2014). Sludge recycling is the crucial factor in an activated sludge system as it keeps the high concentration of active biomass in the system, which increases the solids retention time (SRT) along with a short hydraulic retention time (HRT) (Rittmann and McCarty, 2001; Metcalf & Eddy, 2014).

Activated sludge systems mainly aim to achieve a "secondary treatment" standard by removing BOD and TSS. However, they could also be designed to remove the nutrients. Nitrifying activated sludge processes require higher SRT to develop the slow-growing nitrifying bacteria, while the SRT is limited to a range of 4 to 10 days for the BOD removal process. The SRT not only can control the system performance but also can control the sludge's physical and biological

properties that can affect the flocs settling characteristics. Once the microbial flocs are not able to compact well, a major settling problem called "sludge bulking" will occur due to a non-optimal operational condition and the ecological complexity of the activated sludge systems. Sludge bulking leads to a significant loss of the microbiological population and hence high suspended solids concentrations in the effluent, which results in a decrease in system performance (Rittmann and McCarty, 2001; Metcalf & Eddy, 2014).

### **2.1.2 Attached growth systems – Biofilm reactors**

In an attached growth process, the required microorganisms treating the wastewater are attached to inert packing material. The attached growth systems employ various microorganisms to convert the organic material or nutrients (Equation 2-1) to simple end-products similar to the suspended growth systems. Both systems' approaches rely on natural biomass aggregation. Whereas, attachment of microorganisms to a substratum is the basis for biofilm accumulation in attached growth systems (Rittmann and McCarty, 2001; Metcalf & Eddy, 2014). The similarity of fundamental metabolic processes for both systems is inevitable because the microorganisms utilize the same electron donors and acceptors, and are exposed to the same environmental conditions. However, biofilm formation in attached growth systems offers advantages that can result in better system performance and cost benefits (Rittmann and McCarty, 2001; WEF, 2011; Metcalf & Eddy, 2014). Biofilm processes are simple, reliable, and stable because the attachment allows excellent biomass accumulation and biomass retention in the reactor without requiring recycling the active biomass from the clarifiers. This may reduce energy and operational cost and intensity (Rittmann and McCarty, 2001; WEF, 2011).

The packing materials, which provide suitable substratum for microbial growth in the attached growth system, could be either natural or synthetic material, including rock, gravel, slag, sand and

a wide range of plastics. These mediums can be non-submerged, partially submerged, or completely submerged in the liquid. The application of the attached growth systems originated from trickling filter, which is an example of a non-submerged biofilm process. Trickling filters have been commonly used for secondary treatment since the late 1800s. Afterward, rotating biological contactor (RBC), an example of a partially submerged biofilm process, has been introduced and became widespread through the 1970s (Rittmann and McCarty, 2001; Metcalf & Eddy, 2014). In the late 1980s, a submerged attached growth system called moving bed biofilm reactor (MBBR) was developed in Norway by Kaldness Miljøteknologi. The MBBR is the most recent biofilm technology introduced as a robust reactor with no need for sludge recirculation and backwashing (Ødegaard et al., 1994; Ødegaard, 2006; Bassin and Dezotti, 2018). The unique advantage of the submerged attached growth system is the need for a small footprint. An area requirement is a fraction (one-fifth to one-third) of the area needed for activated sludge treatment (Metcalf & Eddy, 2014). Therefore, the biofilm technologies could be an efficient alternative wastewater treatment process, which provides advantages over the activated sludge system.

## **2.2 Biofilm development and detachment**

The key difference between the attached and suspended growth systems is biofilm formation on the surface of the packing material. A biofilm is a layer-like aggregate of microbial cells embedded in a self-produced matrix of extracellular polymeric substances (EPS) and adherent to an inert or living surface (Rittmann and McCarty, 2001; Flemming and Wingender, 2010). EPS is an essential component for biofilm formation. It is responsible for the adhesion of microorganisms to the solid surfaces, and it provides a three-dimensional biofilm structure. Research has demonstrated that the bacteria cells in the biofilm (sessile state) act differently than the planktonic state (free-floating microorganisms). Therefore the biofilm-associated organisms show more

robust biological survival properties, increased resistance and stability to deal with fluctuations in environmental conditions such as toxicity and cold climate (Dunne, 2002; Flemming and Wingender, 2010).

The growth rates and substrate utilization of organisms in the biofilm are limited by the mass transfer of the substrate into the biofilm. The biofilm separates from the bulk liquid through a viscous interface called the mass transfer boundary layer (MTBL), where convective transport does not occur due to the decreased flow. Therefore, the substrate diffuses through the MTBL and the biofilm itself, causing the substrate concentration gradients through the depth of the biofilm (Figure 2-1). This can be considered as a notable feature of the biofilm, where different environmental conditions in different layers of the biofilm will lead to the presence of variable microbial communities, moving from aerobic to anoxic conditions depending on the biofilm thickness (WEF, 2011).

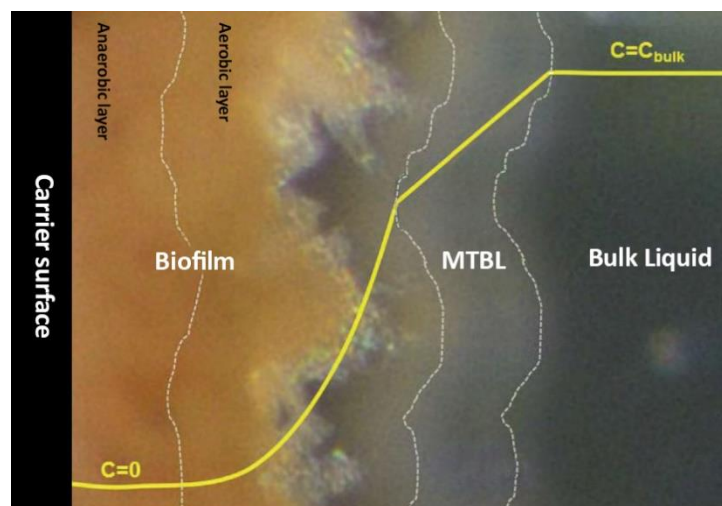


**Figure 2-1:** Substrate concentration gradients through the depth of biofilm, i.e. yellow line illustrates the oxygen concentration gradient through the biofilm, creating aerobic and anaerobic zones (Piculell, 2016)

The biofilm formation process consists of three main steps: attachment, growth, and detachment (Figure 2-2). The single floating planktonic cells land on the substratum, attach to the surface and start bacterial aggregation through the initial attachment event. Then the surface-bound organisms begin to replicate, grow and die actively. The availability of nutrients in the bulk liquid, the hydrodynamic flow, and other conditions such as temperature, pH, dissolved oxygen (DO), carbon source, and etcetera, can control the biofilm growth and morphology. The biofilm may become smooth, rough, or maintain a mushroom-like structure. (Dunne, 2002; Garrett et al., 2008). Once the overall density, mass and complexity of the biofilm increased and the extracellular components are generated, the biofilm is matured and begins to generate planktonic organisms. These organisms are free to escape the biofilm and colonize other surfaces (Watnick and Kolter, 2000; Donlan, 2001; Dunne, 2002).

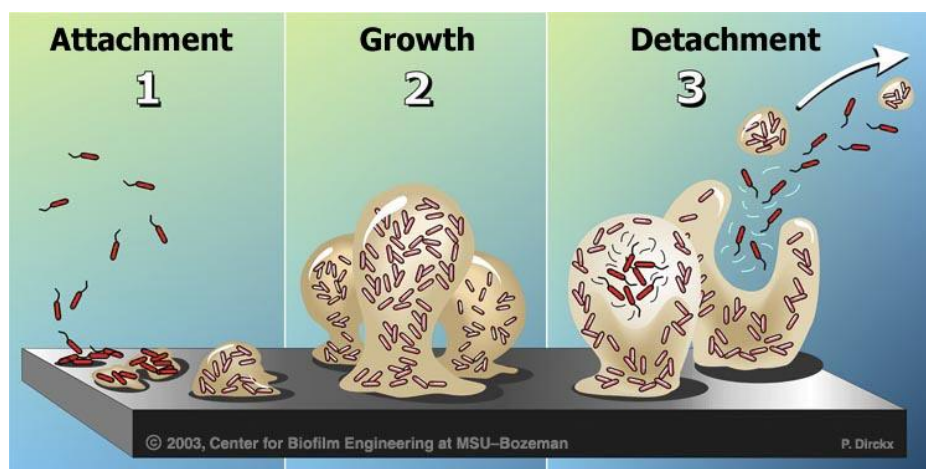


**Figure 2-2:** Three steps of biofilm formation

There is a continuous detachment of biomass as the biofilms grow on the substratum. The biofilm detachment is the last step in biofilm formation. In this process, the biofilm loses the particulate component into the bulk liquid. Bryers (1987) characterized four general biofilm detachments: abrasion, erosion, sloughing, and predator grazing. Abrasion and erosion are a

continuous detachment of excess biomass in small pieces, which is associated with well-operating biofilm reactors. Abrasion is caused by particle collision, carriers colliding and scraping against each other. However, hydrodynamics shear forces in the bulk liquid surrounding the biofilm can cause erosion. Moreover, predation of higher organisms on biofilm can cause predator grazing detachment. Moderate predator activity can be considered as a usual detachment mechanism in biofilm reactors. Nonetheless, the sloughing is uncontrollable and undesirable dislodgement of biomass from the substratum interface. Sloughing and excessive predator grazing are the detachment of large segments of the biofilm, which is detrimental to the reactor performance as it increases the BOD and TSS in the effluent and reduces the removal efficiency (WEF, 2009, 2011).

The biofilm detachment is a critical process that can govern the accumulation of bacterial cells in the biofilm reactors. Therefore, it can influence the biological survival, the biofilm structure, the biofilm thickness, the production of suspended solids, and generally the reactor performance. All the mentioned detachment mechanisms might be observed in various biofilm systems depending on the shear forces in the reactor (hydrodynamic forces or particle collision), substrate loading, and the presence of higher organisms (predators) (WEF, 2009; Goode, 2010).

### **2.3 MBBR technology**

MBBR is a submerged attached growth biological process developed in the late 1980s as a simple yet robust, compact, standalone and flexible technology for wastewater treatment (Ødegaard et al., 1994; WEF, 2011; Bassin and Dezotti, 2018). The MBBR technology relies on free-floating plastic carriers with a high surface area that provides a substratum for bacterial growth and maintains most of the biomass on suspended media in the reactor (Ødegaard et al., 1994, 2000b). Therefore, the treatment capacity could be easily increased by adding additional carriers,

up to 70% of the reactor volume, to manage the growing population and increase the loading rates without performing costly infrastructure retrofits (Ødegaard, 1999; Metcalf & Eddy, 2014).

Since the invention of MBBR technology, many studies have been done to demonstrate the reactor's effectiveness in different treatment conditions. Several studies have evaluated the application of MBBR processes in different configurations for carbonaceous and nutrient removal to treat various types of wastewaters, including industrial, municipal, synthetic or real wastewater (Ødegaard, 2006; McQuarrie and Boltz, 2011; Shahot et al., 2014; Almomani and Khraisheh, 2016; Leyva-Díaz et al., 2017; Bassin and Dezotti, 2018; Chaali et al., 2018). These applications have demonstrated success in meeting a wide range of effluent quality standards, including stringent nutrient limits (WEF, 2011). Recently, an excellent performance of MBBR has been proven at low temperatures, which is a promise for cold countries to attain low-temperature nitrification (Hoang et al., 2014; Young et al., 2016; Ahmed et al., 2019).

In addition to high treatment efficiency; high load tolerance, small footprint, cost and energy effectiveness, low vulnerability to cold temperature, low operational intensity, low sludge production and no sludge recirculation and backwashing requirements are some other advantageous characteristics of this technology (Ødegaard, 2004; Åhl et al., 2006; WEF, 2011; Loupasaki and Diamadopoulos, 2013; Young et al., 2016; Ramli and Abdul Hamid, 2017; Mannacharaju et al., 2018; Dias et al., 2018c; Tian and Delatolla, 2019). However, like any other technology, the MBBR also has its drawbacks. As such, several studies have highlighted the poor settling characteristics of the biologically produced solids leaving MBBR systems, which clarify the necessity for using intense solids separation methods such as filtration, lamella settling, and using enhanced sedimentation with pre-coagulation (Ødegaard et al., 2010; Ivanovic and Leiknes, 2012; Karizmeh et al., 2014; Bassin and Dezotti, 2018).

The studies have shown that loading rate, HRT, filling degrees of the carriers, carrier types, temperature and DO concentration in the reactors could influence the MBBR performance (Aygun et al., 2008; Barwal and Chaudhary, 2014; Young et al., 2016; Chaali et al., 2018). However, it should be noted that the removal efficiency of a biological reactor is not only dependant on the soluble organic matter and nutrient removal but also the particulate suspended solids removal. Therefore, solid-liquid separation could play an essential role in any biological wastewater treatment process, as it significantly impacts the effluent quality. Since a settling tank is a conventional solid-liquid separation technology to remove particulate matter from the wastewater, it is imperative to study the solids characteristics, settleability and settling behaviour of suspended solids in MBBRs' effluent while studying the system performance.

### **2.3.1 Effect of carrier type on MBBR system performance**

A variety of carrier media are possible for use in MBBR processes, but most of the research and the existing installations have used the plastic AnoxKaldnes™ carriers with a specific gravity of 0.96 to 0.98 g/cm<sup>3</sup> (WEF, 2011; Metcalf & Eddy, 2014). Most carriers are designed to provide a large protected surface area (PSA) inside voids and cavities, where biofilms can grow in a protected environment (McQuarrie and Boltz, 2011). Therefore, the SALR and the capacity of the MBBR reactor can be simply adjusted by changing the volumetric filling degree of the carriers (up to 70%) to meet the specific removal requirements. In addition, the constant movement of the carriers is required by continuous mixing in the reactor to prevent carrier clogging, to enhance substrate availability for the biofilm, and hence to improve treatment performance. Mechanical mixers in anaerobic (or anoxic) reactors and aeration systems in aerobic reactors can provide sufficient mixing and continuous movement of the carriers (Ødegaard, 1999; Ødegaard et al., 2000b).

MBBR design is solely based on the carrier's PSA, as researchers have demonstrated that MBBR removal efficiency only depends on the effective surface area regardless of the carriers design, type and shape (Bassin et al., 2016; Forrest et al., 2016; Levstek et al., 2009; Ødegaard et al., 2000b). Therefore, over the years, different carrier types (of varying material, shape and size) have been developed and are still being modified to improve the overall performance of the MBBR systems. They mostly have focused on providing higher PSA due to the assumption that the available area is a dominating design factor (Bassin et al., 2018; Morgan-Sagastume, 2018). Therefore, providing larger PSA for biofilm growth leads to more biofilm fitted into the reactor and hence, a more compact and efficient reactor.

The performance of MBBR carriers made from different materials in various shapes and sizes has been reported in the literature. The carriers are made up of synthetic polymers, either as plastic foam (sponge) or plastic solid elements such as high-density polyethylene (HDPE), polypropylene (PP) or polyethylene (PE) with an approximate density of  $0.95 \text{ g/cm}^3$  (Levstek and Plazl, 2009; McQuarrie and Boltz, 2011; Zhang et al., 2012; Barwal and Chaudhary, 2014; Liu et al., 2019). The available carrier surface area per packed volume can vary in the range of 200 to  $1,200 \text{ m}^2/\text{m}^3$  for some of the most commonly used HDPE carrier types (Figure 2-3), where the carrier diameter can range from 7 mm to 64 mm (McQuarrie and Boltz, 2011; Barwal and Chaudhary, 2014; Bassin and Dezotti, 2018).

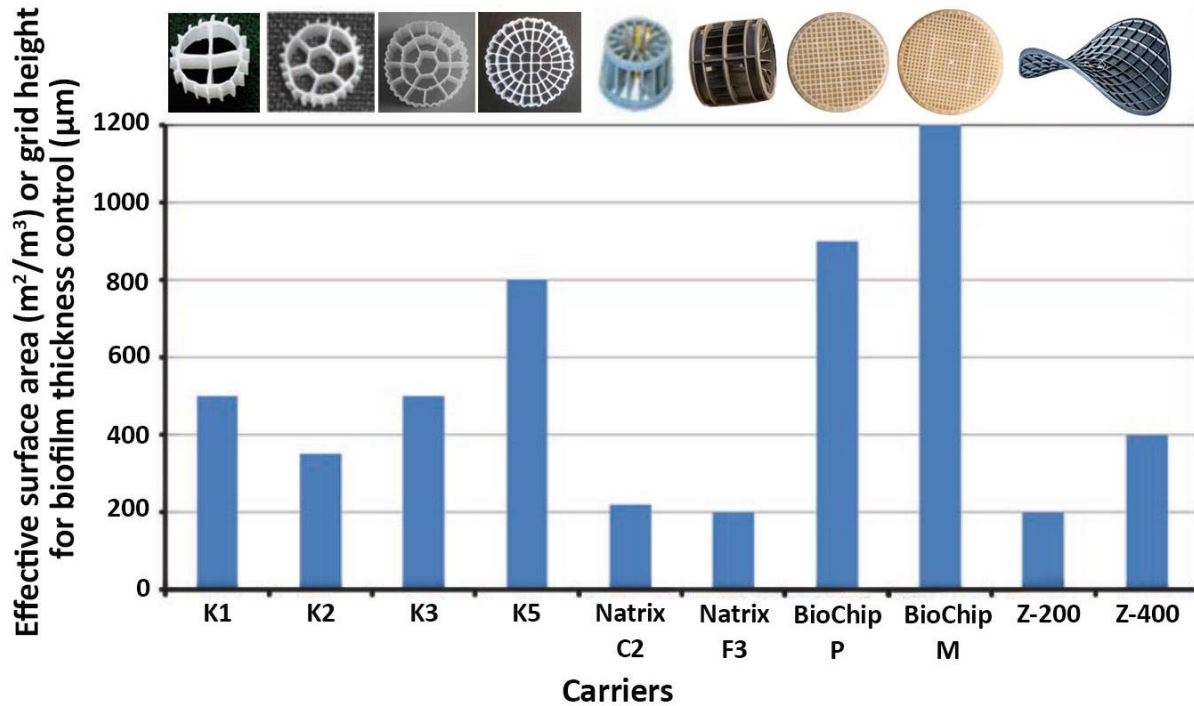


**Figure 2-3:** Effective surface area ( $\text{m}^2/\text{m}^3$ ) or grid height to control the biofilm thickness of AnoxKaldnes® (Bassin and Dezotti, 2018)

Some other studies have proved the carrier material and substratum surface properties significantly affect the biofilm formation rate, attachment, growth and MBBR performance during both start-up and operational periods (Chu et al., 2011; Morgan-Sagastume, 2018; Sonwani et al., 2019). Some researchers highlighted that the physical properties of carriers are important in the design of MBBR because the biofilm formation rate is highly correlated with the shape of the carriers and not with the carrier surface area during the start-up period (Martínez-Huerta et al., 2009; Lopez-Lopez et al., 2012; Bassin et al., 2016; Dias et al., 2018b). Furthermore, the physical and geometrical properties of the carriers play an important role in wastewater hydrodynamic and oxygen transfer efficiency in the MBBR reactors (Dias et al., 2018a), which ultimately would contribute to reactor performance. Similar shapes (cylinder-shaped with a cross inside) but different sizes of carriers showed significantly different nitrogen removal efficiency because of

the different attached biomass distribution patterns and biofilm thickness (Ashrafi et al., 2019). Higher nitrogen removal is achieved for thicker biofilm due to the oxygen mass transfer limitation and hence anoxic condition establishment at a deeper layer of the biofilm (Ashrafi et al., 2019; Bassin et al., 2016; Piculell et al., 2016).

Recently, MBBR carriers have been the focus of further developments aimed to control bacterial attachment, biofilm growth and to optimize the overall MBBR operational performance. It is known that the biofilm thickness, density and effective surface area influence the MBBR system performance (Li et al., 2016a; Morgan-Sagastume, 2018), but no means existed to precisely control the biofilm thickness before the invention of Z-carriers. The Z-carriers are a new series of carriers that have been designed with the specific purpose of controlling biofilm thickness based on the height of the grid walls and biofilm surface area in MBBR reactors (Torresi et al., 2016; Piculell et al., 2016). Therefore, the influence of limiting the biofilm thickness on system performance and solids characteristics in various experimental conditions is not well known and needs more study.

### **2.3.2 Effect of SALR on MBBR system performance**

As the effective biofilm area is a key parameter to design the MBBR, the loading and removal rates of the MBBR can be expressed as a function of the carrier's surface area (Ødegaard, 1999). Therefore, the MBBR reactor loading rate and performance usually are present as surface area loading rate (SALR) and surface area removal rate (SARR), respectively (WEF, 2011). In other words, the SALR ( $\text{g}/\text{m}^2\cdot\text{d}$ ) is the substrate concentration normalized to the surface area while the SARR ( $\text{g}/\text{m}^2\cdot\text{d}$ ) is the quantity of substrate removed per unit of surface area, which can be calculated as follow:

$$SALR = \frac{\text{substrate loading rate}}{\text{m}^2 \text{ of carriers in the reactor}} = \frac{Q \cdot C_{in}}{V \cdot \%fill \cdot S_{ab}} \quad \text{Equation 2-2}$$

$$SARR = \frac{\text{substrate removal rate}}{\text{m}^2 \text{ of carriers in the reactor}} = \frac{Q \cdot (C_{in} - C_{eff})}{V \cdot \%fill \cdot S_{ab}} \quad \text{Equation 2-3}$$

Where  $Q$  is the influent flowrate ( $\text{m}^3/\text{d}$ ),  $C_{in}$  is the influent substrate concentration ( $\text{g}/\text{m}^3$ ),  $C_{eff}$  is the effluent substrate concentration ( $\text{g}/\text{m}^3$ ),  $V$  is the reactor volume ( $\text{m}^3$ ),  $\%fill$  is the fraction of reactor volume that is occupied by carriers, and  $S_{ab}$  is the specific surface area of the carriers ( $\text{m}^2/\text{m}^3$ ) (provided by the manufacturer).

A wide range of SALRs was used in previous studies. Some studies have demonstrated only a little difference in COD removal performance at low organic loading rates up to approximately  $13 \text{ g-COD}/\text{m}^2 \cdot \text{d}$  (Table 2-1). Despite the gradual decrease in the organic removal rate by increasing the loading rate, the reactors showed a good carbonaceous removal performance and stability for all the ranges. However, the nitrification functionality may be hindered in high organic load conditions due to the development of fast-growing heterotrophs (Rusten et al., 1998; Melin et al., 2005; Javid et al., 2013; Bassin et al., 2016). Some other studies showed a significant decrease in organic removal rate with increasing the organic loading rate up to  $96 \text{ g COD}/\text{m}^2 \cdot \text{d}$  (Aygün et al., 2008; Javid et al., 2013).

**Table 2-1:** Effect of various SALR ranges on removal efficiency, used in previous researches

Authors	Carriers	SALR (g-COD/m <sup>2</sup> ·d)	Removal Efficiency (%)	Description	
Bassin et al., 2016	AnoxK™ K1 and Mutag Biochip	3.2	>90%	DO between 4-5 mg/L HRT= 12 hr Synthetic wastewater	
		6.4	>95%		
		9.6	>95%		
		12.8	>95%		
Aygun et al. 2008	AnoxK™ K1	6	95.1%	DO ranges 2.5-3 mg/L (for SALR 6-24) DO= 0.84 and 0.3 mg/L for SALR 48 and 96, respectively (Low DO concentrations could affect COD removal efficiency) HRT= 8 hr Synthetic wastewater	
		12	94.9%		
		24	89.3%		
		48	68.7%		
		96	45.2%		
Javid et al. 2013	AnoxK™ K1	5.3 (1.58) <sup>a</sup>	92.30%	The flowrate was decreased along with the increase in HRT at lower SALRs. DO between 2-3 mg/L HRT between 1 to 4 hr Municipal wastewater	
		7 (2.10)	88.23%		
		7.9 (2.37)	83.49%		
		10.8 (3.24)	79.19%		
		13.5 (4.05)	75.10%		
Karizmeh et al., 2014	AnoxK™ K1	9	75%	DO= 4.2 mg/L HRT= 1 hr Synthetic wastewater	
		32	74%		
		64	65%		
Melin et al. 2005	AnoxK™ K1	Low rate: 4.1 to 6.8 (2.3 to 3.8) <sup>b</sup>	73% (HRT=4h) 70% (HRT=3h)	DO between 2.7-6.3 mg/L HRT was 3 and 4 hr Municipal wastewater	
		high rate: 14.5–26.6 (7.8–16.6)	55% (HRT=1h) 45% (HRT=0.75h)		HRT was 0.75 and 1 hr

<sup>a</sup> The values in the parenthesis is calculated by the given information in the article to convert the loading rate of kg-COD/m<sup>3</sup>·d to g-COD/m<sup>2</sup>·d

<sup>b</sup> The number in the parenthesis is according to filtered COD

Although the varying SALR in some specific ranges has not significantly influenced the carbonaceous removal efficiency, researchers have demonstrated that increased SALR in the carbonaceous MBBR system results in increased solids production (Aygun et al., 2008; Javid et al., 2013). This increase is accompanied by reductions in the solids' settleability due to the production of different floc structures at high and low loading rates (Ivanovic et al., 2006; Ivanovic

and Leiknes, 2012). However, the literature showed that high removal efficiencies might be obtained even at extremely high loading rates if good biomass separation can be assured (Ødegaard, 1999, 2006).

### **2.3.3 Effect of biofilm characteristics on MBBR system performance**

Researchers have linked biofilm characteristics and MBBR reactor performance to operational conditions. They have noticed distinct differences in biofilm morphology (evident changes in thickness and densities) at high (48 g-COD/m<sup>2</sup>·d) and low (12 g-COD/m<sup>2</sup>·d) SALRs for COD removal MBBRs (Ivanovic et al., 2006). High carbonaceous loading rates (approximately 30 g-COD/m<sup>2</sup>·d) in the reactor produced the compact bacterial biofilm. In contrast, reducing loading rates to moderate and low resulted in less dense and fluffy biofilm with a different protozoan population (Ødegaard, 1999). The oxygen penetration into the biofilm is less limited in fluffy biofilms, resulting in higher microbial activity rates than the dense and smooth biofilms. Thin and dense biofilm was observed in a reactor with higher carrier concentration (% fill) due to the higher turbulence in the reactor, the increased carrier collision and the detachment rate, while low carrier concentration promoted rough and fluffy biofilm (Wang et al., 2005).

In other studies, a more filamentous biofilm structure with smaller pores was observed at a medium carbonaceous SALR and lower HRT. While increasing the HRT has reduced the filamentous structure of the biofilm and increased the dimensions of the pores. Moreover, the biofilm thickness has shown a negative correlation with HRT, as the thinnest biofilm corresponded to the higher HRT at medium carbonaceous SALR of 32 g-COD/m<sup>2</sup>·d (Karizmeh et al., 2014). Besides, previous studies on nitrifying MBBR systems have demonstrated a significant increase in nitrifying biofilm thickness with a reduction in temperature. This increase was likely because of the increased oxygen solubility at lower temperatures and decreased cellular activity in the

biofilm (Delatolla et al., 2010; WEF, 2011; Hoang et al., 2014; Young et al., 2016). Moreover, the thicker biofilms indicated a reduction of dry density that can be explained by the biofilm morphology converting to a porous and loose filamentous structure (Jang et al., 2003; Young et al., 2016).

## **2.4 MBBR solids characteristics**

The total solids content in wastewater is the most important physical characteristic of wastewater. The removal of suspended solids is a crucial step in wastewater treatment processes, as it has a significant impact on effluent quality. The MBBR effluent contains a fraction of the influent particulate matter, as well as biologically produced solids that are detached from the carriers in the reactor, colloidal and soluble non-biodegradable organic matter, and soluble microbial products (Ivanovic and Leiknes, 2012; Karizmeh et al., 2014). The total suspended biomass in the pure MBBR system is as low as several hundred mg/L, which is approximately ten to twenty times lower than the activated sludge systems. Therefore, the solid-liquid separation differs from other conventional wastewater systems because the separation of solids from the purified water is dependent on the concentration of the particles and flocs (Ødegaard, 2006; Ødegaard et al., 2010; Ivanovic and Leiknes, 2012). Although solids concentration is an important factor influencing the settling velocity of particles, physical solids characteristics such as particle size, shape and structure also play an important role in settling processes (Guan and Waite, 2006). However, the particle characteristics are not constant over time and can be affected by changes in HRT, SALR, carrier percent fill, carrier type, aeration rate and etcetera.

Since the TSS is a lumped parameter, it cannot indicate enough information on particle characteristics. Therefore, to assess the effectiveness of the treatment process, more understanding about the nature of the particles, particle size distribution, and particle physical and geometrical

characteristics are required. Measurement of particle size is important as it can influence the settling behaviour and treatment efficiency. Moreover, the biological conversion of biodegradable particles is dependent on size. Two approaches can be used to determine particle size. The first approach includes the methods based on observation and measurement, and the second one includes the methods based on separation and analysis techniques (Metcalf & Eddy, 2014). In this study, the measurement is based on the microscopic observation and further image analyses used to investigate the MBBR particles.

Although any changes in operational condition (such as HRT, SALR, carriers percent fill, carrier types, and aeration rate) can affect the soluble constituents removal performance in the MBBR reactors, the operational conditions might also affect the biofilm characteristics, biofilm detachment and consequently particle characteristics, particle size distribution, and settling characteristics of the MBBR solids. Therefore, carrier types, organic SALR and controlling the biofilm thickness are the focus of this study in order to investigate the effects of these parameters on solids characteristics and settling behaviour of solids.

#### **2.4.1 Effect of carrier type on MBBR solids characteristics**

Investigation of biofilm growth on different carrier types demonstrated that the biofilm is not uniformly distributed over the carrier surface. The carrier material, shape and substratum surface properties significantly affect the biofilm formation rate, attachment and biofilm growth (Chu et al., 2011; Morgan-Sagastume, 2018; Sonwani et al., 2019). Consequently, the biofilm at the corners and ridges of the inner surface of the carriers, where the biofilm was well protected from abrasion and erosion, was thicker than the biofilm along the straight surfaces.

The exposure of carriers to shear forces and attrition in the reactor can control the biofilm thickness to some extent. However, the biofilm thickness and the amount of biomass growth on

the conventional carriers is variable because there is no means to control the biofilm thickness exclusively (Dias et al., 2018b; Piculell, 2016; Piculell et al., 2014). Therefore, various conventional carrier types are exposed to different levels of clogging risk under higher loading conditions due to their physical and geometrical properties. Carriers with higher surface area and smaller voids (such as AnoxK™ M carriers) are at the risk of uncontrolled biofilm growth and clogging more than the carriers with lower surface area (such as AnoxK™ K3 and P)(Forrest et al., 2016). In addition, clogging the carriers resulted in decreased treatment performance as well as increased unwanted suspended solids in the effluent, which can cause different settleability and solids characteristics. However, studies on nitrifying MBBR systems have indicated that the solids production rate is not significantly different for different types of carriers when they are not clogged (Brosseau et al., 2016; Forrest et al., 2016; Young et al., 2016; Hayder et al., 2017; Morgan-Sagastume, 2018). Variances in the biofilm morphology for different types of carriers and the potential differences in the bacterial communities might explain the changes in effluent solids characteristics and settleability (Ødegaard et al., 2000b).

Despite the impact of experimental conditions on suspended solids production and settleability, only a few studies have focused on the effect of different carrier types on the MBBR solids' characteristics. Although it has been shown how biofilm properties can differ between different carriers (Li et al., 2016b; Forrest et al., 2016), there is a lack of understanding of how the physical and geometrical characteristics of the carriers and limiting the biofilm thickness would affect the biofilm properties. To achieve this goal, a new series of carriers (AnoxK™ Z-carriers) invented recently (Piculell et al., 2016) were used in this study to prevent clogging and to maintain the thickness of the biofilm to the predetermined maximum thickness.

#### 2.4.2 Effect of SALR on MBBR solids characteristics

The effects of SALR and HRT on particle size distribution for nitrifying and carbonaceous MBBR systems have been investigated. The studies have demonstrated that decreasing the SALR in the reactor as well as increasing the HRT could cause larger particles in the MBBR effluent, and consequently, better settling properties was observed at lower SALRs and higher HRTs (Åhl et al., 2006; Ødegaard et al., 2010). Moreover, the fraction of the colloidal particle decreased by increasing the HRT, which can be a reason for the enhanced settling behaviour at higher HRTs (Melin et al., 2005). The studies on a wide range of SALRs (10-120 g-COD/m<sup>2</sup>·d) have shown a negative correlation with the settling performance of the solids in the MBBR effluent (Ødegaard et al., 2000a; Karizmeh, 2012). However, SALR is not the only factor that affects the suspended solids removal in the settling tank. As a summary, according to the literature, efficient solids removal is dependent on settling tank overflow rates as well as SALRs (Figure 2-4). Such that, the maximum suspended solids removal could be achieved at low SALR (less than 10 g-COD/m<sup>2</sup>·d) and low surface overflow rate (below 0.05 m/h), where the particles produced well-formed and compact flocs that tend to settle more easily (Ødegaard, 2000; Ødegaard et al., 2000a; Ivanovic and Leiknes, 2012).

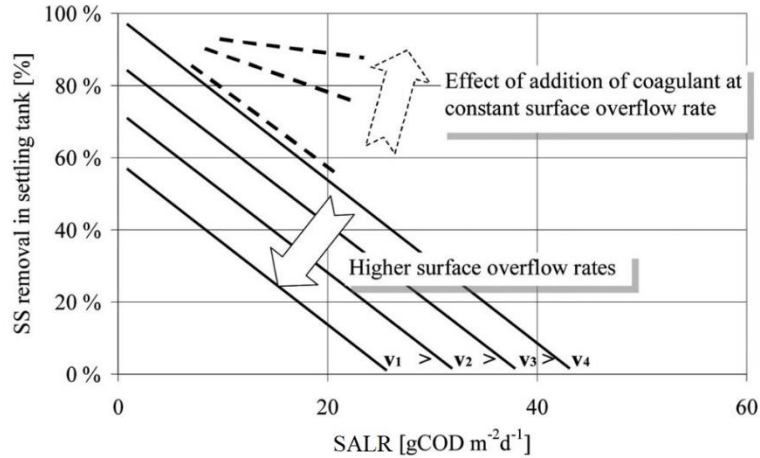


**Figure 2-4:** Effect of SALR and surface overflow rates ( $v_i$ ) on solids removal efficiency (Ivanovic and Leiknes, 2012)

In addition to the impact of varying SALRs on the particle size distribution, the increased SALR also resulted in higher solids production in the MBBR systems (Aygun et al., 2008; Bassin et al., 2016). High loading rate not only demonstrated higher suspended solids concentration but also increased the number of submicron particles, undesirable flocs structures and filaments in the effluent, which are not favourable characteristics for further sludge treatment as compared to low rate biofilm reactors (Ivanovic et al., 2006).

### 2.4.3 Effect of biofilm characteristics on MBBR solids characteristics

The MBBR produced solids are mostly fragments of biofilm detached from the substratum due to erosion, abrasion, and sometimes sloughing or predator grazing, which considerably depends on the operational conditions of the reactors (Wuertz et al., 2003; Metcalf & Eddy, 2014). The biofilm detachment rate is an important process that controls the biofilm structure and the MBBR system performance, which yet is poorly understood. The detachment of cells from biofilm surfaces controls the accumulation and the thickness of the biofilm and hence the quantity of biomass in the reactor, as well as the suspended solids in the bulk liquid phase (Rittmann, 2007).

The biofilm properties might influence the characteristics of the solids in the MBBR effluent. The possibility of a difference in biofilm morphology and hence the bacterial communities might potentially affect the effluent solids characteristics and settleability (Ødegaard et al., 2000b). Some studies have indicated that different operational conditions (such as SALR, HRT, C/N ratio and temperature) can change the thickness of biofilm and the quantity of biomass in the reactor and thus the overall MBBR system performance (Barwal and Chaudhary, 2014; Young et al., 2016; Chaali et al., 2018; Patry et al., 2018). However, up to date, there is a gap of knowledge on how controlling the biofilm thickness could affect the solids production, detachment rate, particle characteristics and settleability, conversely.

## **2.5 Solids characteristics and settling behaviour**

The physical properties of biological solids, such as density, porosity, size and shape of the particles, affect the settling and compression behaviour in secondary clarifiers and hence, the solid-liquid separation processes. Since settling is the most conventional solid-liquid separation method widely used in wastewater treatment plants, understanding the settling behaviour of MBBR produced solids and detailed particle characteristics is essential to determine the performance of the secondary clarifiers. Therefore, this knowledge can help to improve the particle settleability and achieve better solids removal in settling clarifiers, which improves the overall performance of the wastewater treatment plants (Kinnear, 2002; Hasler, 2007). However, the particles that exist in wastewater are not homogenized and have different properties, thus different settling behaviour.

Suspended solids can settle in one of four remarkably different regimes (Figure 2-5): discrete non-flocculent particle settling (Class I), discrete flocculent settling (Class II), hindered settling or zone settling (Class III) and compressive settling (Class IV). These classifications of settling

behaviour are based on the concentration and flocculation tendency of the particles in the suspension (Clercq, 2006; Metcalf & Eddy, 2014; Torfs et al., 2016).

At low solids concentrations, there is a considerable distance between the flocs with no significant interaction with other particles. The flocs can settle independently without any impact on each other's settling behaviour, and at their own settling velocity based on the individual particle properties. For example, some spherical-shaped particles may settle readily, while the filaments may exhibit worse settling behaviour. Class I settling, or discrete non-flocculent settling, happens in a dilute suspension, where there is no tendency for aggregation in particles.

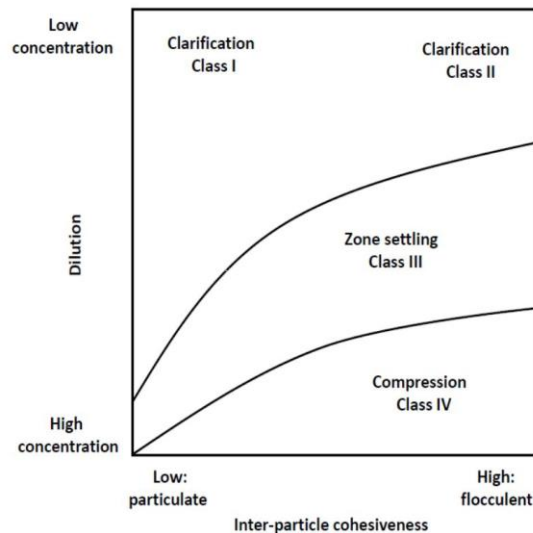


**Figure 2-5:** Settling regimes (Ekama et al., 1997)

However, if the particles tend to flocculate at low solids concentration, larger flocs are formed due to the aggregation process and can settle at increased rates (Class II, discrete flocculent settling). Once the solids concentration in the tank increases to the intermediate level (above 500 mg/l), the particles no longer settle independently because they would be hindered by the inter-particle forces of neighbouring particles and dragged along other particles (Mancell-Egala et al., 2016; Droste and Gehr, 2018). Therefore, the particles settle as one mass with the same velocity

regardless of the size or density of the individual solids, known as the hindered settling regime (Class III). Above the critical solids concentration (5-10 g/L), the physical contact and interaction between flocs become so large that it may affect the floc geometry. Therefore, the settling behaviour changes to compressive settling (Class IV), where the particles are compacted due to the weight of overlying particles. The settling velocity in the compressive settling regime is much lower than in the hindered settling regime (Vesilind, 2003; Metcalf & Eddy, 2014; Torfs et al., 2016).

All the four settling regimes mentioned above could occur in a secondary clarifier, simultaneously. Discrete flocculent and non-flocculent settling could occur in the top and upper-middle regions. The dominant settling behaviour at the lower middle region of the tank would be hindered settling, and the dominant settling behaviour in the bottom region would be the compressive settling behaviour (Clercq, 2006). However, the MBBR effluent solids concentration is approximately ten to twenty times lower than that for the activated sludge systems (Ødegaard, 2006; Ødegaard et al., 2010; Ivanovic and Leiknes, 2012; Metcalf & Eddy, 2014). Therefore, the relatively low solids concentrations in MBBR systems do not allow an efficient bio-flocculation as in activated sludge secondary settlers, where hindered settling occurs. It hence leads to a significantly different settling potential of MBBR produced solids, which is yet to be studied (Melin et al., 2005; Karizmeh et al., 2014).

### **2.5.1 Particle settling velocity**

The settling velocities of the particles must be known to design an efficient settling clarifier. Particle settling velocity can be evaluated either by i) theoretical law or ii) direct measurement of the velocity in quiescent or dynamic devices (Chebbo and Gromaire, 2009). The first one is based

on the measurement of the particle settling distributions (PSD). A theoretical law can be used to calculate the settling velocity from the PSD and the corresponding density distribution. Usually, the classic laws of sedimentation by Newton and Stokes have been applied to analyze the settling velocity of discrete and non-flocculating particles (Class I). To simplify the calculation, they assumed single and spherical particles settling in a viscous and quiescent fluid without changing in size and shape. Therefore, the effective downward force ( $F_g$ ) is the difference between a particle's gravitational force and the buoyant force. This force is equal to the drag force ( $F_d$ ) (Equation 2-4) as the particles ultimately settle with a constant settling velocity (Figure 2-6) (Metcalf & Eddy, 2014; Droste and Gehr, 2018).

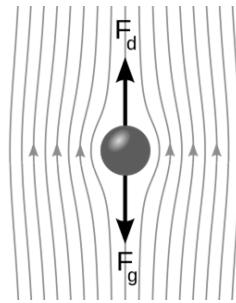


**Figure 2-6:** The forces acting on a particle

$$F_g = F_d \quad \rightarrow \quad (\rho_p - \rho_w)gV_p = \frac{1}{2}\rho_w C_d A_p (v_p)^2 \quad \text{Equation 2-4}$$

$$\text{Therefore,} \quad v_p = \sqrt{\frac{2gV_p (\rho_p - \rho_w)}{C_d A_p \rho_w}} \quad \text{Equation 2-5}$$

Where  $\rho_p$  is the density of particle ( $\text{kg/m}^3$ ),  $\rho_w$  is the water density ( $\text{kg/m}^3$ ),  $g$  is the acceleration due to gravity, which is equal to  $9.81 \text{ m/s}^2$ ,  $V_p$  is the volume of the particle ( $\text{m}^3$ ),  $C_d$  is the drag coefficient,  $A_p$  is the cross-sectional area of the particle and  $v_p$  is the settling velocity of the particle ( $\text{m/s}$ ).

The drag coefficient ( $C_d$ ) is not constant but varies with Reynold's number ( $Re$ ) and the shape of the particles (Figure 2-7). In the laminar range,  $C_d$  is equal to  $24/Re$  regardless of the particle's shape (Droste and Gehr, 2018).

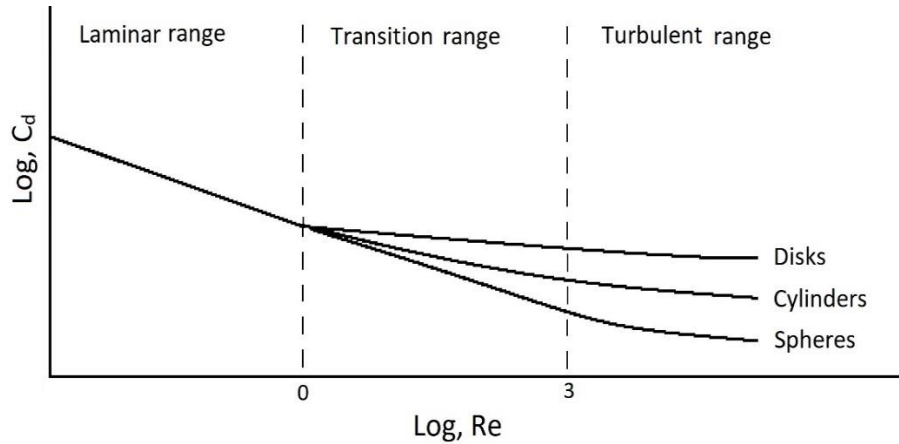


**Figure 2-7:** Variation of  $C_d$  with particle geometry (Droste and Gehr, 2018)

The settling velocity will be calculated as Stoke's law (Equation 2-6) by solving Equation 2-4 for  $v_p$ , logging the volume ( $V_p$ ) and area ( $A_p$ ) of the spherical particle with the diameter of  $d_p$ , and considering a quiescent and laminar fluid regime (Reynold's number  $< 1$ ).

$$v_p = \frac{gd_p^2}{18\mu} \left( \frac{\rho_p - \rho_w}{\rho_w} \right) \quad \text{Equation 2-6}$$

Where  $\mu$  is the dynamic viscosity of water ( $N.s/m^2$ ).

However, suspended particles, especially the biologically produced particles in the real wastewater, are heterogeneous and not always entirely dispersed. They might exhibit a natural tendency to agglomerate, or the addition of chemical coagulants promotes this tendency (Class II). Therefore, the average settling velocity for the particle continuously changes over time, as other particles attach to it. At higher solids concentration, the forces between the particles become significant as the settling can be hindered by other particles (Class III and IV). In these cases, there

are no theoretical means to predict the amount of flocculation and settling velocity distribution in the suspension (Metcalf & Eddy, 2014; Droste and Gehr, 2018). Therefore, a direct measurement of the particle settling velocity distribution (PSVD) is required.

Available literature shows that several protocols have been developed since the early 1990s by several research teams to measure the PSVD of wastewater samples in a quiescent condition (Aiguier et al., 1996; Lucas-Aiguier et al., 1998; Maus et al., 2008; Chebbo and Gromaire, 2009). All the protocols have quite different measurement principles with different utilized apparatus characteristics (Table 2-2). Each protocol has its own benefits and drawbacks in terms of sample preparation, time and energy requirements, accuracy, and repeatability of the result (Aiguier et al., 1996; Lucas-Aiguier et al., 1998; Hasler, 2007). Therefore, the best method should be chosen according to the research objectives by considering the range of measurable settling velocity, the sample volume required, the necessity of sample pretreatment, and the complexity of the test. Some methods require large samples that make it hard to carry out the test and handle the samples, and some others are time-consuming. Among all the protocols, the newest protocol called ViCAs (a French acronym for settling velocity in wastewater) has been developed in the CERREVE research laboratory by Chebbo and Gromaire (2009) to measure the suspended solids settling velocity through a compact, inexpensive and easy-to-operate settling column. In this study, the ViCAs method was applied to directly measure the PSVD of MBBR effluent for the first time.

**Table 2-2:** The comparison of various methods used to measure the settling velocity distribution (Aiguier et al., 1996; Tyack and Hedges, 1996; Lucas-Aiguier et al., 1998; Hasler, 2007; Berrouard, 2010)

Method	Apparatus	Settling depth (m)	Diameter (cm)	Sample volume (L)	Range of Vs (m/h)	Description
<b>Dutch method</b>	5 settling columns	0.4 (each column)	8	10 (total) 2 (each column)	0.01–2.67	There is not enough detail on the procedure.
<b>UFT<sup>a</sup></b> (German method)	Vertical Perspex cylinder on the top of a cone	0.7	5	1	0.36–630	The solids are settled for 2 hours in an Imhoff cone before placing it into the cylinder. The distribution curve is not representative of the total solids settling velocity as the method takes only settleable solids into account.
<b>Cergrene method</b>	IFTS <sup>b</sup> settling column for particles > 50 µm	1.8	5	20	0.71–288	
	Andreasen pipette for particles < 50 µm	0.2	10		0.05–14.76	
<b>ASTON</b> (British method)	One settling column	1.5	5	5	0.65–97.2	It is difficult to transport due to the large size.
<b>Camp</b> (American method)	One settling column	five levels of settling: 0.6, 0.9, 1.2, 1.5, 1.8	15	45-50	0.072–108	There are several portholes (1 cm diameter) over the height of the column (2.6m) for sampling.
<b>VICTOR<sup>c</sup> method</b>	7-10 settling column	0.5 (each column)	5	15-25 (total) 2.1 (each column)	0.022–9	
<b>VICPOL method</b>	5 settling columns	0.5	9	25	0.072–108	It is a modification of the Dutch method.
<b>VICAS protocol</b>	One settling column	0.64	7	4.5	0.036–35.64	

<sup>a</sup> Umwelt and Fluid Technik

<sup>b</sup> Institut de Filtration et des Techniques Separatives

<sup>c</sup> Vitesse de Chute des pOlluants des Rejets urbains

## 2.6 References

- Åhl, R. M., Leiknes, T., and Ødegaard, H. (2006). “Tracking particle size distributions in a moving bed biofilm membrane reactor for treatment of municipal wastewater.” *Water Science and Technology*, 53(7), 33–42.
- Ahmed, W., Tian, X., and Delatolla, R. (2019). “Nitrifying moving bed biofilm reactor: Performance at low temperatures and response to cold-shock.” *Chemosphere*, 229, 295–302.
- Aiguier, E., Chebbo, G., Bertrand-Krajewski, J.-L., Hedges, P., and Tyack, N. (1996). “Methods for determining the settling velocity profiles of solids in storm sewage.” *Water Science and Technology*, 33(9), 117–125.
- Almomani, F. A., and Khraisheh, M. A. M. (2016). “Treatment of septic tank effluent using moving-bed biological reactor: kinetic and biofilm morphology.” *International Journal of Environmental Science and Technology*, 13(8), 1917–1932.
- Ashrafi, E., Allahyari, E., Torresi, E., and Andersen, H. R. (2019). “Effect of slow biodegradable substrate addition on biofilm structure and reactor performance in two MBBRs filled with different support media.” *Environmental Technology*, 1–10.
- Aygun, A., Nas, B., and Bertay, A. (2008). “Influence of high organic loading rates on COD removal and sludge production in moving bed biofilm reactor.” *Environmental Engineering Science*, 25(9), 1311–1316.
- Barwal, A., and Chaudhary, R. (2014). “To study the performance of biocarriers in moving bed biofilm reactor (MBBR) technology and kinetics of biofilm for retrofitting the existing aerobic treatment systems: A review.” *Reviews in Environmental Science and Biotechnology*, 13(3), 285–299.
- Bassin, J. P., and Dezotti, M. (2018). “Moving Bed Biofilm Reactor (MBBR).” *Advanced Biological Processes for Wastewater Treatment*, Springer, Cham, 37–75.
- Bassin, J. P., Dias, I. N., Cao, S. M. S., Senra, E., Laranjeira, Y., and Dezotti, M. (2016). “Effect of increasing organic loading rates on the performance of moving-bed biofilm reactors filled with different support media: Assessing the activity of suspended and attached biomass

- fractions.” *Process Safety and Environmental Protection*, Institution of Chemical Engineers, 100, 131–141.
- Berrouard, E. (2010). “Caractérisation de la décantabilité des eaux pluviales.” M.Sc. thesis, Université Laval, QC, Canada.
- Brosseau, C., Émile, B., Labelle, M. A., Laflamme, É., Dold, P. L., and Comeau, Y. (2016). “Compact secondary treatment train combining a lab-scale moving bed biofilm reactor and enhanced flotation processes.” *Water Research*, 106, 571–582.
- Bryers, J. D. (1987). “Biologically active surfaces: processes governing the formation and persistence of biofilms.” *Biotechnology Progress*, 3(2), 57–68.
- Chaali, M., Naghdi, M., Brar, S. K., and Avalos-Ramirez, A. (2018). “A review on the advances in nitrifying biofilm reactors and their removal rates in wastewater treatment.” *Journal of Chemical Technology and Biotechnology*, 93(11), 3113–3124.
- Chebbo, G., and Gromaire, M.-C. (2009). “VICAS—An operating protocol to measure the distributions of suspended solid settling velocities within urban drainage samples.” *Journal of Environmental Engineering*, 135(9), 768–775.
- Chu, L., and Wang, J. (2011). “Comparison of polyurethane foam and biodegradable polymer as carriers in moving bed biofilm reactor for treating wastewater with a low C/N ratio.” *Chemosphere*, 83(1), 63–68.
- Clercq, J. De. (2006). “Batch and continuous settling of activated sludge : In-depth monitoring and 1-D compression modelling.” Ph.D. thesis, Gent University.
- Delatolla, R., Tufenkji, N., Comeau, Y., Gadbois, A., Lamarre, D., and Berk, D. (2010). “Investigation of laboratory-scale and pilot-scale attached growth ammonia removal kinetics at cold temperature and low influent carbon.” *Water Quality Research Journal of Canada*, 45(4), 427–436.
- Dias, J., Bellingham, M., Hassan, J., Barrett, M., Stephenson, T., and Soares, A. (2018a). “Impact of carrier media on oxygen transfer and wastewater hydrodynamics on a moving attached growth system.” *Chemical Engineering Journal*, Elsevier, 351, 399–408.

- Dias, J., Bellingham, M., Hassan, J., Barrett, M., Stephenson, T., and Soares, A. (2018b). "Influence of carrier media physical properties on start-up of moving attached growth systems." *Bioresource Technology*, Elsevier, 266, 463–471.
- Dias, R. A., Martins, R. C., Castro, L. M., and Quinta-Ferreira, R. M. (2018c). "Biosolids production and COD removal in activated sludge and moving bed biofilm reactors." *WASTES – Solutions, Treatments and Opportunities II*, Taylor & Francis Group, London, 271–276.
- Donlan, R. M. (2001). "Biofilm formation: A clinically relevant microbiological process." *Clinical Infectious Diseases*, 33(8), 1387–1392.
- Droste, R. L., and Gehr, R. L. (2018). *Theory and practice of water and wastewater treatment*. John Wiley & Sons.
- Dunne, W. M. (2002). "Bacterial adhesion : Seen any good biofilms lately?" *Clinical Microbiology Reviews*, 15(2), 155–166.
- Ekama, G. A., Barnard, J. L., Gunthert, F. W., Krebs, P., McCorquodale, J. A., Parker, D. S., and Wahlberg, E. J. (1997). "Secondary settling tanks: Theory." *Modelling, Design and Operation*, 12–39.
- Flemming, H.-C., and Wingender, J. (2010). "The biofilm matrix." *Nature Reviews Microbiology*, Nature Publishing Group, 8(9), 623–633.
- Forrest, D., Delatolla, R., and Kennedy, K. (2016). "Carrier effects on tertiary nitrifying moving bed biofilm reactor: An examination of performance, biofilm and biologically produced solids." *Environmental Technology*, 37(6), 662–671.
- Garrett, T. R., Bhakoo, M., and Zhang, Z. (2008). "Bacterial adhesion and biofilms on surfaces." *Progress in Natural Science*, 18(9), 1049–1056.
- Gazette, C. (2012). "Wastewater systems effluent regulations, Part II." 145(15), 1632–1812.
- Gazette, C. (2018). "Wastewater systems effluent regulations, Part II." 152(21), 3388–3401.
- Goode, C. (2010). "Understanding biosolids dynamics in a moving bed biofilm reactor." *Department of Chemical Engineering and Applied Chemistry*, University of Toronto.
- Guan, J., and Waite, T. D. (2006). "Impact of aggregate size and structure on biosolids

- settleability.” *Drying Technology*, 24(10), 1209–1215.
- Hasler, M. (2007). “Field and laboratory experiments on settling process in stormwater storage tanks.” Graz University of Technology, Austria.
- Hayder, G., Ahmed, A. N., and Fu’ad, N. F. S. M. (2017). “A review on media clogging in attached growth system.” *International Journal of Applied Engineering Research*, 12(19), 8034–8039.
- Hoang, V., Delatolla, R., Abujamel, T., Mottawea, W., Gadbois, A., Laflamme, E., and Stintzi, A. (2014). “Nitrifying moving bed biofilm reactor (MBBR) biofilm and biomass response to long term exposure to 1 °C.” *Water Research*, 49, 215–224.
- Ivanovic, I., and Leiknes, T. O. (2012). “Particle separation in moving bed biofilm reactor: Applications and opportunities.” *Separation Science and Technology*, 47(5), 647–653.
- Ivanovic, I., Leiknes, T., and Ødegaard, H. (2006). “Influence of loading rates on production and characteristics of retentate from a biofilm membrane bioreactor (BF-MBR).” *Desalination*, 199(1–3), 490–492.
- Jang, A., Bishop, P. L., Okabe, S., Lee, S. G., and Kim, I. S. (2003). “Effect of dissolved oxygen concentration on the biofilm and in situ analysis by fluorescence in situ hybridization (FISH) and microelectrodes.” *Water Science and Technology*, 47(1), 49–57.
- Javid, A. H., Hassani, A. H., Ghanbari, B., and Yaghmaeian, K. (2013). “Feasibility of utilizing moving bed biofilm reactor to upgrade and retrofit municipal wastewater treatment plants.” *International Journal of Environmental Research*, 7(4), 963–972.
- Karizmeh, M. S. (2012). “Investigation of biologically-produced solids in moving bed bioreactor (MBBR) treatment systems.” M.Sc. thesis, University of Ottawa, Canada.
- Karizmeh, M. S., Delatolla, R., and Narbaitz, R. M. (2014). “Investigation of settleability of biologically produced solids and biofilm morphology in moving bed bioreactors (MBBRs).” *Bioprocess and Biosystems Engineering*, 37(9), 1839–1848.
- Kinnear, D. J. (2002). “Biological solids sedimentation: a model incorporating fundamental settling and compression properties.” Ph.D. thesis, University of Utah, US.
- Levstek, M., and Plazl, I. (2009). “Influence of carrier type on nitrification in the moving-bed

- biofilm process.” *Water Science and Technology*, 59(5), 875–882.
- Leyva-Díaz, J. C., Martín-Pascual, J., and Poyatos, J. M. (2017). “Moving bed biofilm reactor to treat wastewater.” *International Journal of Environmental Science and Technology*, 14(4), 881–910.
- Li, C., Felz, S., Wagner, M., Lackner, S., and Horn, H. (2016a). “Investigating biofilm structure developing on carriers from lab-scale moving bed biofilm reactors based on light microscopy and optical coherence tomography.” *Bioresource Technology*, 200, 128–136.
- Li, C., Wagner, M., Lackner, S., and Horn, H. (2016b). “Assessing the influence of biofilm surface roughness on mass transfer by combining optical coherence tomography and two-dimensional modeling.” *Biotechnology and Bioengineering*, 113(5), 989–1000.
- Liu, J., Zhou, J., Xu, N., He, A., Xin, F., Ma, J., Fang, Y., Zhang, W., Liu, S., Jiang, M., and Dong, W. (2019). “Performance evaluation of a lab-scale moving bed biofilm reactor (MBBR) using polyethylene as support material in the treatment of wastewater contaminated with terephthalic acid.” *Chemosphere*, 227, 117–123.
- Lopez-Lopez, C., Martín-Pascual, J., González-Martínez, A., Calderón, K., González-López, J., Hontoria, E., and Poyatos, J. M. (2012). “Influence of filling ratio and carrier type on organic matter removal in a moving bed biofilm reactor with pretreatment of electrocoagulation in wastewater treatment.” *Journal of Environmental Science and Health - Part A Toxic/Hazardous Substances and Environmental Engineering*, 47(12), 1759–1767.
- Loupasaki, E., and Diamadopoulos, E. (2013). “Attached growth systems for wastewater treatment in small and rural communities: A review.” *Journal of Chemical Technology and Biotechnology*, 88(2), 190–204.
- Lucas-Aiguier, E., Chebbo, G., Bertrand-Krajewski, J. L., Gagné, B., and Hedges, P. (1998). “Analysis of the methods for determining the settling characteristics of sewage and stormwater solids.” *Water Science and Technology*, 37(1), 53–60.
- Mancell-Egala, W. A. S. K., Kinnear, D. J., Jones, K. L., De Clippeleir, H., Takács, I., and Murthy, S. N. (2016). “Limit of stokesian settling concentration characterizes sludge settling velocity.” *Water Research*, 90, 100–110.

- Mannacharaju, M., Natarajan, P., Villalan, A. K., Jothieswari, M., Somasundaram, S., and Ganesan, S. (2018). “An innovative approach to minimize excess sludge production in sewage treatment using integrated bioreactors.” *Journal of Environmental Sciences*, Elsevier B.V., 67, 67–77.
- Martínez-Huerta, G., Prendes-Gero, B., Ortega-Fernández, F., and Mesa-Fernández, J. M. (2009). “Design of a carrier for wastewater treatment using moving bed bioreactor.” *Proceedings of the 2nd International Conference on Environmental and Geological Science and Engineering*, 44–49.
- Maus, C., Holtrup, F., and Uhl, M. (2008). “Measurement method for in situ particle settling velocity.” 1–10.
- McQuarrie, J. P., and Boltz, J. P. (2011). “Moving bed biofilm reactor technology: Process applications, design, and performance.” *Water Environment Research*, 83(6), 560–575.
- Melin, E., Leiknes, T., Helness, H., Rasmussen, V., and Ødegaard, H. (2005). “Effect of organic loading rate on a wastewater treatment process combining moving bed biofilm and membrane reactors.” *Water Science and Technology*, 51(6–7), 421–430.
- Metcalf & Eddy. (2014). *Wastewater Engineering: Treatment and Resource Recovery*. McGraw-Hill, New York.
- Morgan-Sagastume, F. (2018). “Biofilm development, activity and the modification of carrier material surface properties in moving-bed biofilm reactors (MBBRs) for wastewater treatment.” *Critical Reviews in Environmental Science and Technology*, 48(5), 439–470.
- Ødegaard, H. (1999). “The moving bed biofilm reactor.” *Water Environmental Engineering and Reuse of Water*, 250–305.
- Ødegaard, H. (2000). “Advanced compact wastewater treatment based on coagulation and moving bed biofilm processes.” *Water Science and Technology*, 42(12), 33–48.
- Ødegaard, H. (2006). “Innovations in wastewater treatment: The moving bed biofilm process.” *Water Science and Technology*, 53(9), 17–33.
- Ødegaard, H., Cimbritz, M., Christensson, M., and Dahl, C. P. (2010). “Separation of biomass

- from moving bed biofilm reactors (MBBRs).” *Proceedings of the Water Environment Federation*, 2010(7), 212–233.
- Ødegaard, H., Gisvold, B., Helness, H., Sjøvold, F., and Zuliang, L. (2000a). “High rate biological/chemical treatment based on the moving bed biofilm process combined with coagulation.” *Chemical Water and Wastewater Treatment VI*, 245–255.
- Ødegaard, H., Gisvold, B., and Strickland, J. (2000b). “The influence of carrier size and shape in the moving bed biofilm process.” *Water Science and Technology*, 41(4–5), 383–391.
- Ødegaard, H., Rusten, B., and Westrum, T. (1994). “A new moving bed biofilm reactor: applications and results.” *Water Science and Technology*, 29(10–11), 157–165.
- Ødegaard, H. (2004). “Sludge minimization technologies - An overview.” *Water Science and Technology*, 49(10), 31–40.
- Patry, B., Boutet, É., Baillargeon, S., and Lessard, P. (2018). “Solid-liquid separation of an effluent produced by a fixed media biofilm reactor.” *Water Science and Technology*, 77(3), 589–596.
- Piculell, M. (2016). “New dimensions of moving bed biofilm carriers influence of biofilm thickness and control possibilities.” Ph.D. thesis, Lund University, Sweden.
- Piculell, M., Welander, P., Jönsson, K., and Welander, T. (2016). “Evaluating the effect of biofilm thickness on nitrification in moving bed biofilm reactors.” *Environmental Technology*, 37(6), 732–743.
- Piculell, M., Welander, T., and Jönsson, K. (2014). “Organic removal activity in biofilm and suspended biomass fractions of MBBR systems.” *Water Science and Technology*, 69(1), 55–61.
- Ramli, N. A., and Abdul Hamid, M. F. (2017). “A review on two different systems in municipal sewage treatment plant.” *2017 IEEE Conference on Energy Conversion*, 207–211.
- Rittmann, B. E. (2007). “Where are we with biofilms now? Where are we going?” *Water Science and Technology*, 55(8–9), 1–7.
- Rittmann, B. E., and McCarty, P. L. (2001). *Environmental Biotechnology: Principles and Applications*. McGraw-Hill, New York.

- Rusten, B., McCoy, M., Proctor, R., and Siljudalen, J. G. (1998). "The innovative moving bed biofilm reactor/solids contact reaeration process for secondary treatment of municipal wastewater." *Water Environment Research*, 70(5), 1083–1089.
- Shahot, K., Idris, A., Omar, R., and Yusoff, H. M. (2014). "Review on biofilm processes for wastewater treatment." *Life Science Journal*, 11(11), 11.
- Sonwani, R. K., Swain, G., Giri, B. S., Singh, R. S., and Rai, B. N. (2019). "A novel comparative study of modified carriers in moving bed biofilm reactor for the treatment of wastewater: Process optimization and kinetic study." *Bioresource Technology*, 281, 335–342.
- Tian, X., and Delatolla, R. (2019). "Meso and micro-scale effects of loading and air scouring on nitrifying bio-cord biofilm." *Environmental Science Water Research & Technology*, 5, 1183–1190.
- Torfs, E., Nopens, I., Winkler, M., Vanrolleghem, P., Balemans, S., and Smets, I. (2016). "Settling Tests." *Experimental Methods In Wastewater Treatment*, IWA Publishing, London, UK, 235–262.
- Torresi, E., Fowler, S. J., Polesel, F., Bester, K., Andersen, H. R., Smets, B. F., Plósz, B. G., and Christensson, M. (2016). "Biofilm thickness influences biodiversity in nitrifying MBBRs - Implications on micropollutant removal." *Environmental Science and Technology*, 50(17), 9279–9288.
- Tyack, J. N., and Hedges, P. (1996). "The relationship between settling velocity grading and the characteristics of the contributing catchment." *Water Science and Technology*, 33.
- Vesilind, P. (2003). *Wastewater treatment plant design*. IWA publishing.
- Wang, J. (2012). "Fundamentals of biological processes for wastewater treatment." *Biological Sludge Minimization and Biomaterials/Bioenergy Recovery Technologies*, John Wiley & Sons, Inc., Hoboken, NJ, USA, 1–80.
- Wang, R. C., Wen, X. H., and Qian, Y. (2005). "Influence of carrier concentration on the performance and microbial characteristics of a suspended carrier biofilm reactor." *Process Biochemistry*, 40(9), 2992–3001.

- Watnick, P., and Kolter, R. (2000). "Biofilm, city of microbes." *Journal of Bacteriology*, 182(10), 2675–2679.
- WEF. (2009). *Design of Municipal Wastewater Treatment Plants: WEF Manual of Practice No. 8*. McGraw-Hill, New York.
- WEF. (2011). *Moving Bed Biofilm Reactors: WEF Manual of Practice No. 35*. McGraw-Hill, New York.
- Wuertz, S., Bishop, P. L., and Wilderer, P. A. (2003). *Biofilms in Wastewater Treatment: An Interdisciplinary Approach*. IWA publishing.
- Young, B. (2017). "Nitrifying MBBR performance optimization in temperate climates through understanding biofilm morphology and microbiome." Ph.D. thesis, University of Ottawa, ON, Canada.
- Young, B., Delatolla, R., Ren, B., Kennedy, K., Laflamme, E., and Stintzi, A. (2016). "Pilot-scale tertiary MBBR nitrification at 1°C: Characterization of ammonia removal rate, solids settleability and biofilm characteristics." *Environmental Technology*, 37(16), 2124–2132.
- Zhang, L., Sun, K., and Hu, N. (2012). "Degradation of organic matter from domestic wastewater with loofah sponge biofilm reactor." *Water Science and Technology*, 65(1), 190–195.

# **Chapter 3 – The Impact of Biofilm Thickness-Restraint and Carrier Type on Attached Growth System Performance, Solids Characteristics and Settleability**

## **3.1 Context**

Chapter 3 presents the published research entitled “*The Impact of Biofilm Thickness-Restraint and Carrier Type on Attached Growth System Performance, Solids Characteristics and Settleability*” by R. Arabgol, P.A. Vanrolleghem, M. Piculell, and R. Delatolla (Environmental Science: Water Research & Technology, 2020, 6(10), 2843-2855). The influence of carrier types and limiting the biofilm thickness are investigated on carbonaceous and nitrifying kinetics, in addition to biofilm thickness and solids characteristics.

## **3.2 Abstract**

The moving bed biofilm reactor (MBBR) technology is a proven standalone and add-on technology for carbon and nutrient removal from municipal wastewaters. The key challenge of the carbon removal MBBR technology is the production of poor settling biological solids and the need for intense solid separation methods. This study investigates the effect of carrier type and biofilm thickness-restraint on MBBR system performance, biofilm thickness, solids production, detachment rate, solids characteristics and settleability. Two new emerging "thickness-restraint" carriers, AnoxK™ Z-200 and Z-400 (allowing for 200 and 400 µm maximum biofilm thickness, respectively), are compared to the conventional AnoxK™ K5 carrier at BOD loading rates of 6 g-sBOD/m<sup>2</sup>·d. The obtained results indicate that carrier type has a significant effect on MBBR carbonaceous removal, biofilm thickness, detachment and solids production. The K5 carrier MBBR system demonstrated statistically significant higher carbonaceous removal rates of 3.8 ±

0.3 g-sBOD/m<sup>2</sup>·d, higher biofilm thickness ( $281.1 \pm 8.7 \mu\text{m}$ ), lower solids production ( $7.7 \pm 3.2 \text{ mg-TSS/L}$ ) and greater stability with respect to the detachment rate compared to the two Z-carriers. Particle size distribution analysis demonstrates a higher percentage of small particles in Z-carrier system effluent and hence significantly lower solids settling efficiency. Therefore, the K5 carrier produced solids with improved settling characteristics compared to Z-carriers. No significant difference was observed in removal efficiency, solids production, detachment rate, particle characteristics and settling behaviour when comparing the Z-200 to the Z-400, indicating that biofilm thickness-restraint carrier design was not a controlling factor in the settling potential of produced solids.

### **3.3 Introduction**

New regulations and more stringent wastewater discharge standards are increasingly enforced due to a raised awareness regarding the detrimental effects of wastewater discharge into surface water bodies (Di Trapani et al., 2010; Dias et al., 2018b). Therefore, wastewater treatment facilities are being required to improve their treatment and reduce the concentration of organic matter, nutrients and solids prior to discharge (Gazette, 2012). In order to improve the quality of treated wastewater, the use of advanced, cost-effective and efficient technologies is required to upgrade or replace ageing, existing wastewater treatment infrastructure (Delatolla and Babarutsi, 2005; Di Trapani et al., 2010; Delatolla et al., 2010; Young et al., 2016b, 2017; Mannacharaju et al., 2018). In this regard, the carbon removal moving bed biofilm reactor (MBBR) technology is a proven, compact, standalone biological treatment unit and a means to upgrade passive and conventional wastewater treatment systems (Delatolla et al., 2010; Karizmeh et al., 2014; Ødegaard, 2016; Young et al., 2016b). The MBBR system is an attached growth biological treatment process that was developed approximately 25 years ago by Kaldnes Miljøteknologi, as

a robust reactor with no need for sludge recirculation and backwashing (Ødegaard et al., 1994; Bassin and Dezotti, 2018). High load tolerance, elevated biomass maintained in a small footprint, high treatment efficiency, cost and energy effectiveness, low vulnerability to cold temperature, low operational intensity and low sludge production are additional advantageous characteristics of this technology (Ødegaard, 2004; Åhl et al., 2006; WEF, 2011; Loupasaki and Diamadopoulos, 2013; Young et al., 2016b; Ramli and Abdul Hamid, 2017; Mannacharaju et al., 2018; Dias et al., 2018b; Tian and Delatolla, 2019). With these advantageous characteristics, it should be noted that relatively poor settleability of biologically produced solids in carbon removal MBBR effluent is a potential drawback and remains a concern of the MBBR technology compared to conventional suspended growth systems (Ødegaard et al., 2010; Ivanovic and Leiknes, 2012; Karizmeh et al., 2014; Bassin and Dezotti, 2018). Several studies have highlighted the necessity of using intense solids separation methods (such as filtration, lamella settling, or using enhanced sedimentation with pre-coagulation) due to the poor settling characteristics of the biomass leaving MBBR systems (Ødegaard et al., 2010; Ivanovic and Leiknes, 2012).

The MBBR technology relies on freely moving plastic carriers with a high surface area that provides a substratum for bacterial growth and maintenance. The carriers are exposed to other carriers, interaction with aeration, and the surrounding liquid in the MBBR reactors. As the exposure to the shear forces in the reactor affects the biofilm thickness and quantity of attached biomass along with the potential characteristics of the dispersed and detached solids, the physical characteristics of the carriers in the MBBR technology likely play a considerable role in solids production, characteristics and the settleability of these particles (Ødegaard et al., 1994, 2000b).

The effective carrier surface area is an important parameter in MBBR design. A higher effective surface area of a carrier will promote a higher biofilm surface area for the same quantity

of carriers and hence will augment the performance of a system with a specified reactor volume or will allow for the design of a smaller reactor volume at the same reactor performance. Therefore, over the years, different types of carriers (of different material, shape, and size) have been developed and still are being modified to improve removal efficiency by providing a higher effective surface area (Bassin and Dezotti, 2018; Morgan-Sagastume, 2018). Several studies performed individually on various carriers have evaluated organic matter removal, ammonia removal and solids production of MBBR reactors to treat various types of wastewaters (Ødegaard, 2006; McQuarrie and Boltz, 2011; Shahot et al., 2014; Almomani and Khraisheh, 2016; Chaali et al., 2018). Previous studies demonstrated that the physical and geometrical properties of the carriers play an important role in wastewater hydrodynamics and oxygen transfer efficiency in the MBBR reactors (Dias et al., 2018a), which ultimately might contribute to reactor performance. Similar performance results have been observed in the investigation of various media for biofiltration (Delatolla et al., 2015). The previous studies on MBBR systems have mainly focused on how the removal efficiency and solids production change as a result of different surface area loading rate (SALR), hydraulic retention time (HRT), temperature and filling degrees of the carriers (Barwal and Chaudhary, 2014; Young et al., 2016b; Chaali et al., 2018; Patry et al., 2018). Research has demonstrated that MBBR carbon removal efficiency depends on the effective surface area that is available for biomass growth regardless of carrier type and shape (Ødegaard et al., 2000b; Levstek and Plazl, 2009; Barwal and Chaudhary, 2014; Bassin et al., 2016; Young et al., 2016a; Forrest et al., 2016). Particle characteristics and especially particle size distribution along with the settleability of the particles in MBBR effluent have shown a good correlation with HRT and SALR (Ødegaard et al., 2000, 2010; Melin et al., 2005; Åhl et al., 2006; Karizmeh et al., 2014). Enhanced settleability of MBBR effluent solids has been demonstrated at lower SALR and,

consequently, longer HRT due to larger particle sizes (Ødegaard et al., 2010; Karizmeh et al., 2014). Moreover, a significant difference has been demonstrated between the settleability and the characteristics of the solids for different types of carriers when high loading was applied, and the carrier was clogged (Forrest et al., 2016; Young et al., 2016b). Although previous studies have proven that the carrier material and substratum surface properties have a significant effect on biofilm formation rate, biofilm distribution pattern and biofilm thickness (Chu and Wang, 2011; Piculell et al., 2016b; Morgan-Sagastume, 2018; Ashrafi et al., 2019; Sonwani et al., 2019); there remains uncertainty regarding the impact of physical and geometrical characteristics of carriers on MBBR system performance, solids production and settling potential of suspended solids associated to different carrier types. Moreover, it is not well understood how the biofilm thickness affects system performance and solids characteristics regardless of the carrier type.

Furthermore, carriers have been shown to suffer clogging due to uncontrolled biofilm growth, with the effective surface area of the system becoming considerably decreased and the performance of the system being negatively impacted. Moreover, the uncontrolled growth of biofilm may lead to heavier carriers and hence systems that require more energy for mixing and more consumption of oxygen by the inactive and thick biofilm (Piculell et al., 2016a). Therefore, to avoid potential negative impacts of clogging on MBBR performance, researchers were encouraged to develop new types of carrier to control the biofilm thickness and decrease the difference between the exposed biofilm area (EBA) and the effective surface area used for the design (Piculell, 2016).

Recently, a new series of carriers (AnoxK™ Z-carriers) have been designed to control and maintain the thickness of the biofilm to a predetermined maximum thickness (Piculell et al., 2016b; Bassin and Dezotti, 2018; Morgan-Sagastume, 2018). Before the invention of the Z-carriers,

evaluating the direct effect of biofilm thickness on the MBBR system performance was not possible. Currently, there is limited research on nitrogen removal, carbonaceous removal and calcium scaling effects using the "thickness-restraint" carriers (Piculell, 2016; Piculell et al., 2016b). Controlling biofilm thickness may impact the detachment mechanism of biological mass from the carriers and hence impact the effluent solids and, ultimately, their settleability. Although some studies have indicated that different operational conditions (such as SALR, HRT, C/N ratio and temperature) can change the thickness of biofilm and the quantity of biomass in the reactor and hence the overall MBBR system performance (Barwal and Chaudhary, 2014; Young et al., 2016b; Chaali et al., 2018; Patry et al., 2018); there are no studies to date that demonstrate how controlling the biofilm thickness affects the MBBR system performance along with the solids production, detachment rate, particle characteristics and settleability, conversely.

Based on the literature, it is hypothesized that an enhanced understanding of the impact of various carrier types and the use of newly designed thickness-restraint carriers can be used to optimize the design of MBBR systems and their subsequent downstream solids separation units. Therefore, this study aims to improve the current understanding of the effects of carrier type and newly designed thickness-restraint carriers on the kinetic performance of MBBR systems, the effluent solids characteristics and subsequent downstream solids settleability. In particular, the objective of this study is to investigate the effects of different types of carriers, the conventional AnoxK™ K5 carrier compared to the newly designed "thickness-restraint" AnoxK™ Z-carriers, as well as the effect of biofilm thickness-restraint on carbonaceous removal rates (soluble biological oxygen demand (sBOD) and soluble chemical oxygen demand (sCOD)), total ammonia nitrogen (TAN) removal rates, effluent solids, effluent particle size distribution and characteristics, and effluent solids settleability.

## 3.4 Materials and methods

### 3.4.1 Experimental setup

This study was conducted at the Gatineau municipal secondary treatment water resource recovery facility (WRRF), Quebec, Canada. Three identical laboratory-scale MBBR reactors with volumes of 4 L were operated in parallel. A reservoir feed tank was used to collect the primary clarified wastewater and distribute it to the reactors to ensure constant flow rates of  $3.7 \pm 0.1$  L/h in the reactors (Figure 3-1).

The reactors housed three different types of carriers; the conventional AnoxK™ K5 carrier and two types (AnoxK™ Z-200 and AnoxK™ Z-400) of newly designed "thickness-restraint" Z-carriers (AnoxKaldnes, Lund, Sweden). It should be noted that in order to maintain similar carrier surface areas and loading rates in the three reactors within conventional ranges, different numbers of carriers were housed in each of the reactors (Table 3-1). In addition, it is noted that the carrier fill percentage of all reactors in this study was maintained below maximum fill percent capacities.

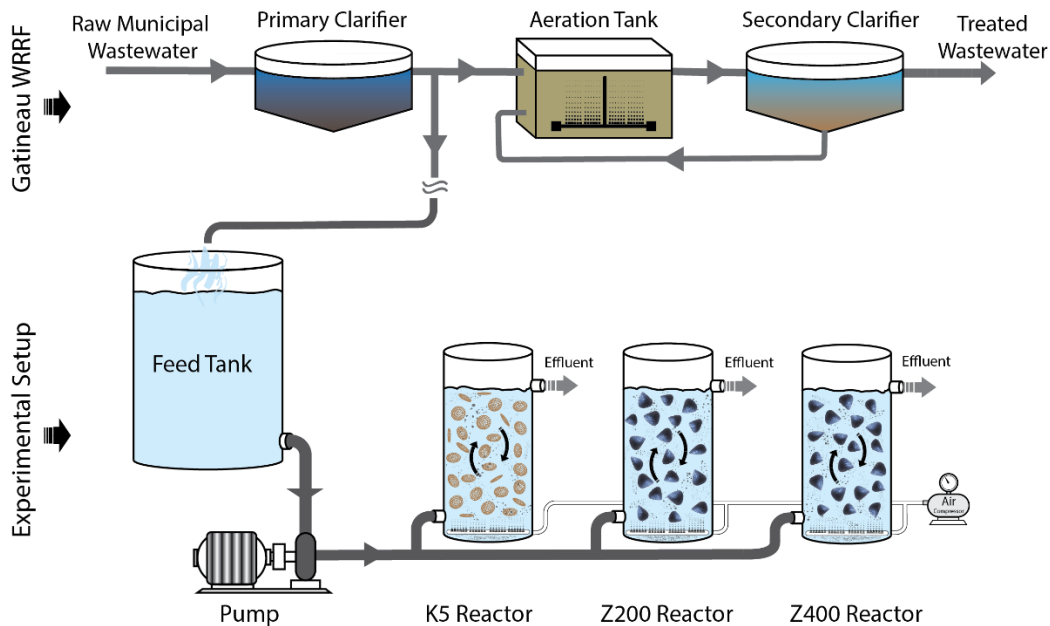


**Figure 3-1:** Experimental setup

**Table 3-1:** Reactor properties at SALR of  $6 \pm 0.8$  g-sBOD/m<sup>2</sup>·d

	Reactor volume (L)	No. of carriers	Carrier surface area (mm <sup>2</sup> /carrier)*	Reactor surface area (m <sup>2</sup> /reactor)	Carrier image
<b>K5</b>	4	160	2420	0.38	
<b>Z-200</b>	4	300	1280	0.38	
<b>Z-400</b>	4	300	1280	0.38	

\* Protected surface area (PSA) for K5, and exposed biofilm area (EBA) for Z carriers (Piculell, 2016)

### 3.4.2 Carrier characteristics

Two different types of carriers, conventional K5 carrier and newly designed Z-carriers, were used in this study. The conventional K5 carrier is a porous cylindrical carrier (Table 3-1), which is a commonly used carrier in full-scale carbonaceous and nitrogen removal applications (Barwal and Chaudhary, 2014). The saddle-shaped Z-carriers, on the other hand, is a newly designed carrier to control biofilm thickness, and as such, they are significantly different in shape compared to the conventional K5 carrier (Table 3-1). Z-carriers are covered with a grid of specific height, allowing the biofilm to grow on the outside of the carrier in a protected compartment rather than biofilm growing inside the protected inner voids of K5 carriers (Piculell, 2016). Therefore, Z-carriers limit the maximum thickness of the biofilm growth on the carrier to the height of the pre-defined carrier's grid wall. The excess biomass could scrape off due to abrasion caused by the collision between carriers in the reactor and also due to erosion caused by hydraulic shear forces acting on the biofilm attached to the carriers (Piculell, 2016; Bassin and Dezotti, 2018). The Z-200 and Z-400 carriers are identical in shape and provide a similar exposed biofilm area (EBA) of 1280 mm<sup>2</sup> per carrier and a projected diameter of 30 mm (with the two types of Z-carriers having different grid wall heights). While the cylindrical K5 carrier has a diameter of 25 mm and a height of 3.5 mm and provides a surface area of 2420 mm<sup>2</sup> per carrier (Table 3-1) (Piculell, 2016; Bassin and

Dezotti, 2018). In this study, the Z-200 and Z-400 carriers, with grid wall heights of 200 and 400  $\mu\text{m}$ , respectively, were used to study the effects of the thickness-restraint on system performance. In particular, the biofilm thickness on the Z-200 carrier is restrained to a predefined thickness of 200  $\mu\text{m}$  compared to the Z-400 carrier that is allowed to increase in thickness up to 400  $\mu\text{m}$ .

### 3.4.3 Wastewater characteristics

Primary clarified municipal wastewater from the city of Gatineau WRRF (Table 3-2) was used as the influent for all of the MBBR reactors operated in this study. The primary clarifiers of the WRRF were conventional sedimentary basins and were operated without chemical addition.

**Table 3-2:** Characteristics of raw wastewater entering the Gatineau WRRF and the clarified feed wastewater entering the on-site MBBR reactors

Constituent	Raw Influent Wastewater*	Clarified Wastewater entering MBBRs**
	Average $\pm$ 95 % CI	Average $\pm$ 95 % CI
TSS (mg/L)	212.7 $\pm$ 12.2	49.3 $\pm$ 4.2
VSS (mg/L)	207.5 $\pm$ 12.2	38.1 $\pm$ 2.4
COD (mg/L)	233.6 $\pm$ 10.2	118.8 $\pm$ 6.8
BOD (mg/L)	100.5 $\pm$ 5.1	53.6 $\pm$ 4.4
sCOD (mg/L)	NA	58.7 $\pm$ 4.5
sBOD (mg/L)	NA	23.0 $\pm$ 2.4
TAN(NH <sub>3</sub> /NH <sub>4</sub> <sup>+</sup> -N mg/L)	15.6 $\pm$ 0.5	16.0 $\pm$ 0.9
Nitrite (NO <sub>2</sub> <sup>-</sup> -N mg/L)	0.0 $\pm$ 0.0	0.0 $\pm$ 0.0
Nitrate (NO <sub>3</sub> <sup>-</sup> -N mg/L)	1.0 $\pm$ 0.2	2.7 $\pm$ 0.1
VSS/TSS ratio (%)	97.5 $\pm$ 0.7	79.3 $\pm$ 2.7
COD/BOD	2.5 $\pm$ 0.1	2.3 $\pm$ 0.1
sCOD/sBOD	NA	2.7 $\pm$ 0.2
Temperature ( $^{\circ}\text{C}$ )	15.0 $\pm$ 1.0	15.0 $\pm$ 1.0
DO (mg/L)	NA	2.1 $\pm$ 0.6
pH	7.3 $\pm$ 0.0	7.7 $\pm$ 0.1

\* Average and 95% confidence interval (95% CI) across the study (n  $\approx$  365)

\*\* Average and 95% confidence across the study (n  $\approx$  50)

NA: not available

Although coagulant is not added during primary clarification, the raw municipal wastewater (Table 3-2) entering the Gatineau WRRF includes reject water from three water treatment plants servicing the community. Therefore, the residual alum in the reject water is a portion of the WRRF raw wastewater and, as such, may affect solids removal in the primary clarifiers. The primary clarifiers demonstrated approximately 76% total suspended solids (TSS) removal throughout the experimental phase prior to entering the MBBR reactors. The influent characteristics of this study are in the range of typical strength raw wastewater for Canadian WRRFs.

#### **3.4.4 Biofilm inoculation and start-up**

All carriers were inoculated with non-diluted, return activated sludge (RAS) harvested from the Gatineau WRRF. The TSS and volatile suspended solids (VSS) concentrations of the RAS and hence within the reactors during inoculation were 9.2 g-TSS/L and 6.8 g-VSS/L. The reactors were operated in batch mode, housing virgin carriers, for one week with RAS wastewater. Following one week of operation with RAS as batch reactors, when biofilm growth was observed on the carriers, the reactors were continuously fed with primary clarified wastewater (Table 3-2) for a continued inoculation period of four additional weeks with increasing flow rates up to 3.7 L/h. Subsequently, the reactors were operated at the experimental conditions with a flow rate of 3.7 L/h and a loading rate of approximately 6.0 g-sBOD/m<sup>2</sup>·d for another three weeks (with three weeks equal to 504 times HRTs) to monitor the biofilm development, maturation and acclimatization on the carriers. The MBBR reactors were deemed to be fully inoculated once the systems demonstrated steady-state operation (after three weeks of operation at 3.7 L/h and 6.0 g-sBOD/m<sup>2</sup>·d). The steady-state operation was validated within all the MBBR reactors by ensuring a maximum of ±15% variance of carbonaceous removal rates, changes in biofilm thickness and changes in biofilm mass per carrier across time.

### 3.4.5 Reactor operation

During the experimental phase of the study, 15 months, the three reactors were fed from the same feed tank with identical flowrates of  $3.7 \pm 0.1$  L/h and an identical HRT of 1.1 h. Approximately  $14 \text{ m}^3/\text{d}$  ( $\approx 10$  litres per minute (LPM)) of air was supplied to each of the reactors by an air compressor and air diffusers located at the bottom of each reactor (Figure 3-1). The number of carriers in the three reactors was modified during the experimental phase; specifically, carriers were removed from the three reactors to provide a range of operational SALR values and responses to best evaluate the carbonaceous removal kinetics of the carriers. The range of carbonaceous SALR was 0.7 to  $9.3 \text{ g-sBOD}/\text{m}^2\cdot\text{d}$ , and the range of TAN SALR was 0.6 to  $5.2 \text{ g-TAN}/\text{m}^2\cdot\text{d}$ . All three reactors were operated at a set carbonaceous SALR of  $6.0 \pm 0.8 \text{ g-sBOD}/\text{m}^2\cdot\text{d}$  and TAN SALR of  $4.1 \pm 0.3 \text{ g-TAN}/\text{m}^2\cdot\text{d}$  to compare carbonaceous removal kinetics and solids characteristics at the same loading rates. At this operational condition, which corresponds to a conventional loading rate for MBBR systems (Ødegaard et al., 2010; WEF, 2011), the reactors were tested for biofilm thickness, solids production, detachment rates, particle characteristics and settleability to compare the three reactors at the same operational condition.

At a carbonaceous SALR of  $6.0 \pm 0.8 \text{ g-sBOD}/\text{m}^2\cdot\text{d}$  and TAN SALR of  $4.1 \pm 0.3 \text{ g-TAN}/\text{m}^2\cdot\text{d}$ , the reactors housed surface areas for biofilm attachment of  $0.38 \text{ m}^2$  per reactor; with 160 K5 carriers and 300 of Z-200 and Z-400 carriers being housed in the reactors (Table 3-1). All three reactors were operated in parallel with non-limiting dissolved oxygen (DO) conditions and sufficient aeration to ensure movement of the carriers in the reactors. The DO concentration ranged between 6 to 7 mg/L for the three reactors, which is above conventional values of 4 mg/L as slightly higher aeration rates were required to keep the carriers in motion within the laboratory-

scale sized reactors used in this study. Moreover, pH and temperature were maintained at  $7.8 \pm 0.1$  and  $18.0 \pm 1.0$  °C, respectively, throughout the experimental period.

### **3.4.6 Constituent analytical methods**

Influent and effluent grab samples were collected from the reactors and analyzed for the following parameters throughout the study: total BOD and sBOD, total COD and sCOD, TSS, VSS, TAN, nitrite, nitrate, DO, pH and temperature. The grab samples were taken two to three times a week during data collection periods and tested in triplicate within 4 hours of collection. The average of the triplicated measurements is reported in this study. The following methods were used to analyze total and soluble BOD, all nitrogen constituents and solids in accordance with standard methods: 5210B-5 day BOD, 4500-NH<sub>3</sub>, 4500-NO<sub>3</sub><sup>-</sup>, 4500-NO<sub>2</sub><sup>-</sup>, 2540 D-TSS (TSS dried at 103–105°C) and 2540 E-VSS (fixed and volatile solids ignited at 550°C). A HACH DR 5000 Spectrophotometer (HACH, Loveland, CO, USA) was used to determine total and soluble COD concentrations according to HACH methods 8000. DO, pH and temperature were measured using an HQ40d portable PH/DO meter (HACH, USA).

### **3.4.7 Solids analysis**

In addition to TSS and VSS concentration measurements, further calculations were performed to quantify the solids production and the solids detachment rate. As the HRT of the MBBR reactors is short (1.1 h) in this study, it can be assumed that the influent particles remain unchanged, and the effects of hydrolysis of the particles in the reactors is negligible. Therefore, the TSS production is calculated as the difference between the effluent TSS and the influent TSS. Moreover, the detachment rate is defined as the difference between the MBBR influent and effluent TSS, normalized per surface area of carriers in the reactor.

### 3.4.8 Biofilm thickness analysis

The biofilm thickness was measured by acquiring top view stereoscopy images of the void spaces of the K5 carriers and cross-sectional images of the cut compartments of the Z-carriers due to the different shape of the carriers. Images were obtained using a Zeiss Stemi 305 stereoscope (Toronto, Canada), and the acquired images were analyzed using the Fiji open-source software (<http://fiji.sc/Fiji>) (Schindelin et al., 2012). Three different randomly selected carriers were harvested from each reactor and imaged within 1 hour to minimize the potential effects of biofilm dehydration. The biofilm thickness was measured using fresh, wet biofilm but not biofilm submerged in liquid. The biofilm thickness reported in this study is the average height of the biofilm growth on the surface of the carriers. The average height of the biofilm was calculated by measuring the top view occupied area by biofilm over the length of the available surface for the biofilm. The occupied area of the biofilm is the integrated area between the substratum and the bulk-liquid interface (Figure 3-2). The biofilm thickness for at least one side of all 64 void spaces of K5 carriers were imaged and analyzed. On the other hand, to achieve a better vision of biofilm thickness on Z-carriers, the longest strip was cut to acquire cross-sectional images and analyzed for both sides of all the cut compartments, including compartments close to the edges as well as the compartments in the center of the carriers. The average of all measurements ( $n \approx 160$ ) was reported as the overall average of biofilm thickness per carrier with deviation based on a comparison between average thicknesses measured for the carriers.

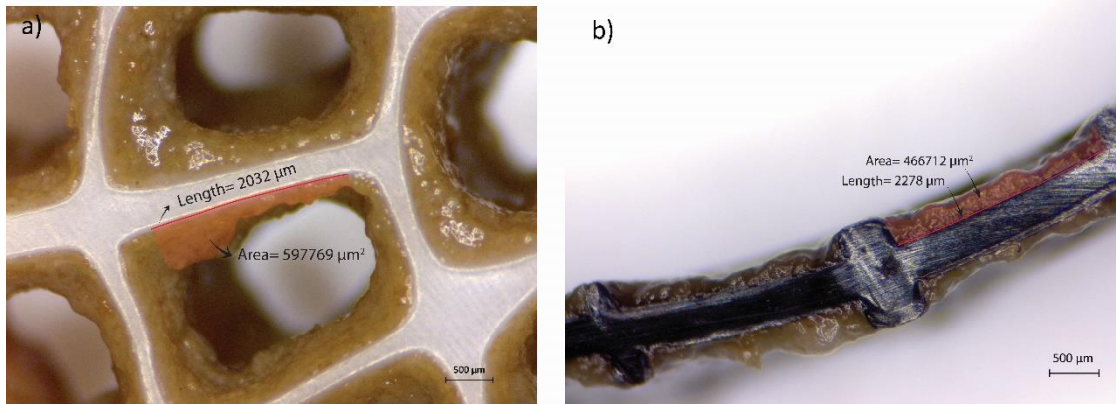


**Figure 3-2:** (a) top view occupied area of biofilm in one void of the K5 carriers, and (b) cross-sectional images of biofilm thickness in a compartment of Z-carries

### 3.4.9 Particle size distribution analysis of solids

Along with the chemical constituent testing, micro-flow imaging (MFI) technology was used to quantify the number of particles, particle size, concentration, area, and circularity coefficients of the particles in the MBBR reactors. In particular, a Brightwell Technologies Dynamic Particle Analyzer (DPA) equipped with a BP-4100-FC-400-Uflow cell (Brightwell Technologies, Canada, ON) was operated at low magnification to observe and quantify particles in the range of 2.25–400  $\mu\text{m}$  in diameter, according to Forrest et al. (2016) and Karizmeh et al. (2014). The acquired DPA images were analyzed to determine particle properties based on the two-dimensional projection of the particles by the analyzer. The volume of the particles was calculated using  $\pi(\text{ECD})^3 \times \text{circularity} / 6$ . ECD is defined as the equivalent circular diameter and is based on the assumption that all the particles are spheres. ECD is equal to the diameter of a circle with an equivalent area of the irregular-shaped particle, calculated as  $2 \times (\text{Area} / \pi)^{0.5}$ . Circularity is defined as the perimeter of the equivalent area circle divided by the perimeter of the actual particle. This dimensionless number varies between zero (for noncircular particles) and 1 (for circular particles) (Karizmeh et al., 2014; Forrest et al., 2016).

Finally, the DPA graphs are displayed in this study as the percent volume of particles across particle size. The integrated area under the particle distribution curves reveals the total volume percentage of unsettled particles in the sample. Therefore, the settleability is calculated as the percentage of total solids that are settled during a specific settling time. In this study, solids distribution samples were analyzed before and after 4 hours of settling to mimic the secondary clarifier retention time at the full-scale WRRF, where the reactors in this study were operated. Particle size distribution was analyzed to investigate the effects of carrier type and biofilm thickness-restraint on particle characteristics and settleability of particles. The particle distribution of effluent MBBR samples was measured in triplicate throughout the study during the steady-state operation of each system.

#### **3.4.10 Statistical analyses**

The student t-test was used to validate significant statistical differences between the measured constituents, the solids concentration, solids production and detachment rates, with a  $p$ -value less than 0.05 indicating significance in this study. Average and 95% confidence intervals (95% CI) shown as error bars are displayed in all figures.

### **3.5 Results and discussion**

#### **3.5.1 Reactor carbonaceous and ammonia removal performance**

Carbonaceous removal (sBOD and sCOD) along with TAN removal by the three MBBR reactors were quantified across numerous loading conditions, and a maintained HRT at 1.1 hours to determine the effects of carrier type and thickness-restraint on system performance (Figure 3-3). Due to the short HRT of the MBBR technology and the lack of a settling unit in this study, the carbonaceous material is tracked in the soluble phase. The concentration of carbonaceous substrate

in the influent wastewater was  $58.7 \pm 4.5$  mg-sCOD/L and  $23.0 \pm 2.4$  mg-sBOD/L with the sCOD to sBOD ratio of  $2.7 \pm 0.2$ . The carbonaceous removal rate (SARR) across the SALR demonstrated a strong linear correlation between the measured sBOD loading rate and the removal rate (Figure 3-3a) in all three reactors ( $0.79 < R^2 < 0.94$ ). As such, all three reactors demonstrate first-order sBOD kinetics and sBOD mass transfer rate-limited conditions, likely due to the low loading rate of the substrate (WEF, 2011). Similar conditions are also commonly observed in full-scale MBBR carbonaceous removal installations (WEF, 2011; Siciliano and De Rosa, 2016; Bassin et al., 2016). The substrate removal performance in attached growth wastewater systems, including the MBBR technology, is mediated by the mass transfer of the substrate (carbonaceous matter or nutrients) or the electron acceptor (DO) from the bulk liquid to the biofilm surface and subsequently through the biofilm itself to the embedded biomass. The linear relation in this study between the sBOD SARR and the sBOD SALR values are indicative that the sBOD SARR is limited by the mass transfer effects of the carbonaceous matter. The order of the sBOD kinetics of these attached growth MBBR systems has been shown to shift from sBOD mass transfer-dependent (first-order relation) to DO mass transfer-dependent (zero-order relation) at increased sBOD SALR values to the DO aeration rates (WEF, 2011; Qiqi et al., 2012; Barwal and Chaudhary, 2014).

Moreover, a linear correlation and first-order kinetics were also observed for the sCOD removal rate with respect to the loading rate (Figure 3-3b). Unlike the carbonaceous removal rate, a weak correlation is detected between the measured TAN loading rate and removal rate, likely due to the pathway of TAN removal being via assimilation by microorganisms (Figure 3-3c). The lack of nitrification in the system, as is evident by the not remarkable change in influent and effluent  $\text{NO}_x$  concentrations, is likely due to the heterotrophic community outcompeting the nitrifying autotrophic community. BOD to total Kjeldahl nitrogen (TKN) ratios larger than 1.0,

influent sBOD concentrations larger than 12 mg/L and organic loads above 5 g-sBOD/m<sup>2</sup>·d are known to limit the TAN removal in MBBR reactors via heterotrophs outcompeting the nitrifying autotrophs (Hem et al., 1994; WEF, 2009). The BOD to TAN ratio of this study was 1.4 ± 0.1, assuming that organic nitrogen concentrations do not contribute to nitrification, the influent sBOD was 23.0 ± 2.4 mg-sBOD/L, and the organic load studied for biofilm and solids responses was 6.0 ± 0.8 g-sBOD/m<sup>2</sup>·d; hence nitrification was limited in this study.

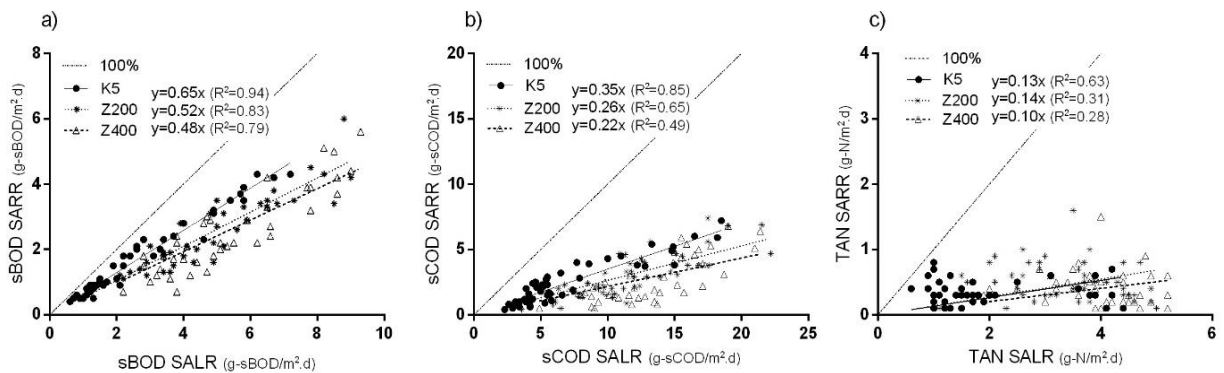


**Figure 3-3:** SARR versus SALR across a range of loading rates for various carriers with respect to (a) sBOD (b) sCOD, and (c) TAN removal

The results demonstrate that the carrier type (i.e., the physical properties of the carriers) has a statistically significant impact on the carbonaceous removal performance, as demonstrated by the sBOD and sCOD kinetics across different loading conditions (Figure 3-3a, b). Although the DO concentrations in this study were elevated compared to conventional values, the elevated DO concentration likely results in improved carbonaceous removal rates for the three carrier types due to the similar DO concentrations and mixing configuration of the three reactors. At a selected operational SALR of 6.0 ± 0.8 g-sBOD/m<sup>2</sup>·d, the measured sBOD and sCOD SARR values and removal efficiencies also demonstrate that carbonaceous removal performance is significantly affected by carrier type (Figure 3-4a, b). Cylindrically shaped K5 carriers with protected biofilm

show significantly better removal rates and removal efficiencies in terms of sBOD and sCOD ( $p < 0.05$ ) as compared to the saddle-shaped Z-carriers with exposed surface biofilm. Therefore, the K5 carrier with a SARR of  $3.8 \pm 0.3$  g-sBOD/m<sup>2</sup>·d (or  $5.0 \pm 0.7$  g-sCOD/m<sup>2</sup>·d) and  $59.9 \pm 3.0\%$  sBOD removal efficiency (or  $31.5 \pm 4.0\%$  sCOD removal efficiency) shows statistically significantly higher removal rates compared to the Z-carriers. 45 to 80% better sCOD SARR is observed for K5 as compared to Z-carriers, which implies a significant effect of carrier type on carbonaceous removal (Figure 3-4a, b). However, TAN removal rates and efficiencies are not significantly different across carrier types ( $p > 0.05$ ), likely due to the low TAN removal performance of the systems and the likely pathway of removal being cell assimilation. The changes in NO<sub>x</sub> concentration were not remarkable between influent and effluent of the reactors, and TAN:sCOD removal ratio varies between 7 and 14%, which is consistent with theoretical TAN:COD ratios of cell synthesis for aerobic heterotrophs (Metcalf & Eddy, 2014). This ratio of removal supports the hypothesis that nitrification was not occurring in the reactors, and the low TAN removal is likely due to nitrogen assimilation by heterotrophic microorganisms. The TAN removal rate was approximately  $0.4 \pm 0.1$  g-TAN/m<sup>2</sup>·d in all three reactors, and the removal efficiency was between  $9.1 \pm 2.6\%$  and  $11.1 \pm 3.0\%$  (Figure 3-4c).

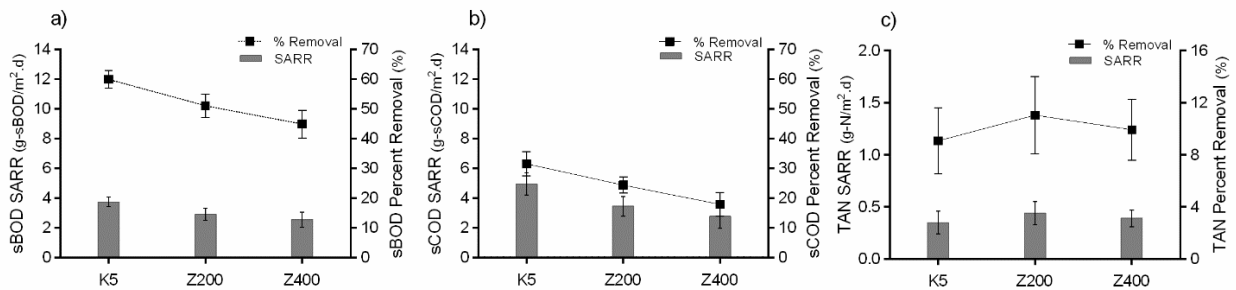


**Figure 3-4:** SARR and percent removal at SALR of  $6 \pm 0.8$  g-sBOD/m<sup>2</sup>·d for (a) sBOD (b) sCOD and (c) TAN removal

A comparison of the performance of the Z-200 carriers to the Z-400 carriers demonstrates that restraining the thickness of the Z-200 carriers compared to the Z-400 carriers did not affect the overall removal rates or efficiencies of the systems. An SARR of  $2.9 \pm 0.4$  g-sBOD/m<sup>2</sup>·d (or  $3.4 \pm 0.7$  g-sCOD/m<sup>2</sup>·d) and  $2.6 \pm 0.5$  g-sBOD/m<sup>2</sup>·d (or  $2.8 \pm 0.8$  g-sCOD/m<sup>2</sup>·d) was observed for Z-200 and Z-400, respectively. Therefore, the thickness-restraint did not show any significant effect for either carbonaceous or TAN removal rates and efficiencies (Figure 3-4).

### 3.5.2 Biofilm thickness

The thickness of the biofilm was characterized at the loading rate of  $6.0 \pm 0.8$  g-sBOD/m<sup>2</sup>·d to investigate the effects of carrier type and thickness-restraint on biofilm thickness and hence solids production, characteristics and settleability. The thickest biofilm was observed on K5 carriers ( $281.1 \pm 8.7$  μm), which can be explained by the protected and non-limited area for biofilm growth inside the voids of the carrier as opposed to the exposed surface area for biofilm growth of the Z-carriers (Figure 3-5). The overall average biofilm thickness on the Z-carriers was approximately  $111.6 \pm 11.3$  μm and  $174.3 \pm 11.1$  μm for Z-200 and Z-400, respectively (Figure 3-5). Therefore, as expected, a thinner biofilm is observed on the Z-200 as compared to the Z-400. However, the measured biofilm thickness was approximately half of the maximum allowed biofilm thickness for the two Z-carriers. Even though the maximum biofilm thickness on Z-carriers is pre-defined by the grid wall height (200 μm for the Z-200 carrier and 400 μm for the Z-400 carrier), the biofilm growth can also be limited by substrate availability, shear force or carrier interaction dynamics in the reactor, as with any other carriers.

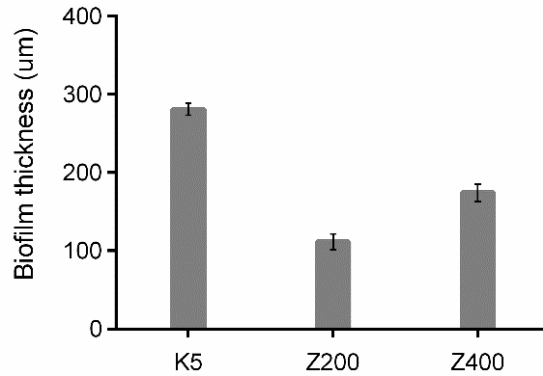


**Figure 3-5:** Biofilm thickness of various carriers, average and 95% confidence interval

In this study, it was observed that the biofilm thicknesses often varied from one side of the Z-carrier to the other side of the same carrier (Figure 3-6b, c). In particular, a thicker and more uniform biofilm was observed to be formed on one side of the Z-carriers with a thinner biofilm on the other side of the same carrier. The difference in biofilm thickness between the two sides of a carrier was more recognizable on the Z-400 carriers as compared to the Z-200 (Figure 3-6b, c). This phenomenon may have been the result of different reasons such as the carriers mould, the tendency of Z-carriers in the reactor to stack in pairs and the scraping depth, which lead to a thinner biofilm in the center of each compartment (Piculell et al., 2016b). Although the continuous aeration in the reactor keeps the carriers in constant movement, it was observed in this study that likely due to the shape of the Z-carriers, some carriers may stack in pairs and move together as pairs in the reactor. Therefore, the depth of the biofilm being limited on one side of the carrier that may not have been exposed to an adequate substrate supply due to stacking. This effect may be due to the bench-scale size of the MBBRs systems used in this study and, in particular, an effect of the mixing dynamics of carriers in the small volume reactors. Similar to previous studies, thicker biofilm was observed along the grid walls and thinner biofilm towards the center of each compartment that could be explained as a result of the carriers scraping each other (Piculell et al., 2016b). Therefore, thinner biofilm in the center of each compartment, as well as thinner biofilm on one side of some

carriers, has likely resulted in both Z-200 and Z-400 carriers demonstrating the overall average biofilm thickness lower than the predefined maximum thickness. It should be noted that previous studies that measured biofilm thicknesses while carriers were submersed in water show that the overall average of biofilm thickness on Z-400 carriers was approximately the height of the Z-400 grid walls, in a nitrifying system (Piculell, 2016; Piculell et al., 2016b).

Previous studies demonstrated that biofilm thickness and structure affect the performance of the MBBR (Forrest et al., 2016), where thicker biofilm with higher biofilm porosity may lead to deeper oxygen penetration depth (Piculell, 2016). Therefore, higher carbonaceous removal rates for the K5 carriers with the thickest biofilm, observed in this study, could be explained by the higher substrate availability and an increased bacteria activation at deeper layers of biofilm because of more porosity. On the other hand, the saddle-shaped Z-carriers, which are three-dimensional carriers as compared to flat K5 carriers, could be hit by the rising aeration bubbles and change moving direction more than K5. Therefore, the increase of turbulence in the reactor results in an elevated shear on the biofilm as the biofilm surface is more exposed in Z-carriers than K5 carriers (Piculell, 2016). Thus, thinner biofilm observed on Z-carriers might be indicative of potentially higher shear stress, which results in a denser biofilm on Z-carriers as compared to K5. Therefore, the possibility of inadequate substrate supply into the biofilm due to the carrier stacking, as well as thinner and denser biofilm, could limit the kinetics of the Z-reactors as compared to K5 (the difference in removal kinetics for different carrier types is shown in Figure 3-4).

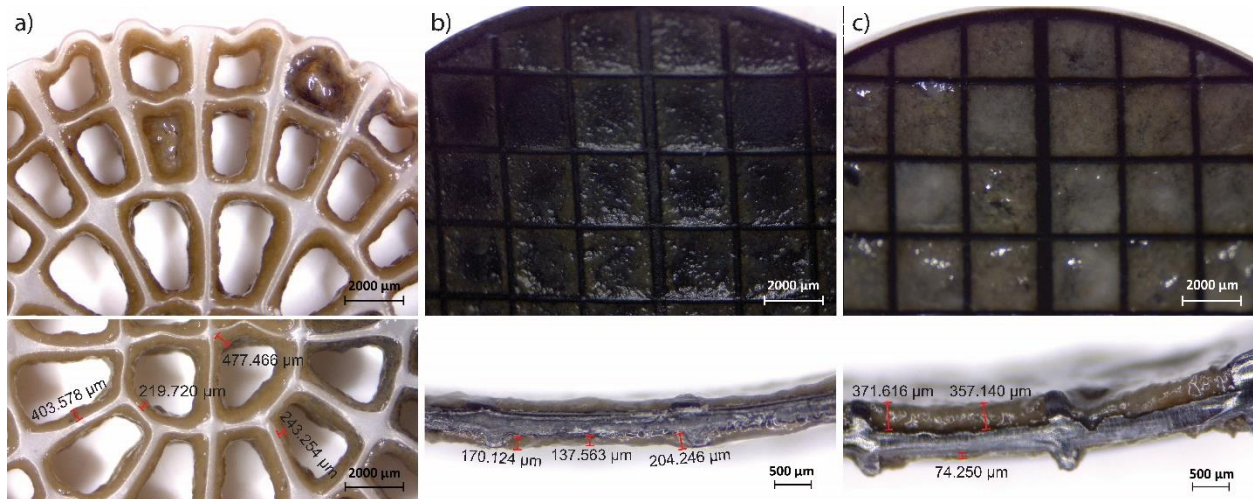


**Figure 3-6:** Stereomicroscopy images of carriers showing biofilm thickness measurements, (a) top view of K5 carrier, (b) top view of Z-200 carrier and side view of cut Z-200 carrier, and (c) top view of Z-400 carrier and side view of cut Z-400 carrier

Overall, the investigation of the biofilm thickness indicates that carrier type, shape and physical properties significantly affect the biofilm thickness, as the thickest biofilm was observed on protected and non-limited voids of K5 carriers. The newly designed thickness-restraint Z-carriers demonstrate different thicknesses compared to the conventional K5 carriers. Z-carriers successfully hence restrain the biofilm thickness and maintain the biofilm thickness within predefined maximum values.

### 3.5.3 Solids concentration, production, detachment

TSS, VSS, solids production and detachment rate were measured for the three reactors under the same experimental conditions of an SALR of  $6.0 \pm 0.8$  g-sBOD/m<sup>2</sup>·d, an HRT of 1.1 hours along with consistent DO, pH, and temperatures (Table 3-3). The MBBR effluent TSS concentration is a combination of biologically produced solids, detached biofilm from the carriers, and influent suspended solids. Since the particulate matter in the influent wastewater can be assumed to remain unchanged in high flowrate MBBR systems, with HRT values lower than 2

hours, the effect of hydrolysis was deemed negligible in this study (Ivanovic and Leiknes, 2012). The TSS production is calculated as the difference between the effluent TSS and the influent TSS. The detachment rate is defined as the mass flux of the difference between the MBBR influent and effluent TSS and is normalized per reactor surface area. The lowest TSS, VSS, solids production and detachment rate were measured for K5 (Table 3-3). The K5 reactor solids production resulted in  $7.7 \pm 3.2$  mg-TSS/L with a detachment rate of  $1.7 \pm 0.7$  g-TSS/ m<sup>2</sup>·d solids, which is statistically significantly lower than the solids production and detachment rate of the Z-carrier systems. Therefore, it can be concluded that the carrier type has a significant impact on solids production and biofilm detachment rate. On the other hand, the thickness-restraint carriers, comparison the Z-200 and Z-400 carriers, did not show a significant difference in the solids production and detachment rate.

**Table 3-3:** Effluent solids concentration, production and detachment rates in MBBR reactors (n=10)

	<b>SALR</b> (g-sBOD/m <sup>2</sup> ·d)	<b>TSS</b> (mg/L)	<b>VSS</b> (mg/L)	<b>Production*</b> (mg-TSS/L)	<b>Detachment rate</b> (g-TSS/m <sup>2</sup> ·d)
<b>K5</b>	6.0 ± 0.8	53.4 ± 8.5	42.2 ± 4.0	7.7 ± 3.2	1.7 ± 0.7
<b>Z-200</b>	6.0 ± 0.8	70.4 ± 13.0	53.3 ± 6.5	19.4 ± 7.6	5.0 ± 2.0
<b>Z-400</b>	6.0 ± 0.8	65.5 ± 10.5	50.9 ± 6.6	15.1 ± 4.0	3.7 ± 1.0

\*The amount of solids produced per day in each reactor can simply be calculated as the production multiplied by the reactor flow rate, which is equal to  $0.7 \pm 0.3$ ,  $1.7 \pm 0.7$  and  $1.3 \pm 0.4$  g-TSS/d in K5, Z-200 and Z-400 reactors, respectively.

An average observed yield, defined as the production of TSS over the soluble substrate consumption, of  $0.5 \pm 0.2$  g-TSS/g-sBOD<sub>removed</sub> was measured for K5, which is comparable with previous studies (0.12 to 0.56 g-TSS/g-COD<sub>removed</sub>) (Brosseau et al., 2016). Moreover,  $1.9 \pm 0.7$  and  $1.6 \pm 0.5$  g-TSS/g-sBOD<sub>removed</sub> were measured for Z-200 and Z-400, respectively. Hence, the Z-carriers showed three times higher yields compared to K5 carriers. Since all three reactors were

started on the same date and operated for 15 months, it is expected that the biofilm maturation on all carriers in this study was similar, and as such, differences in biofilm maturation did not affect the results. However, differences between the solids production and observed yield for different carrier types could be an important characteristic for downstream sludge treatment and subsequent biogas potential in full-scale applications, which can be an interest for future studies.

### **3.5.4 Solids characteristics and settleability**

The total suspended solids removal efficiency of a WRRF is highly dependent on the behaviour of the solids. The particle size distribution of MBBR effluent solids along with MBBR effluent solids settled for 4 hours are presented in this section. DPA was performed directly on the effluent of the three reactors immediately after sampling and also after 4 hours of settling to mimic the secondary clarifier retention time at the full-scale WRRF where the reactors were operated. The study on the settleability of solids was conducted at an SALR of  $6.0 \pm 0.8$  g-sBOD/m<sup>2</sup>·d and a constant HRT of 1.1 hours. The particle size distribution curves in the range of 2-400 µm were graphed along with the corresponding bar graphs for particles larger than 400 µm, before (Figure 3-7) and after settling (Figure 3-8). The graphs show the average of triplicate measurements of total volume percentage of particles with 95% confidence intervals. The volume percentages for both unsettled and settled effluent solids were normalized by the total volume of the particles presented in the unsettled effluent to enable a comparison of the unsettled and settled solids (Karizmeh et al., 2014).

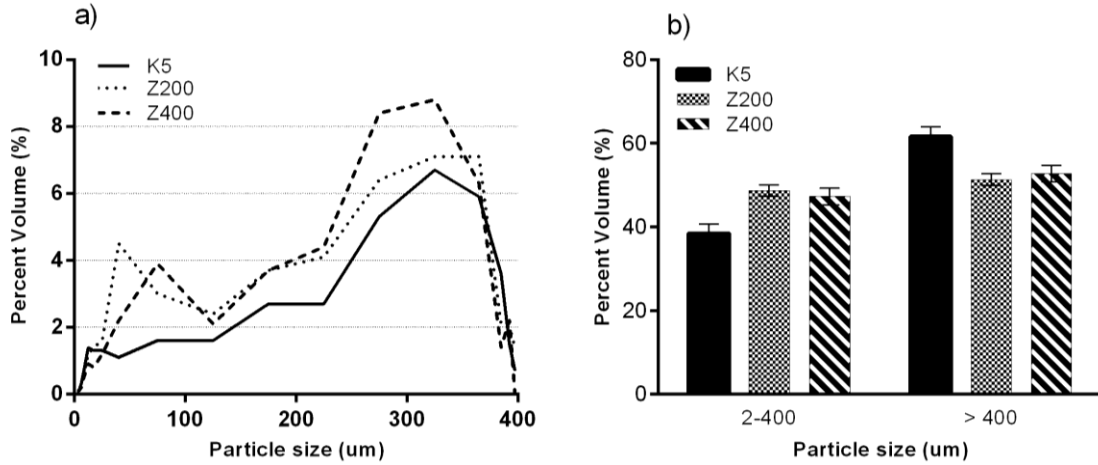


**Figure 3-7:** Impact of various carrier types on unsettled effluent particle distribution at SALR of  $6.0 \pm 0.8$  g-sBOD/m<sup>2</sup>·d, (a) particle size distribution of particles between 2–400 μm, and (b) total volume percentages of particles smaller and larger than 400 μm

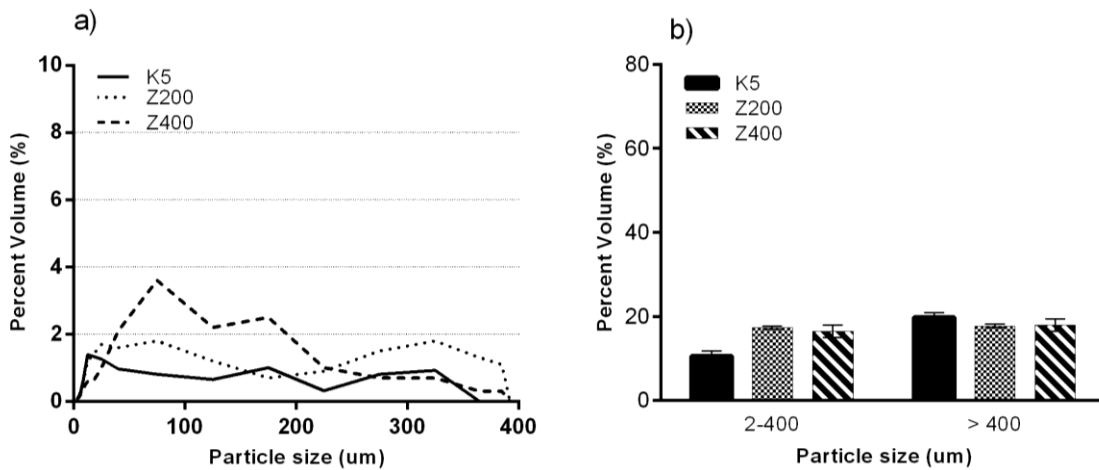


**Figure 3-8:** Impact of various carrier types on effluent particle distribution at SALR of  $6.0 \pm 0.8$  g-sBOD/m<sup>2</sup>·d after 4 hours of settling, (a) particle size distribution of particles between 2–400 μm, and (b) total volume percentages of particles smaller and larger than 400 μm

The integrated area under the particle distribution curves (Figure 3-7a) shows that  $38.4 \pm 2.3\%$ ,  $48.7 \pm 1.4\%$  and  $47.3 \pm 2\%$  of the total volume of unsettled effluent particles in the K5, Z-200 and Z-400 reactors, respectively, existed in the range of 2-400 μm. Therefore, statistically,

significantly lower percent volume of particles between 2-400  $\mu\text{m}$  ( $38.4 \pm 2.3\%$ ), and accordingly, significantly higher percent volume of particles larger than 400  $\mu\text{m}$  ( $61.6 \pm 2.3\%$ ) is observed for K5 as compared to Z-carriers. However, the thickness-restraint carriers do not show statistically significant differences between percent volume of particles for Z-200 and Z-400, neither for particles between 2-400  $\mu\text{m}$  nor for particles larger than 400  $\mu\text{m}$  (Figure 3-7b). Generally, greater than 50 % of the total solids volume was observed to be larger than 400  $\mu\text{m}$  in all three reactors (Figure 3-7b). However, previous studies have shown that approximately 20% of the total particles volume is larger than 400  $\mu\text{m}$  for carbon removal systems using synthetic wastewater at various loading rates (Karizmeh et al., 2014). The interference of influent solids with produced solids in systems fed with real wastewaters, such as in this study, may result in the agglomeration of solids and hence a higher percentage of large particles.

The trend of all three particle size distribution curves is similar for unsettled effluent particles in the range of 150-400  $\mu\text{m}$ . However, Z-carriers were shown to produce a larger quantity of particles smaller than 150  $\mu\text{m}$  as compared to K5 (Figure 3-7a). An obvious distinction between Z-carriers and K5 carriers was observed for unsettled effluent particle size distribution in the range of 2-150  $\mu\text{m}$ , where there is less distinction when comparing the effects of thickness-restraint on the Z-carriers in this range (Figure 3-7a).

In addition, the peak quantity of unsettled effluent particles in the range of 2–400  $\mu\text{m}$  is shown to shift slightly towards smaller particles (Figure 3-7a), and in accordance, a slight decrease in mean particle diameter is also observed for Z-carriers as compared to K5 carrier. Therefore, the measured median particle diameter was  $289 \pm 20 \mu\text{m}$  for K5,  $267 \pm 10 \mu\text{m}$  for Z-200 and  $271 \pm 17 \mu\text{m}$  for Z-400. The median particle diameter is the diameter of the particle for which 50% of a sample's volume is smaller than and 50% of a sample's volume is larger than this value. The

unsettled median particle diameter did not show a statistically significant difference for different carrier types ( $p > 0.05$ ). However, after 4 hours of settling, the K5 showed a statistically significantly smaller median particle diameter ( $38 \pm 14 \mu\text{m}$ ) as compared to the two Z-carriers ( $p < 0.05$ ), which implies the potential of better settling for solids detached from K5 carriers. The thickness-restraint carriers, comparison of Z-200 and Z-400, did not show a significant difference in the median particle diameter after 4 hours of settling ( $96 \pm 4 \mu\text{m}$  and  $82 \pm 11 \mu\text{m}$  for Z-200 and Z-400, respectively).

The settled particle distribution curves (Figure 3-8) indicate that K5 contains a statistically significantly lower percent volume of particles between 2-400  $\mu\text{m}$  ( $10.5 \pm 1.2\%$ ) and larger than 400  $\mu\text{m}$  ( $19.7 \pm 1.1\%$ ) as compared to the Z-carriers. The lowest removal for all carriers occurred in the ranges of 2–200  $\mu\text{m}$  particles, which implies the poor settleability of smaller particles (Figure 3-8a). Furthermore, a large volume fraction of the particles is related to relatively large particles or aggregates of particles (in the range of 20 – 400  $\mu\text{m}$ ). Although the very small particles may not be the dominant volume fraction of particles, they may cause various challenges in solids separation (Ødegaard et al., 2010).

The effect of carrier type on settleability indicates that the K5 carrier, with  $69.7 \pm 2.0\%$  of total solids settling, showed statistically significantly higher settling efficiency compared to the Z-carriers. This can be explained by the larger particle size volume percentage of the particles and the distinct particle size distribution observed for the K5 carrier solids. As such, carrier design is herein shown to affect not only the quantity of particles detached from the carriers but also the size and settleability of the particles. On the other hand, the thickness-restraint effects of the Z-200 carrier compared to the Z-400 carriers did not significantly affect the settleability of the solids. Lower solids production, lower detachment rate (Table 3-3) and lower volume percentage of small

particles indicate potentially better settleability for the K5 carrier. Although the small particles (2-150  $\mu\text{m}$ ) produced by Z-200 carriers appear to agglomerate and preferentially settle better than the small particles produced by Z-400 carriers, thickness-restraint Z-carriers did not differ significantly in terms of the overall settleability, as  $65.0 \pm 0.7\%$  and  $65.7 \pm 1.1\%$  of total solids settling was observed for Z-200 and Z-400, respectively. This demonstrates that carrier design, as opposed to thickness-restraint versions of similarly designed carriers, affects particle detachment and, in turn, the settleability of the effluent solids.

### **3.6 Conclusion**

This study investigated the effects of carrier type and the biofilm thickness-restraint carrier design on the carbonaceous and TAN removal performance, biofilm thickness and subsequent solids production, particle characteristics and settleability. The application of various carriers at an SALR of  $6 \pm 0.8 \text{ g-sBOD/m}^2 \cdot \text{d}$  and a constant HRT of 1.1 hours demonstrated that the carrier type has a significant effect on the carbonaceous removal rate (both sBOD and sCOD) and not a significant effect on TAN removal. TAN removal via nitrification was likely suppressed in all reactors due to the elevated carbonaceous loading of the reactors. Biofilm thickness-restraint was shown to not significantly affect the carbonaceous removal efficiency. The K5 carriers show lower TSS concentrations, lower solids production and lower detachment rates compared to the Z-carriers. The thickness-restraint carrier design of the Z-200 carrier and the corresponding thinner attached biofilm of the Z-200 carrier did not demonstrate statistically significant differences in solids production or biofilm detachment rate compared to the less thickness-restraint Z-400 carrier. The volume-based particle size distribution analysis of the MBBR effluent demonstrates a higher volume percentage of particles smaller than 400  $\mu\text{m}$  for Z-carriers compared to K5 carriers. In particular, a significant distinction is observed in the particle size distribution range of 2-150  $\mu\text{m}$

between the Z-carriers and the K5 carriers, which is likely related to the lower overall settleability of the Z-carriers effluent solids. As such, the carrier's physical properties have a significant effect on the solids production, detachment and, subsequently, the solids distribution size and settleability. In contrast, biofilm thickness and the restraint of biofilm thickness due to carrier design did not significantly affect the solids production, the detachment rate or the settling behaviour of the effluent solids.

### 3.7 References

- Åhl, R. M., Leiknes, T., and Ødegaard, H. (2006). "Tracking particle size distributions in a moving bed biofilm membrane reactor for treatment of municipal wastewater." *Water Science and Technology*, 53(7), 33–42.
- Almomani, F. A., and Khraisheh, M. A. M. (2016). "Treatment of septic tank effluent using moving-bed biological reactor: kinetic and biofilm morphology." *International Journal of Environmental Science and Technology*, 13(8), 1917–1932.
- Ashrafi, E., Allahyari, E., Torresi, E., and Andersen, H. R. (2019). "Effect of slow biodegradable substrate addition on biofilm structure and reactor performance in two MBBRs filled with different support media." *Environmental Technology*, 1–10.
- Barwal, A., and Chaudhary, R. (2014). "To study the performance of biocarriers in moving bed biofilm reactor (MBBR) technology and kinetics of biofilm for retrofitting the existing aerobic treatment systems: A review." *Reviews in Environmental Science and Biotechnology*, 13(3), 285–299.
- Bassin, J. P., and Dezotti, M. (2018). "Moving Bed Biofilm Reactor (MBBR)." *Advanced Biological Processes for Wastewater Treatment*, Springer, Cham, 37–75.
- Bassin, J. P., Dias, I. N., Cao, S. M. S., Senra, E., Laranjeira, Y., and Dezotti, M. (2016). "Effect of increasing organic loading rates on the performance of moving-bed biofilm reactors filled with different support media: Assessing the activity of suspended and attached biomass fractions." *Process Safety and Environmental Protection*, Institution of Chemical Engineers,

100, 131–141.

- Brosseau, C., Émile, B., Labelle, M. A., Laflamme, É., Dold, P. L., and Comeau, Y. (2016). “Compact secondary treatment train combining a lab-scale moving bed biofilm reactor and enhanced flotation processes.” *Water Research*, 106, 571–582.
- Chaali, M., Naghdi, M., Brar, S. K., and Avalos-Ramirez, A. (2018). “A review on the advances in nitrifying biofilm reactors and their removal rates in wastewater treatment.” *Journal of Chemical Technology and Biotechnology*, 93(11), 3113–3124.
- Chu, L., and Wang, J. (2011). “Comparison of polyurethane foam and biodegradable polymer as carriers in moving bed biofilm reactor for treating wastewater with a low C/N ratio.” *Chemosphere*, 83(1), 63–68.
- Delatolla, R. A., and Babarutsi, S. (2005). “Parameters affecting hydraulic behavior of aerated lagoons.” *Journal of Environmental Engineering*, 131(10), 1404–1413.
- Delatolla, R., Seguin, C., Springthorpe, S., Gorman, E., Campbell, A., and Douglas, I. (2015). “Disinfection byproduct formation during biofiltration cycle: Implications for drinking water production.” *Chemosphere*, 136, 190–197.
- Delatolla, R., Tufenkji, N., Comeau, Y., Gadbois, A., Lamarre, D., and Berk, D. (2010). “Investigation of laboratory-scale and pilot-scale attached growth ammonia removal kinetics at cold temperature and low influent carbon.” *Water Quality Research Journal*, 45(4), 427–436.
- Dias, J., Bellingham, M., Hassan, J., Barrett, M., Stephenson, T., and Soares, A. (2018a). “Impact of carrier media on oxygen transfer and wastewater hydrodynamics on a moving attached growth system.” *Chemical Engineering Journal*, 351, 399–408.
- Dias, R. A., Martins, R. C., Castro, L. M., and Quinta-Ferreira, R. M. (2018b). “Biosolids production and COD removal in activated sludge and moving bed biofilm reactors.” *WASTES – Solutions, Treatments and Opportunities II*, Taylor & Francis Group, London, 271–276.
- Forrest, D., Delatolla, R., and Kennedy, K. (2016). “Carrier effects on tertiary nitrifying moving bed biofilm reactor: An examination of performance, biofilm and biologically produced solids.” *Environmental Technology*, 37(6), 662–671.

- Gazette, C. (2012). "Wastewater systems effluent regulations, Part II." 145(15), 1632–1812.
- Hem, L., Rusten, B., and Ødegaard, H. (1994). "Nitrification in a moving bed biofilm reactor." *Water Research*, 28(6), 1425–1433.
- Ivanovic, I., and Leiknes, T. O. (2012). "Particle separation in moving bed biofilm reactor: Applications and opportunities." *Separation Science and Technology*, 47(5), 647–653.
- Karizmeh, M. S., Delatolla, R., and Narbaitz, R. M. (2014). "Investigation of settleability of biologically produced solids and biofilm morphology in moving bed bioreactors (MBBRs)." *Bioprocess and Biosystems Engineering*, 37(9), 1839–1848.
- Levstek, M., and Plazl, I. (2009). "Influence of carrier type on nitrification in the moving-bed biofilm process." *Water Science and Technology*, 59(5), 875–882.
- Loupasaki, E., and Diamadopoulou, E. (2013). "Attached growth systems for wastewater treatment in small and rural communities: A review." *Journal of Chemical Technology and Biotechnology*, 88(2), 190–204.
- Mannacharaju, M., Natarajan, P., Villalan, A. K., Jothieswari, M., Somasundaram, S., and Ganesan, S. (2018). "An innovative approach to minimize excess sludge production in sewage treatment using integrated bioreactors." *Journal of Environmental Sciences*, Elsevier B.V., 67, 67–77.
- McQuarrie, J. P., and Boltz, J. P. (2011). "Moving bed biofilm reactor technology: Process applications, design, and performance." *Water Environment Research*, 83(6), 560–575.
- Melin, E., Leiknes, T., Helness, H., Rasmussen, V., and Ødegaard, H. (2005). "Effect of organic loading rate on a wastewater treatment process combining moving bed biofilm and membrane reactors." *Water Science and Technology*, 51(6–7), 421–430.
- Metcalf & Eddy. (2014). *Wastewater Engineering: Treatment and Resource Recovery*. McGraw-Hill, New York.
- Morgan-Sagastume, F. (2018). "Biofilm development, activity and the modification of carrier material surface properties in moving-bed biofilm reactors (MBBRs) for wastewater treatment." *Critical Reviews in Environmental Science and Technology*, 48(5), 439–470.

- Ødegaard, H. (2006). “Innovations in wastewater treatment: The moving bed biofilm process.” *Water Science and Technology*, 53(9), 17–33.
- Ødegaard, H. (2016). “A road-map for energy-neutral wastewater treatment plants of the future based on compact technologies (including MBBR).” *Frontiers of Environmental Science & Engineering*, Springer, 10(4), 2.
- Ødegaard, H., Cimbritz, M., Christensson, M., and Dahl, C. P. (2010). “Separation of biomass from moving bed biofilm reactors (MBBRs).” *Proceedings of the Water Environment Federation*, 2010(7), 212–233.
- Ødegaard, H., Gisvold, B., and Strickland, J. (2000). “The influence of carrier size and shape in the moving bed biofilm process.” *Water Science and Technology*, 41(4–5), 383–391.
- Ødegaard, H., Rusten, B., and Westrum, T. (1994). “A new moving bed biofilm reactor: applications and results.” *Water Science and Technology*, 29(10–11), 157–165.
- Ødegaard, H. (2004). “Sludge minimization technologies - An overview.” *Water Science and Technology*, 49(10), 31–40.
- Patry, B., Boutet, É., Baillargeon, S., and Lessard, P. (2018). “Solid-liquid separation of an effluent produced by a fixed media biofilm reactor.” *Water Science and Technology*, 77(3), 589–596.
- Piculell, M. (2016). “New dimensions of moving bed biofilm carriers influence of biofilm thickness and control possibilities.” Ph.D. thesis, Lund University, Sweden.
- Piculell, M., Lidén, S., Henningsson, G., Wessman, F., Thomson, C., Welander, T., and Ekenberg, M. (2016a). “Minimizing Clogging and Scaling Issues in the Moving Bed Biofilm Reactor Using Biofilm Control.” *Proceedings of the Water Environment Federation*, 2015(13), 4294–4303.
- Piculell, M., Welander, P., Jönsson, K., and Welander, T. (2016b). “Evaluating the effect of biofilm thickness on nitrification in moving bed biofilm reactors.” *Environmental Technology*, Taylor & Francis, 37(6), 732–743.
- Qiqi, Y., Qiang, H., and T. Ibrahim, H. (2012). “Review on moving bed biofilm processes.” *Pakistan Journal of Nutrition*, 11(9), 804–811.

- Ramli, N. A., and Abdul Hamid, M. F. (2017). "A review on two different systems in municipal sewage treatment plant." *2017 IEEE Conference on Energy Conversion*, 207–211.
- Schindelin, J., Arganda-Carreras, I., Frise, E., Kaynig, V., Longair, M., Pietzsch, T., Preibisch, S., Rueden, C., Saalfeld, S., and Schmid, B. (2012). "Fiji: an open-source platform for biological-image analysis." *Nature Methods*, 9(7), 676.
- Shahot, K., Idris, A., Omar, R., and Yusoff, H. M. (2014). "Review on biofilm processes for wastewater treatment." *Life Science Journal*, 11(11), 11.
- Siciliano, A., and De Rosa, S. (2016). "An experimental model of COD abatement in MBBR based on biofilm growth dynamic and on substrates' removal kinetics." *Environmental Technology*, Taylor & Francis, 37(16), 2058–2071.
- Sonwani, R. K., Swain, G., Giri, B. S., Singh, R. S., and Rai, B. N. (2019). "A novel comparative study of modified carriers in moving bed biofilm reactor for the treatment of wastewater: Process optimization and kinetic study." *Bioresource Technology*, 281, 335–342.
- Tian, X., and Delatolla, R. (2019). "Meso and micro-scale effects of loading and air scouring on nitrifying bio-cord biofilm." *Environmental Science Water Research & Technology*, 5, 1183–1190.
- Di Trapani, D., Mannina, G., Torregrossa, M., and Viviani, G. (2010). "Quantification of kinetic parameters for heterotrophic bacteria via respirometry in a hybrid reactor." *Water Science and Technology*, 61(7), 1757–1766.
- WEF. (2009). *Design of Municipal Wastewater Treatment Plants: WEF Manual of Practice No. 8*. McGraw-Hill, New York.
- WEF. (2011). *Moving Bed Biofilm Reactors: WEF Manual of Practice No. 35*. McGraw-Hill, New York.
- Young, B., Banihashemi, B., Forrest, D., Kennedy, K., Stintzi, A., and Delatolla, R. (2016a). "Meso and micro-scale response of post carbon removal nitrifying MBBR biofilm across carrier type and loading." *Water Research*, 91, 235–243.
- Young, B., Delatolla, R., Abujamel, T., Kennedy, K., Laflamme, E., and Stintzi, A. (2017). "Rapid

start-up of nitrifying MBBRs at low temperatures: nitrification, biofilm response and microbiome analysis.” *Bioprocess and Biosystems Engineering*, 40(5), 731–739.

Young, B., Delatolla, R., Ren, B., Kennedy, K., Laflamme, E., and Stintzi, A. (2016b). “Pilot-scale tertiary MBBR nitrification at 1°C: Characterization of ammonia removal rate, solids settleability and biofilm characteristics.” *Environmental Technology*, 37(16), 2124–2132.

# **Chapter 4 – MBBR effluent particles: Influence of carrier geometrical properties and levels of biofilm thickness restraint on biofilm properties, effluent particle size distribution, settling velocity distribution and settling behaviour**

## **4.1 Context**

Chapter 4 presents a version of the article entitled: “*MBBR effluent particles: Influence of carrier geometric properties and levels of biofilm thickness restraint on biofilm properties, effluent particle size distribution, settling velocity distribution and settling behaviour*”, has been submitted to the journal of Biosystems Engineering. This research describes the MBBR effluent solids characteristics, settling behaviour and the biofilm responses to the various shape of carriers and different levels of biofilm thickness restraint. This study is the first study using the ViCAs method combined with microscopy imaging to investigate the settling behaviour of MBBR produced particles.

## **4.2 Abstract**

The relatively poor settling characteristics of particles produced in moving bed biofilm reactor (MBBR) outline the importance of developing a fundamental understanding of the characterization and settleability of MBBR-produced solids. The influence of carrier geometric properties and different levels of biofilm thickness on biofilm characteristics, solids production, particle size distributions (PSD), and particle settling velocity distributions (PSVD) is evaluated in this study. The analytical ViCAs method is applied to the MBBR effluent to assess the distribution of particle settling velocities. This method is combined with microscopy imaging to relate particle size

distribution to settling velocity. Three conventionally loaded MBBR systems are studied at a similar BOD loading rate of  $6.0 \pm 0.8$  g-sBOD/m<sup>2</sup>·d with two different types of carriers. The conventional AnoxK™ K5, a commonly used carrier, is compared to AnoxK™ Z-carriers, newly designed carriers to restrain the biofilm thickness. Moreover, two levels of biofilm thickness restraint, 200 µm and 400 µm, are studied using AnoxK™ Z-200 and Z-400 "thickness-restraint" carriers. Statistical analysis confirms that K5 carriers demonstrate a significantly different biofilm mass, thickness, and density, in addition to distinct trends in PSD and PSVD in comparison with Z-carriers. However, the results obtained of the thickness-restraint Z-200 carrier did not vary significantly compared to the Z-400 carrier. The K5 carriers show the lowest suspended solids production ( $0.7 \pm 0.3$  g-TSS/d), thickest biofilm ( $281.1 \pm 8.7$  µm) and lowest biofilm density ( $65.0 \pm 1.5$  kg/m<sup>3</sup>). The effluent solids produced by the K5 carriers also show enhanced settling behaviour, consisting of larger particles with faster settling velocities.

### **4.3 Introduction**

The moving bed biofilm reactor (MBBR) technology is a compact wastewater treatment technology often utilized to retrofit and/or upgrade passive and conventional wastewater treatment systems to meet new and stringent regulations (Delatolla et al., 2010; Young et al., 2016b; Ødegaard, 2016). It is an efficient system with a small footprint and low solids production (Ødegaard, 2004; Åhl et al., 2006; WEF, 2011; McQuarrie and Boltz, 2011; Barwal and Chaudhary, 2014; Mannacharaju et al., 2018; Dias et al., 2018). However, several studies have highlighted the poor settling characteristics of the solids produced by MBBR systems as the main drawback of this technology (Ødegaard et al., 2010; Ivanovic and Leiknes, 2012; Karizmeh et al., 2014; Bassin and Dezotti, 2018). Since the separation of biologically produced solids from the liquid is an essential step in any biological treatment system and has an inevitable impact on the

quality of the effluent, more detailed particle characteristics and settling behaviour knowledge related to this technology will advance the design of downstream clarifiers for these systems and ultimately result in enhanced effluent water quality.

Despite the importance of understanding the settling behaviour of MBBR-produced solids and particle characteristics to improve the settleability of MBBR effluent particles, there exists a fundamental lack of understanding of MBBR effluent particle characteristics. Particle size distribution (PSD) and particle settling velocity distributions (PSVD) are two important characteristics used to understand the particle settling behaviour of wastewater treatment systems (Maruéjols et al., 2014). MBBR effluent PSD has previously been studied for different solid-liquid separation technologies, different loading conditions, different hydraulic retention time (HRT), and different carrier types (Melin et al., 2005; Åhl et al., 2006; Ødegaard et al., 2010; Karizmeh et al., 2014; Young et al., 2016a; Forrest et al., 2016). It has been demonstrated that the PSD correlates well with HRT and surface area loading rate (SALR), with larger particles observed at higher HRT (hence, lower SALR) (Ødegaard et al., 2000, 2010; Melin et al., 2005; Åhl et al., 2006). As such, increasing SALR was observed to cause a decrease in solids settleability for both nitrifying and carbon removal MBBR systems (Karizmeh et al., 2014; Young et al., 2016b). Moreover, different types of carriers demonstrated significantly different settleability and particle characteristics at high loading rates, causing excessive biofilm growth and carrier clogging (Forrest et al., 2016; Young et al., 2016b). In these studies, the settleability of solids was estimated by comparing the PSD before and after a short settling time of 30 minutes. However, no research on the PSVD for MBBR systems currently exists. Thus, the effect of various carrier types and the biofilm thickness-restraint carriers on particle settling behaviour has not been studied in sufficient detail, leaving a fundamental gap of knowledge on this topic.

PSVD can be calculated theoretically (i.e. Stoke's law) from PSD and density assuming spherical homogeneous particles. However, since particles are not uniform in real wastewater, and the density distributions of particles associated to PSD are often not evident in wastewaters, the direct evaluation of the settling velocity is necessary to describe real wastewater settling behaviour (Chebbo and Gromaire, 2009; Bachis et al., 2015; Plana et al., 2018). Current literature shows several methods that were developed to measure the PSVD (Aiguier et al., 1996; Hasler, 2007; Berrouard, 2010). The "Vitesse de Chute en Assainissement" (ViCAs) method is becoming a reference method with good repeatability when used to measure the PSVD of wastewaters (Chebbo and Gromaire, 2009; Vallet et al., 2014). This method directly measures the settling velocity of particles in a quiescent settling column. As such, several studies have recently used the ViCAs method to measure the PSVD for different wastewaters and storm waters to estimate the solids removal performance with a comprehensive perception of the particle settling behaviour. These studies mainly focus on solids' settling behaviour in grit chambers, combined sewers, retention tanks, and primary clarifiers (Hasler, 2007; Maruéjols et al., 2013; Bachis et al., 2015; Vanrolleghem et al., 2019; Plana et al., 2020) other than biological wastewater treatment systems such as MBBR effluent. As such, there is still a gap of knowledge and lack of research on particle settling behaviour for MBBR effluent, let alone the influence of carrier's geometric properties and restraining the biofilm thickness on solids settleability. Therefore, the MBBR effluent particle characteristics and settling velocity distribution have yet to be comprehensively studied.

The main objective of this research is to improve the current knowledge of the particle characteristics of MBBR effluents and their solids settling behaviour by developing an understanding of the effects of carrier geometry and levels of biofilm thickness restraint on these parameters. In addition, particle characteristics and settling behaviour are related to the biofilm

characteristics in the study. As such, biofilm thickness, density, mass, detachment rate along with solids concentration, solids production, PSD, and PSVD have all been measured in carbon removal MBBR reactors. Further, this study combines the settling velocity characterization method, ViCAs, along with particle size distribution analysis to characterize MBBR effluent comprehensively. In particular, the conventional AnoxK™ K5 carrier is compared to two newly designed AnoxK™ Z-carriers. The AnoxK™ Z-200 and AnoxK™ Z-400 carriers are used in this study to enable the evaluation of "thickness-restraint" via predefined biofilm thicknesses of 200 and 400 µm, respectively, which has not previously been achievable.

## **4.4 Materials and methods**

### **4.4.1 Experimental setup and operation**

Three identical four-litre MBBR reactors were operated in parallel at the Gatineau municipal water resource recovery facility (WRRF), located in Québec, Canada. Infiltration/inflow in the sewershed feeding the Gatineau WRRF might cause the more dilute wastewater characteristics of the Gatineau WRRF. The reactors were fed with a steady flow rate of  $3.7 \pm 0.1$  L/h with primary clarified wastewater. One reactor filled with the porous cylindrical-shaped K5 carrier and the other two reactors housed the saddle-shaped Z-carriers, Z-200 and Z-400, with the predefined levels of biofilm thickness up to 200 and 400 µm, respectively. 160 AnoxK™ K5 carriers, 300 AnoxK™ Z-200 carriers, and 300 AnoxK™ Z-400 carriers (AnoxKaldnes, Lund, Sweden) were used individually in each reactor to provide the same surface areas of  $0.38 \text{ m}^2$  per reactor for biofilm growth. The study is conducted during the steady-state operation after the inoculation and acclimatization period (Arabgol et al., 2020), when the reactors were working under similar conditions with a moderate carbonaceous SALR of  $6.0 \pm 0.8$  g-sBOD/m<sup>2</sup>·d ( $14.9 \pm 1.6$  g-sCOD/m<sup>2</sup>·d), total ammonia nitrogen (TAN) SALR of  $4.1 \pm 0.3$  g/m<sup>2</sup>·d, HRT of  $1.1 \pm 0.0$  h and

the dissolved oxygen (DO) of  $6.5 \pm 0.5$  at the maintained pH and temperature of  $7.8 \pm 0.1$  and  $18.0 \pm 1.0$  °C, respectively. Sufficient aeration provided the movement of the carriers in the reactors. The operational conditions were selected to be in the range of normally loaded carbon removal MBBR systems (Ødegaard et al., 2010; WEF, 2011) to minimize the impacts of high loaded operational conditions on MBBR system performance, biofilm and solids characteristics. These values (SALR, HRT and % fill) were within the typical design range applicable for the three different carriers with different properties, allowing to provide similar conditions in all three reactors.

#### **4.4.2 Constituent analysis**

Influent and effluent wastewater constituents were analyzed for each reactor. Samples were collected two to three times a week and analyzed for the following constituents within 4 hours of collection. Total and soluble biochemical oxygen demand (BOD and sBOD) (SM 5210B-5 day BOD), total and soluble chemical oxygen demand (COD and sCOD) (HACH methods 8000), total suspended solids (TSS) (SM 2540 D-TSS), volatile suspended solids (VSS) (SM 2540 E-VSS), TAN (SM 4500-NH<sub>3</sub>), nitrite (SM 4500-NO<sub>2</sub><sup>-</sup>), nitrate (SM 4500-NO<sub>3</sub><sup>-</sup>B) (APHA, 2005). The DO concentration, pH and temperature within the reactors were determined using a HACH HQ40d portable multi-meter with Intellical™ LDO101 DO probe and PHC201 pH electrode (Loveland, CO, USA).

#### **4.4.3 Biofilm characteristics analysis**

The biofilm thickness, mass and density are analyzed to characterize the biofilm properties. The images used for biofilm thickness measurement were acquired utilizing a Zeiss Stemi 305 stereoscope (Carl Zeiss Canada Ltd., Toronto, Canada). The acquired images from three randomly harvested carriers from each reactor were analyzed using Fiji software (Schindelin et al., 2012).

The biofilm thickness was quantified as the average height of the biofilm on the surface of the carriers (Arabgol et al., 2020).

To quantify the mass of the attached biofilm, three additional carriers were randomly collected from each reactor, dried at 105°C overnight and weighed. The difference between the weights of dried carriers with the attached biofilm and the carriers after being thoroughly cleaned was used to quantify the mass of biofilm attached to each carrier (Delatolla et al., 2008; Piculell et al., 2016b; Young et al., 2017). The biofilm density is then determined by the biofilm mass per volume of the biofilm (biofilm volume is expressed as thickness  $\times$  carrier surface area) (Tijhuis et al., 1995).

#### **4.4.4 Biofilm Morphology**

A Tescan Vega-II XMU variable pressure scanning electron microscopy (VPSEM) (Tescan USA Inc., US, PA) was used to acquire images from the attached biofilm on the carriers. A total of 15 VPSEM images were acquired from triplicate carriers at the optimized pressure of 40 Pa, and with 60 $\times$  to 600 $\times$  magnifications to analyze the biofilm morphology (Delatolla et al., 2009; Young, 2017). The VPSEM imaging does not require any sample preparation, which minimizes the destruction of biofilm before analysis. The exposure times were restricted in this study to minimize the destructive effects of biofilm shrinkage on the biofilm morphology due to dehydration. Z-carriers were more vulnerable to dehydration due to the exposed surface of biofilm in comparison with K5 carriers.

#### **4.4.5 Particle settling velocity distribution (PSVD)**

The ViCAs protocol was used to assess the PSVD of the MBBR effluent in the study. ViCAs is a sedimentation column developed by Chebbo and Gromaire (2009) as a static settling device that does not require any sample pre-treatment step. The test uses a cylindrical column (H = 70 cm,  $\emptyset$  = 7 cm) quickly filled with a homogenized wastewater sample assuming the solids are

uniformly distributed over the ViCAs column at the beginning of the test ( $t = 0$ ). Then the mass of settled particles is collected in movable cups installed under the column at different time intervals ( $t = 2, 6, 14, 30, 60, 120, \text{ and } 240 \text{ min}$ ) and analyzed for TSS according to standard methods (APHA, 2005; Chebbo and Gromaire, 2009). The measurement of the cumulative mass settled over time allows calculating the settling velocity ( $V_s$ ) distributions corresponding to different mass fractions of solids using a small Excel solver macro (Chebbo and Gromaire, 2009). The obtained ViCAs curves represent the mass percentage of particles with velocities lower than the selected corresponding velocities. The influent and effluent samples of each reactor were collected and analyzed immediately after sampling to minimize the particles' flocculation in the sample (Maruejous et al., 2011; Torfs et al., 2016). Each sample was well mixed before starting the ViCAs test, and the test was considered valid if the mass balance error was less than  $\pm 15\%$  (Chebbo and Gromaire, 2009).

The repeatability of the ViCAs was evaluated in previous studies for different types of wastewaters except for MBBR effluents (Gromaire et al., 2008; Plana et al., 2020). Therefore, during the preliminary work, two different approaches were used to assess the reproducibility of the ViCAs test for MBBR effluent (Plana et al., 2020). In the first approach, two replicates of a single sample were analyzed simultaneously by two ViCAs columns in parallel. In the second one, the ViCAs results for samples taken on three different days were evaluated to confirm the repeatability.

#### **4.4.6 Particle size distribution (PSD)**

The PSD was determined for particles collected at the bottom of the ViCAs settling column after 2, 30 and 240 minutes of settling. 5 ml of collected, homogenized samples were transferred to a glass petri dish for visualization and image acquisition. A Carl Zeiss bright field moving stage

microscope Axio Examiner.Z1 (Carl Zeiss Canada Ltd., Toronto, Canada) with A-plan 2.5×/0.06 objective was used to acquire 16 images per sample. Each image covers an area of 2580 μm × 2680 μm at a resolution of 1388 × 1040 pixels. Therefore, a total area of 14320 μm × 10720 μm was imaged and analyzed. Fiji software (<http://fiji.sc/Fiji>) was used to analyze the images and quantify the particle size, area, perimeter and shape factor (Schindelin et al., 2012). The size of the particles is expressed as the equivalent circular diameter (ECD), calculated as  $2 \times (\text{Area}/\pi)^{0.5}$  with the particle projected area (Grijnspeerdt and Verstraete, 1997).

Moreover, along with characterizing the settled particle using bright-field microscopy images at different ViCAs time intervals, micro-flow imaging (MFI) technology was also used to characterize the PSD in the MBBR effluent before and after 4 hours of settling. Therefore, the PSD was also quantified using a dynamic particle analyzer (DPA) (Brightwell Technologies, Canada, ON) (Arabgol et al., 2020). However, unlike the bright-field microscopy, DPA was only able to analyze particle size distribution in the range of 2.25–400 μm at low magnification (Karizmeh et al., 2014; Forrest et al., 2016).

#### **4.4.7 Statistical analysis**

The statistical significant differences are validated with a *p*-value less than 0.05. The student t-test was applied in this study to assess the statistical significant differences of all the analyses except PSD analysis due to the lack of data. Three sets of t-test were performed to determine the significance of the differences (*p*-values) between K5 and Z-200, between K5 and Z-400, and between Z-200 and Z-400 (Appendix A). The mean values with 95% confidence intervals expressed as error bars are illustrated in all figures.

## 4.5 Results and discussion

### 4.5.1 System performance

The kinetic study of the three MBBR reactors operated under identical experimental conditions (SALR of  $6.0 \pm 0.8$  g-sBOD/m<sup>2</sup>·d, hydraulic flowrate of  $3.7 \pm 0.1$  L/h, HRT of 1.1 h, temperature of  $18.0 \pm 1.0$  °C and pH  $7.8 \pm 0.1$ ) was performed to investigate the effects of carrier's geometric properties and different levels of biofilm thickness on carbonaceous and ammonia removal performance. This study was conducted at normal (moderate) loaded conditions ( $<8$  g-BOD/m<sup>2</sup>·d (Ødegaard et al., 2010)) to reduce the negative impacts of high loadings on MBBR system performance and carrier clogging. The sBOD and sCOD of the influent were  $24.2 \pm 4.1$  mg/L and  $59.8 \pm 9.5$  mg/L, respectively, with an sCOD to sBOD ratio of  $2.5 \pm 0.1$  during the study (Table 4-1). The highest sBOD removal rate of  $3.8 \pm 0.3$  g-sBOD/m<sup>2</sup>·d and removal efficiency of  $59.9 \pm 3.0\%$  sBOD was observed in the reactor housing the K5 carriers, along with the lowest sBOD concentration of  $9.6 \pm 2.4$  mg-sBOD/L in the effluent. Correspondingly, the MBBR with K5 carriers demonstrated sCOD removal rate of  $5.0 \pm 0.7$  g-sCOD/m<sup>2</sup>·d (removal efficiency of  $31.5 \pm 4.0\%$  sCOD) while the obtained sCOD removal rate for Z-200 and Z-400 MBBRs was  $3.4 \pm 0.7$  and  $2.8 \pm 0.8$  g-sCOD/m<sup>2</sup>·d, respectively, which is statistically significantly lower ( $\approx 45-79\%$  lower) than K5 ( $p$ -value  $< 0.05$ ). However, the comparison between the two Z-carriers did not show a statistically significant difference in carbonaceous removal rates and efficiencies ( $p$ -value = 0.65) (Table 4-1).

**Table 4-1:** Influent and effluent wastewater characteristics (n ≈ 10) along with operational conditions for the three reactors.

Constituent & units (Average ± 95 % CI)	Influent	Effluent		
		K5	Z-200	Z-400
TSS (mg/L)	49.8 ± 7.0	53.4 ± 8.5	70.4 ± 13.0	65.5 ± 10.5
VSS (mg/L)	38.2 ± 3.0	42.2 ± 4.0	53.3 ± 6.5	50.9 ± 6.6
COD (mg/L)	111.6 ± 14.1	104.7 ± 10.9	113.2 ± 10.6	110.4 ± 8.4
BOD (mg/L)	51.9 ± 6.3	55.1 ± 6.1	73.0 ± 8.0	60.5 ± 4.9
sCOD (mg/L)	59.8 ± 9.5	41.5 ± 5.8	45.3 ± 4.2	48.4 ± 4.4
sBOD (mg/L)	24.2 ± 4.1	9.6 ± 2.4	11.5 ± 1.3	12.6 ± 1.6
TAN,( NH <sub>3</sub> /NH <sub>4</sub> <sup>+</sup> -N mg/L)	16.8 ± 1.6	15.2 ± 1.6	15.3 ± 1.8	15.6 ± 1.7
Nitrite, (NO <sub>2</sub> <sup>-</sup> -N mg/L)	0.0 ± 0.0	0.2 ± 0.1	0.2 ± 0.1	0.2 ± 0.1
Nitrate, (NO <sub>3</sub> <sup>-</sup> -N mg/L)	2.9 ± 0.2	2.4 ± 0.2	2.7 ± 0.4	2.6 ± 0.1
VSS/TSS ratio (%)	77.6 ± 4.7	82.0 ± 4.4	79.9 ± 5.0	79.5 ± 3.4
COD/BOD	2.2 ± 0.1	1.8 ± 0.1	1.6 ± 0.1	1.8 ± 0.1
sCOD/sBOD	2.5 ± 0.1	4.4 ± 0.5	4.1 ± 0.4	4.0 ± 0.3
sBOD SARR (g-sBOD/ m <sup>2</sup> ·d)	-	3.8 ± 0.3	2.9 ± 0.4	2.6 ± 0.5
sCOD SARR(g-sCOD/ m <sup>2</sup> ·d)	-	5.0 ± 0.7	3.4 ± 0.7	2.8 ± 0.8
TAN SARR(g-TAN/ m <sup>2</sup> ·d)	-	0.4 ± 0.1	0.4 ± 0.1	0.4 ± 0.1
<b>Operational conditions for all reactors</b>				
SALR (g-sBOD/ m <sup>2</sup> ·d)	6.0 ± 0.8	HRT (hr)		1.1 ± 0.0
SALR(g-sCOD/ m <sup>2</sup> ·d)	14.9 ± 1.6	Temperature (°C)		18.0 ± 1.0
SALR(g-TAN/ m <sup>2</sup> ·d)	4.1 ± 0.3	DO (mg/L)		6.5 ± 0.5

Nitrification was not occurred in the reactors, probably due to the high C/N ratio of the influent (Yadu et al., 2018). A low TAN removal rate of  $0.4 \pm 0.1$  g-TAN/m<sup>2</sup>·d (less than 11% removal efficiency) was likely the nitrogen assimilation by cells. Therefore, the results indicated that the carbonaceous removal performance of the MBBR reactors was significantly affected by the carrier geometric properties, K5 versus Z-carriers, and not by the levels of thickness restraint, 200 versus 400 μm of biofilm thickness. Statistical analysis confirmed that cylindrically shaped K5 carriers with protected biofilm inside the voids show significantly higher removal rates compared to the saddle-shaped Z-carriers with the biofilm on the exposed substratum (*p*-value <

0.05 for the t-test). However, the level of biofilm thickness, 200  $\mu\text{m}$  versus 400  $\mu\text{m}$ , did not significantly impact the MBBR removal performance in this study. Previous studies on nitrifying MBBR with Z-carriers also showed that the ammonium removal was not affected by the biofilm thickness (Piculell et al., 2016b).

#### **4.5.2 Biofilm characteristics (Thickness/mass/ density)**

The attached biofilm is an essential factor in MBBR systems to ensure biological treatment. Therefore, biofilm properties such as thickness, mass and density were quantified for various carriers at the experimental conditions of SALR of  $6.0 \pm 0.8 \text{ g-sBOD/m}^2 \cdot \text{d}$  to investigate the effect of carrier geometry and levels of biofilm thickness restraint on the biofilm properties. According to the results, the statistically significant thickest biofilm grew inside the protected and non-limited voids of K5 carriers compared to Z-carriers (Figure 4-1). The biofilm grown on K5 with an average thickness of  $281.1 \pm 8.7 \mu\text{m}$  was 60-150 % thicker than the biofilm grown on the outside of the saddle-shaped Z-carrier. The overall average of biofilm thickness on the Z-carriers was  $111.6 \pm 11.3 \mu\text{m}$  for Z-200 and  $174.3 \pm 11.1 \mu\text{m}$  for Z-400 carrier even though the Z-carriers are designed to limit the biofilm thickness up to the predefined maximum thickness of 200  $\mu\text{m}$  and 400  $\mu\text{m}$ , respectively (Piculell et al., 2016b). Although the Z-carriers successfully maintained the biofilm thickness below the predefined maximum thicknesses, the overall average thickness was lower than the maximum allowed biofilm thicknesses designed for the Z-carriers, similar to previous studies (Piculell et al., 2016b). This difference could be explained by the drastic variation of the biofilm thickness on different sides of each individual Z-carrier (Arabgol et al., 2020). Thinner biofilm on one side and thicker biofilm on the other side of the Z-carriers could result from carrier stacking due to the carrier shape. Two closely stacked carriers could hinder one side of the carrier from exposure to an adequate supply of substrate. This phenomenon affected not only the biofilm

growth but also might affect the removal rates (Table 4-1), as demonstrated by the Z-carriers showing significantly lower carbonaceous removal efficiency (30-45% lower COD removal rate compared to K5).

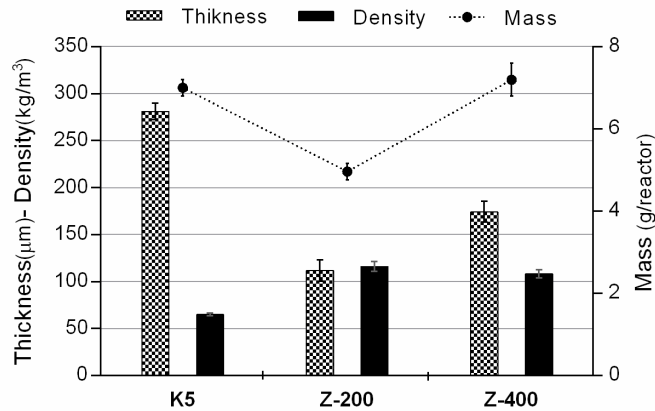


**Figure 4-1:** Biofilm thickness, density and biomass for different reactors

In addition, the total attached biofilm mass in each reactor is calculated by measuring the dry biofilm mass per carrier and multiplying this value with the number of carriers in each reactor. Significantly higher biofilm mass is measured per K5 carrier ( $43.9 \pm 1.0$  mg) compared to Z-carriers, as K5 has a thicker biofilm and higher surface area ( $2420 \text{ mm}^2/\text{carrier}$ ) than Z-carriers. Furthermore, comparing Z-200 and Z-400 with a similar surface area ( $1280 \text{ mm}^2/\text{carrier}$ ) demonstrated an increase in dry biofilm mass with the increase in biofilm thickness per carrier, as higher biofilm mass is observed for Z-400 than Z-200 ( $16.5 \pm 0.7$  mg and  $24.0 \pm 2.1$  mg per Z-200 and Z-400 carrier, respectively). Considering 160 carriers in the K5 reactor and 300 carriers in the Z-reactors, which resulted in a similar surface area of  $0.38 \text{ m}^2$  per reactor, a dry biofilm mass of  $7.0 \pm 0.2$  g,  $5.0 \pm 0.2$  g and  $7.2 \pm 0.4$  g is calculated in K5, Z-200 and Z-400 reactors, respectively (Figure 4-3). These numbers are consistent with previous studies on nitrifying MBBR reactors using Z-400 carriers ( $14.1 \pm 0.5 \text{ g-TS/m}^2$ ) (Piculell et al., 2016b).

Statistical analyses confirmed that the biofilm densities differ between the two carrier types (K5 versus Z-carriers). The biofilm density was calculated from  $65 \pm 1.5 \text{ kg/m}^3$  for K5 to  $116 \pm 5.3$  and  $108 \pm 4.3 \text{ kg/m}^3$  for Z-200 and Z-400, respectively, which is comparable with the range of typical biofilm densities from previous studies (Young et al., 2017). Although similar biofilm mass is measured in the K5 and Z-400 reactors, the statistically significant smaller biofilm thickness of Z-400 resulted in a denser biofilm on Z-400 carriers as compared to K5. Therefore, the highest biofilm thickness led to the lowest biofilm density equal to  $65.0 \pm 1.5 \text{ kg/m}^3$  on K5 carriers. However, the biofilm density is not statistically significantly affected by the different levels of biofilm thickness restraint, comparing Z-200 versus Z-400 carriers ( $p$ -value = 0.11).

The results indicate that the carrier geometric properties significantly affected biofilm characteristics. As such, Z-carriers demonstrated a different biofilm growth pattern and biofilm properties as compared to conventional K5 carriers. Since the hydrodynamic conditions have been shown to affect biofilm density, it may be expected to observe a decrease in biofilm thickness (thinner biofilm) with increasing shear stress and increasing detachment forces related to particle-particle collisions (Vieira et al., 1993; Kwok et al., 1998; Laspidou and Rittmann, 2004). Moreover, previous studies illustrated that biofilm density affects penetration and mass transfer of oxygen and available substrate to embedded cells (Vieira et al., 1993). This study shows that the biofilm thickness and mass in each reactor cannot be used as a direct indicator of system performance, as different performance is observed for K5 and Z-400 carriers with the same amount of attached biofilm mass in the reactor. Different physical properties (i.e. shape and size) of Z-carriers with the exposed biofilm to additional shear stress could explain the relation of thinner and denser biofilm on Z-carriers with the resulting higher solids production and lower system performance in comparison with K5.

### 4.5.3 Biofilm morphology

The acquired VPSEM images illustrate the differences in biofilm structure on different carrier types. As such, more filamentous morphology is observed on the surface of the Z-carriers biofilm as compared to K5 carriers (Figure 4-2). However, the biofilm morphology did not differ between the two Z-carriers. Since the biofilm density on saddle-shaped Z-carriers was significantly higher than cylindrical-porous K5 carriers, the findings of this study contrast with previous studies that have postulated that a decrease in biofilm density in thick biofilms is attributed to filamentous biofilm morphology (Jang et al., 2003; Karizmeh et al., 2014; Young et al., 2016b). Therefore, this study showed that the Z-carriers with a completely different designed shape (Z-carriers with exposed biofilm and surface area compared to porous carriers with protected voids) show a different biofilm morphology, which might lead to different solids characteristics and settleability.

The higher organisms observed at the surface of the biofilm of all carriers in this study were mostly nematodes (the small upper right image in Figure 4-2a), ciliates (the small upper right image in Figure 4-2b) and rotifers (the small upper right image in Figure 4-2c). There were numerous ciliates present in the biofilms of the three carriers. However, stalked ciliates were seen to be a predominant feature on Z-carriers, while the free ciliates were more dominant on K5. Therefore, the results indicate that the meso-scale environments developed on each carrier type could differ and hence might result in the proliferation of different biota (Karizmeh et al., 2014; Young et al., 2016a).

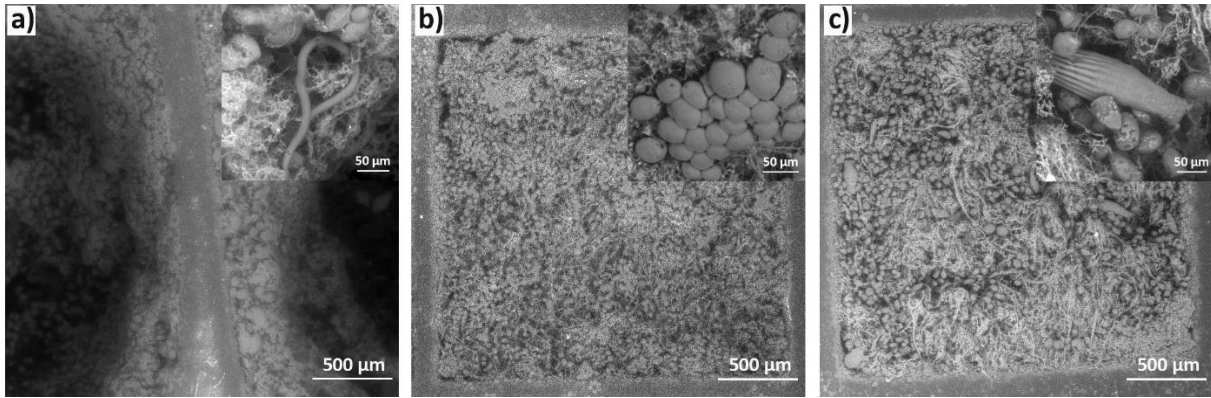


**Figure 4-2:** VPSEM images of biofilm at 60× magnification with a small insert image, at the upper right of each image, at higher magnification of 600× for (a) K5, (b) Z-200, and (c) Z-400 carriers

#### 4.5.4 Solids analysis

The TSS and VSS concentrations (Table 4-1), solids production and biofilm detachment rate in the effluent of each reactor were analyzed to investigate the effect of carrier geometrics and levels of thickness restraint on solids production (Figure 4-3). The effluent TSS contains fragments of detached biofilm from the carriers in addition to the influent suspended solids. Due to the short HRT in this study (~1 hr), the influent particulate matter was presumed to remain unchanged in MBBR systems, and the hydrolysis effects were considered negligible (Ivanovic and Leiknes, 2012) to simplify the calculations. Therefore, solids production is defined as the difference between the influent and effluent TSS mass flow rate, and the detachment rate is the normalized solids production per surface area of carriers in the reactor.

The influent wastewater feeding the reactors contains an average of  $49.8 \pm 7.0$  mg-TSS/L with  $77.9 \pm 4.5\%$  VSS (Table 4-1). Although the effluent TSS concentration for all carriers was not significantly different, the K5 carriers showed the statistically significantly lowest (at 95% confidence level) solids production and biofilm detachment rate of  $0.7 \pm 0.3$  g-TSS/d and  $1.7 \pm 0.7$  g-TSS/ m<sup>2</sup>·d, respectively (Figure 4-3). Low solids production could be an indication of a

stable biofilm that was not actively sloughing. K5 carriers showed a statistically significant 53-65% lower solid production than the Z-carriers of this study ( $p$ -value  $< 0.05$  for the t-test). In addition, a greater solids production stability and detachment rate stability were observed for K5 carriers, as indicated by the lower variation/fluctuation in values and hence smaller confidence intervals.

However, the comparison of the Z-200 and Z-400 carriers did not demonstrate a significant difference in solids production ( $p$ -value = 0.36) and, likewise, does not show a significant change in detachment rates ( $p$ -value = 0.47). The amount of solids produced in the Z-200 reactor was  $1.7 \pm 0.7$  g-TSS/d ( $5.0 \pm 2.0$  g-TSS/  $m^2 \cdot d$ ), which was not scientifically different from the  $1.3 \pm 0.4$  g-TSS/d ( $3.7 \pm 1.0$  g-TSS/  $m^2 \cdot d$ ) produced in the Z-400 reactor. Overall, it can be concluded that the carrier geometric properties significantly affected the solids production and biofilm detachment rate due to the different shapes of the carriers and likely differing hydraulic shear stress. On the contrary, no significant difference in the solids production and biofilm detachment rate could be observed with respect to the levels of biofilm thickness between the two Z-carriers, where the Z-200 carrier being designed for greater biofilm thickness-restraint.

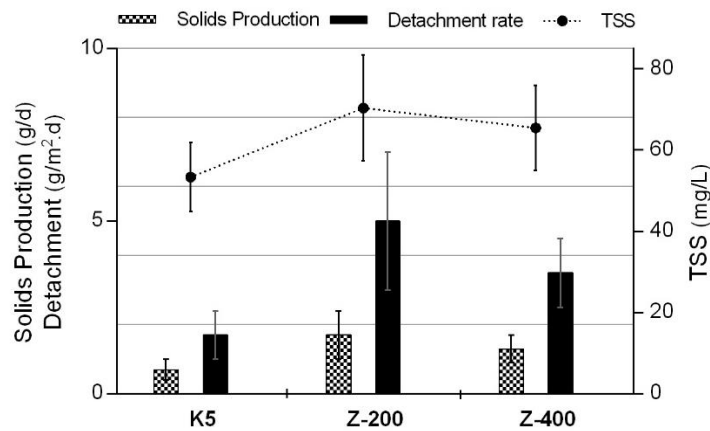


**Figure 4-3:** TSS concentration, solids production and detachment rate for different reactors

#### 4.5.5 Particle settling velocity distribution (PSVD)

To achieve a better understanding of the potential impacts of carrier type and biofilm thickness-restraint on settling behaviour, ViCAs tests were performed on influent and effluent samples collected from the MBBR systems to investigate the particle settling velocity distribution over 4 hours of settling. The ViCAs test reproducibility was first assessed for MBBR effluent during preliminary work in this study, which indicated a good level of repeatability similar to previous studies (Gromaire et al., 2008; Plana et al., 2020). The average of three ViCAs tests is plotted with the 95% confidence intervals shown as error bars (Figure 4-4). The error bars tend to increase for lower settling velocities, as it varies approximately from 1% for higher settling velocity to 5% for lower settling velocities (Gromaire et al., 2008; Plana et al., 2020). The PSVD graphs reveal the cumulative mass percentage of the particles (y-axis) with a corresponding settling velocity below  $V_s$  on the x-axis. Therefore, the lower ViCAs curves are indicative of samples containing a higher fraction of rapidly settling particles. As such, according to the graphs (Figure 4-4), K5 demonstrated statistically different behaviour than Z-carriers ( $p$ -value < 0.05), while the settling behaviour of the two Z-carriers was considerably similar. The K5 PSVD curve is located below the Z-carriers curves, which is an indication of a better settleability of the K5 effluent particles. Since the typical design overflow rate of settling tanks for normally loaded MBBR (< 8 g BOD/m<sup>2</sup>·d) and primary clarified wastewater is 0.5 m/h (Ødegaard et al., 2010), the cumulative mass percentage of particles with  $V_s$  below 0.5 m/h is 46%, 56% and 58% for K5, Z-200 and Z-400 carriers, respectively (Figure 4-4a). In other words, 54%, 44% and 42% of the total particle mass will settle in such a clarifier. This demonstrates that K5 effluent contains a larger, fast settling fraction of solids compared to the Z-carriers effluent.

Previous studies have investigated a wide range of TSS concentrations for different types of wastewater and demonstrated a positive correlation between PSVD and TSS concentration, where the higher TSS concentration has a higher fraction of faster settling particles and a lower located PSVD curve (Maruėjouls et al., 2013; Bachis et al., 2015). However, none of these studies were focused on MBBR effluent with lower solids concentration. In this study, although the TSS concentration for the three different reactors ranged between 50 to 70 mg/L and was not significantly different (Table 4-1), an obvious distinction is observed between the PSVD curves for the different carrier types. K5 with the lowest effluent TSS concentration demonstrated significantly better settling behaviour compared to the effluent of the Z-carriers MBBR reactors. The biofilm thickness-restraint Z-200 carrier showed similar settling behaviour to the Z-400 carrier ( $p$ -value = 0.56).

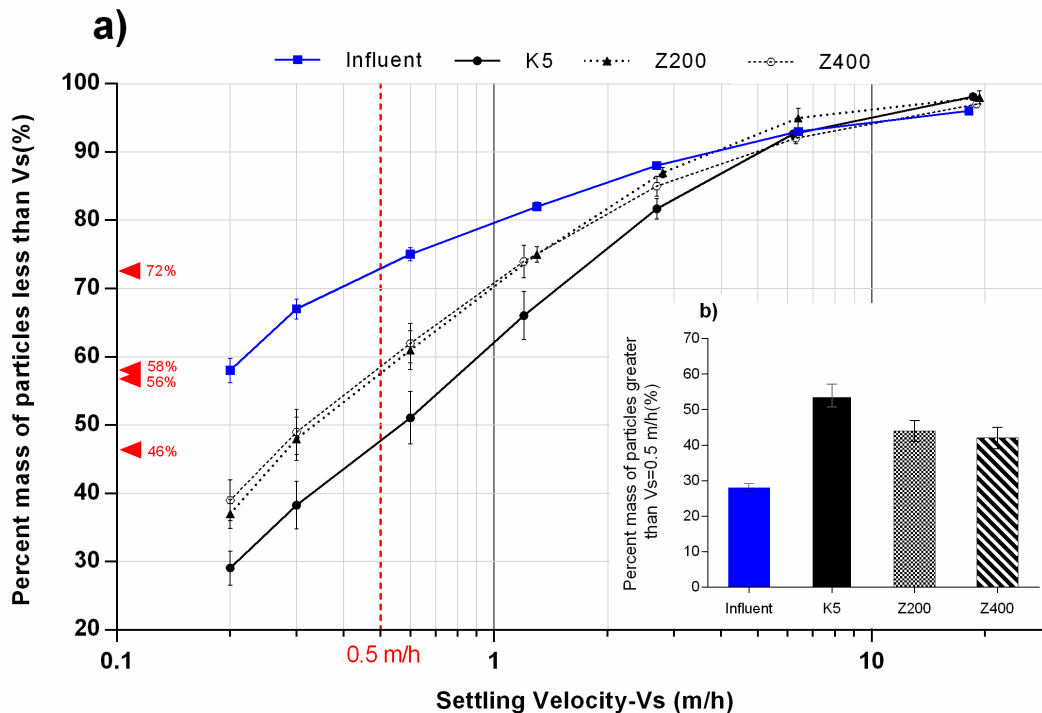


**Figure 4-4:** (a) Particle settling velocity distribution curves for influent and effluent of MBBRs with different types of carriers, and (b) the percentage of particles with a velocity faster than 0.5 m/hr

#### 4.5.6 Particle size distribution (PSD)

The PSD in this study was analyzed for TSS collected at certain time intervals of the ViCAs test. Therefore, the settled particles in the ViCAs cups collected after 2, 30 and 240 minutes of settling were imaged and analyzed to investigate the effect of carrier types and thickness-restraint on particle characteristics over time (Figure 4-5). The size of particles is an important parameter with respect to the settling properties. Since the particles in wastewater are not uniformly circular and spherical, the size of irregular particles are simplified, considering particles as a circle and defining an equivalent circular diameter (ECD). Therefore, the accumulative percent volume of particles across the ECD is graphed to investigate the PSD of each reactor effluent. The results indicate that larger particles settle faster, and the majority of particles with larger ECD settle within the first 30 minutes of the study. Particles of the K5 MBBR demonstrated different characteristics than particles of the Z-carrier MBBR systems as K5 MBBR effluent particles contain considerably larger solids, leading to better settling behaviour.

The excess of smaller particles in the two samples from the Z-carriers MBBRs may lead to lower TSS removal and poor settling behaviour compared to MBBR with K5 carriers. The evolution of the PSD curves across settling time demonstrates similar particle size distributions between the two thickness-restraint Z-carriers MBBR effluent. Moreover, the measured median particle diameter,  $D_{50}$ , shows a drastic decrease for K5 effluent particles from 665  $\mu\text{m}$  to 145  $\mu\text{m}$  after 4 hours of settling. Although a decreasing trend was observed for Z-carriers, Z-carriers show a lower decrease in the particle diameters before and after settling as compared to K5. The  $D_{50}$  decreased from 323  $\mu\text{m}$  to 113  $\mu\text{m}$  and 256  $\mu\text{m}$  to 117  $\mu\text{m}$  for Z-200 and Z-400, respectively (Figure 4-6). It is noteworthy that the influent did not contain large particles, and the particle size did not show drastic changes over time. This may be explained by the fact that all the fast settleable

particles have already settled in the primary clarifier as the primary clarified wastewater was used to feed the reactors in this study.

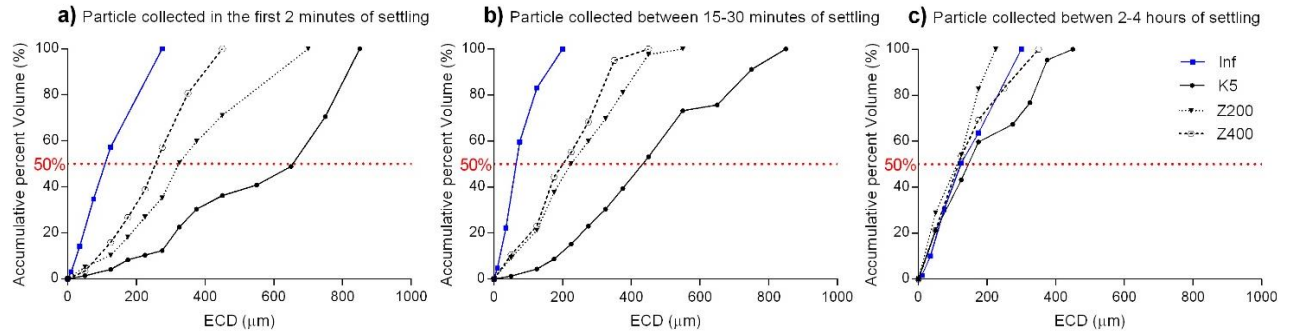


**Figure 4-5:** Accumulative particle size distribution of particles collected (a) in the first 2 minutes, (b) between the 15–30 minutes, and (c) between 2–4hours (= 240 minutes) of settling for different reactors effluents.

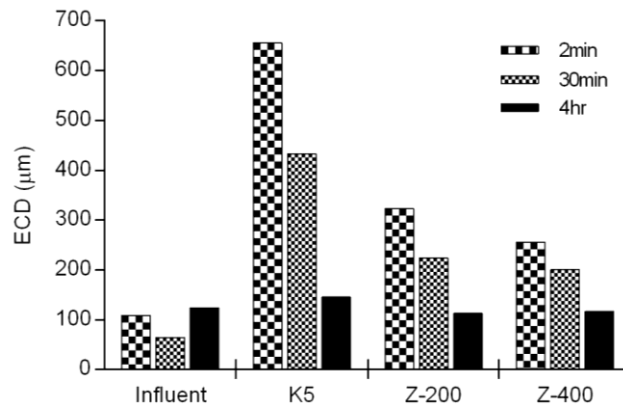


**Figure 4-6:** D<sub>50</sub> measured over different time intervals for different carrier types

Along with characterizing the PSD of settled particles over time by applying bright-field microscopy images, the PSD was also studied using DPA for the three MBBR effluents before and after 4 hours of settling (Arabgol et al., 2020). The integrated area under the curves (Figure 4-7a) shows the total volume of unsettled effluent particles in the K5, Z-200 and Z-400 reactors before and after 4 hours of settling. The results indicated that K5 effluent contains a statistically

significant higher percent volume of large particles as compared to Z-carriers ( $61.6 \pm 2.3\%$  greater than  $400 \mu\text{m}$ ) (Figure 4-7b). However, a similar PSD trend was observed for Z-carriers with a higher percentage of small particles. Since the bright-field microscopy is performed on raw samples without preparation and the DPA test is done after filtering out the particles larger than  $400 \mu\text{m}$  (to enable passage of particles in the measurement chamber), the results of the two PSD tests may not be comparable, especially for samples with high TSS concentration. As such, some particles might have a small ECD with a long chord length (maximum Feret's diameter) larger than  $400 \mu\text{m}$  that could filter out in the DPA test (Figure 4-8). However, the DPA test (Figure 4-7) supported the fact that K5 demonstrated better settleability (Figure 4-4a) in comparison with Z-carriers as it contains larger particles that can settle faster as opposed to the Z-carriers (Figure 4-5). Moreover, the thickness-restraint carriers did not show sufficient difference in particle size distribution and the PSD that can be explained by the different particle characteristics.

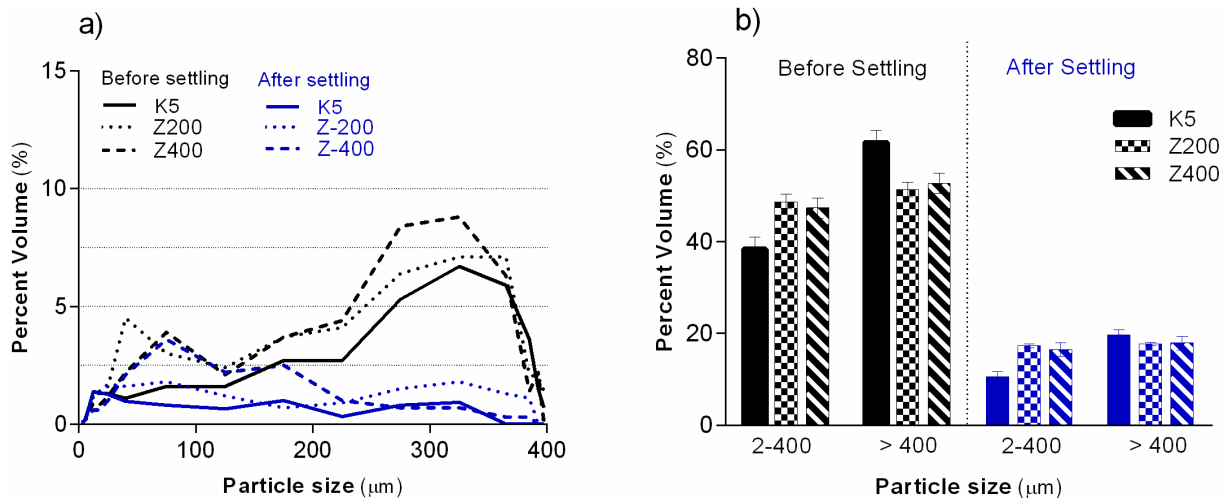


**Figure 4-7:** Particle size distribution curves for different carriers before (in black colour) and after (in blue colour) 4 hours of settling

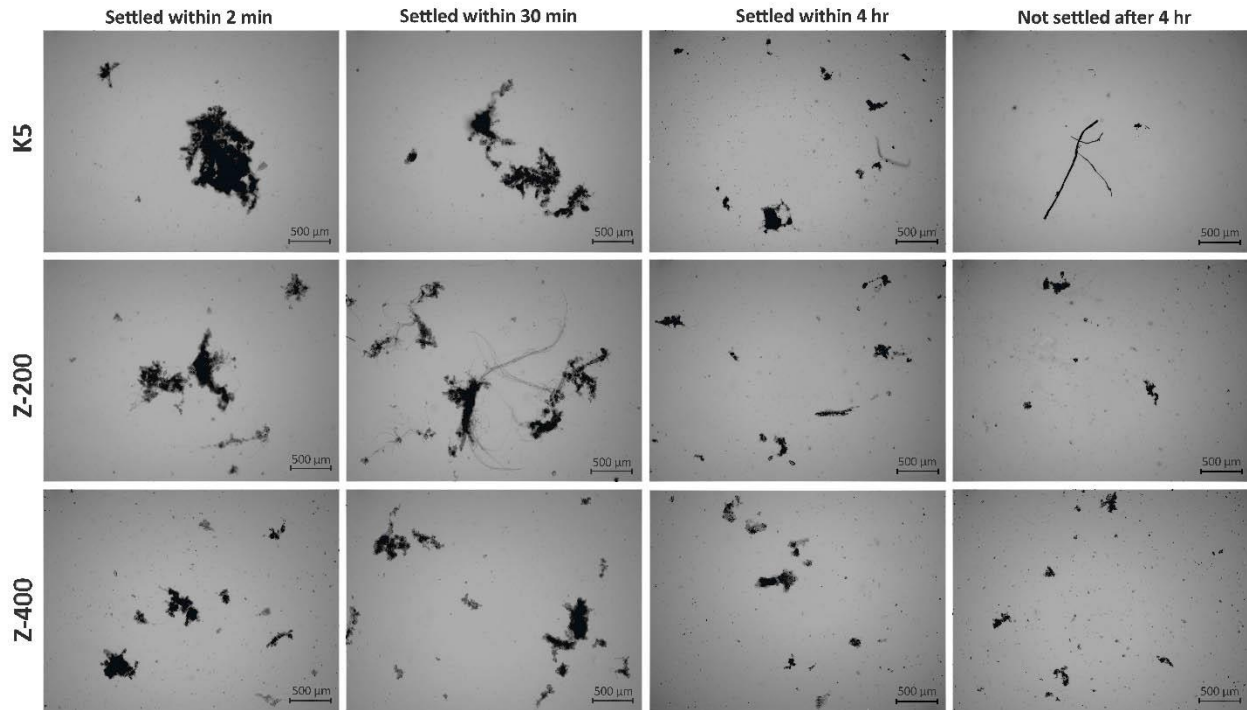


**Figure 4-8:** Microscopy images of settled and non-settled particles over the time for K5, Z-200 and Z-400 effluent

## 4.6 Conclusion

The current literature lacks studies on the characteristics and settling behaviour of MBBR effluent particles. This study aimed to investigate the effects of carrier geometric properties and different levels of biofilm thickness on carbonaceous MBBR system performance, biofilm characteristics and morphology, solids production, effluent particle settling velocity distribution, as well as particle size distribution. The ViCAs assay, which has not previously been used to characterize MBBR-produced solids, was used to quantify the PSVD of the MBBR effluent and settling behaviour of the particles. This method was combined with microscopy imaging to analyze the PSD. The application of two different types of carrier, conventional K5 versus newly designed Z-carriers, under consistent operational conditions (SALR of  $6.0 \pm 0.8$  g-sBOD/m<sup>2</sup>·d and a constant HRT of 1.1) proved a statistically significant effect of carrier geometry on system

performance, biofilm properties and morphology, solids production, PSVD and PSD. The effluent of K5 carriers with higher biofilm mass and higher biofilm thickness showed a higher fraction of larger particles that settle faster. However, the thickness-restraint carrier, Z-200 compared to the Z-400 carrier, did not show significantly different results, which means that the levels of thickness restraint in this study, 200 versus 400  $\mu\text{m}$ , would not significantly affect the system performance, biofilm properties and morphology, solids characteristics, PSVD and PSD. The two Z-carriers showed a similar trend in PSD and PSVD and, hence, similar settling behaviour.

## 4.7 References

- Åhl, R. M., Leiknes, T., and Ødegaard, H. (2006). “Tracking particle size distributions in a moving bed biofilm membrane reactor for treatment of municipal wastewater.” *Water Science and Technology*, 53(7), 33–42.
- Aiguier, E., Chebbo, G., Bertrand-Krajewski, J.-L., Hedges, P., and Tyack, N. (1996). “Methods for determining the settling velocity profiles of solids in storm sewage.” *Water Science and Technology*, 33(9), 117–125.
- APHA, A. (2005). “Standard Methods for the Examination of Water and Wastewater.” *USA: Washington DC, USA*.
- Arabgol, R., Vanrolleghem, P. A., Piculell, M., and Delatolla, R. (2020). “The impact of biofilm thickness-restraint and carrier type on attached growth system performance, solids characteristics and settleability.” *Environmental Science: Water Research & Technology*, 6(10), 2843–2855.
- Bachis, G., Maruéjols, T., Tik, S., Amerlinck, Y., Melcer, H., Nopens, I., Lessard, P., and Vanrolleghem, P. A. (2015). “Modelling and characterization of primary settlers in view of whole plant and resource recovery modelling.” *Water Science and Technology*, 72(12), 2251–2261.
- Barwal, A., and Chaudhary, R. (2014). “To study the performance of biocarriers in moving bed biofilm reactor (MBBR) technology and kinetics of biofilm for retrofitting the existing

- aerobic treatment systems: A review.” *Reviews in Environmental Science and Biotechnology*, 13(3), 285–299.
- Bassin, J. P., and Dezotti, M. (2018). “Moving Bed Biofilm Reactor (MBBR).” *Advanced Biological Processes for Wastewater Treatment*, Springer, Cham, 37–75.
- Berrouard, E. (2010). “Caractérisation de la décantabilité des eaux pluviales.” M.Sc. thesis, Université Laval, QC, Canada.
- Chebbo, G., and Gromaire, M.-C. (2009). “VICAS—An operating protocol to measure the distributions of suspended solid settling velocities within urban drainage samples.” *Journal of Environmental Engineering*, 135(9), 768–775.
- Delatolla, R., Berk, D., and Tufenkji, N. (2008). “Rapid and reliable quantification of biofilm weight and nitrogen content of biofilm attached to polystyrene beads.” *Water Research*, 42(12), 3082–3088.
- Delatolla, R., Tufenkji, N., Comeau, Y., Gadbois, A., Lamarre, D., and Berk, D. (2010). “Investigation of laboratory-scale and pilot-scale attached growth ammonia removal kinetics at cold temperature and low influent carbon.” *Water Quality Research Journal*, 45(4), 427–436.
- Delatolla, R., Tufenkji, N., Comeau, Y., Lamarre, D., Gadbois, A., and Berk, D. (2009). “In situ characterization of nitrifying biofilm: Minimizing biomass loss and preserving perspective.” *Water Research*, 43(6), 1775–1787.
- Dias, R. A., Martins, R. C., Castro, L. M., and Quinta-Ferreira, R. M. (2018). “Biosolids production and COD removal in activated sludge and moving bed biofilm reactors.” *WASTES – Solutions, Treatments and Opportunities II*, Taylor & Francis Group, London, 271–276.
- Forrest, D., Delatolla, R., and Kennedy, K. (2016). “Carrier effects on tertiary nitrifying moving bed biofilm reactor: An examination of performance, biofilm and biologically produced solids.” *Environmental Technology*, 37(6), 662–671.
- Grijpspeerd, K., and Verstraete, W. (1997). “Image analysis to estimate the settleability and concentration of activated sludge.” *Water Research*, 31(5), 1126–1134.

- Gromaire, M. C., Kafi-Benyahia, M., Gasperi, J., Saad, M., Moilleron, R., and Chebbo, G. (2008). “Settling velocity of particulate pollutants from combined sewer wet weather discharges.” *Water Science and Technology*, 58(12), 2453–2465.
- Hasler, M. (2007). “Field and laboratory experiments on settling process in stormwater storage tanks.” Graz University of Technology, Austria.
- Ivanovic, I., and Leiknes, T. O. (2012). “Particle separation in moving bed biofilm reactor: Applications and opportunities.” *Separation Science and Technology*, 47(5), 647–653.
- Jang, A., Bishop, P. L., Okabe, S., Lee, S. G., and Kim, I. S. (2003). “Effect of dissolved oxygen concentration on the biofilm and in situ analysis by fluorescence in situ hybridization (FISH) and microelectrodes.” *Water Science and Technology*, 47(1), 49–57.
- Karizmeh, M. S., Delatolla, R., and Narbaitz, R. M. (2014). “Investigation of settleability of biologically produced solids and biofilm morphology in moving bed bioreactors (MBBRs).” *Bioprocess and Biosystems Engineering*, 37(9), 1839–1848.
- Kwok, W. K., Picioreanu, C., Ong, S. L., Van Loosdrecht, M. C. M., Ng, W. J., and Heijnen, J. J. (1998). “Influence of biomass production and detachment forces on biofilm structures in a biofilm airlift suspension reactor.” *Biotechnology and Bioengineering*, 58(4), 400–407.
- Lapidou, C. S., and Rittmann, B. E. (2004). “Modeling the development of biofilm density including active bacteria, inert biomass, and extracellular polymeric substances.” *Water Research*, 38(14–15), 3349–3361.
- Mannacharaju, M., Natarajan, P., Villalan, A. K., Jothieswari, M., Somasundaram, S., and Ganesan, S. (2018). “An innovative approach to minimize excess sludge production in sewage treatment using integrated bioreactors.” *Journal of Environmental Sciences*, Elsevier B.V., 67, 67–77.
- Maruéjols, T., Lessard, P., and Vanrolleghem, P. A. (2014). “Impact of particle property distribution on hydrolysis rates in integrated wastewater modelling.” *13th International Conference on Urban Drainage, Sarawak, Malaysia*.
- Maruejols, T., Lessard, P., Wipliez, B., Pelletier, G., and Vanrolleghem, P. A. (2011). “Characterization of the potential impact of retention tank emptying on wastewater primary

- treatment: A new element for CSO management.” *Water Science and Technology*, 64(9), 1898–1905.
- Maruéjols, T., Vanrolleghem, P. A., Pelletier, G., and Lessard, P. (2013). “Characterisation of retention tank water quality: particle settling velocity distribution and retention time.” *Water Quality Research Journal*, 48(4), 321–332.
- McQuarrie, J. P., and Boltz, J. P. (2011). “Moving bed biofilm reactor technology: Process applications, design, and performance.” *Water Environment Research*, 83(6), 560–575.
- Melin, E., Leiknes, T., Helness, H., Rasmussen, V., and Ødegaard, H. (2005). “Effect of organic loading rate on a wastewater treatment process combining moving bed biofilm and membrane reactors.” *Water Science and Technology*, 51(6–7), 421–430.
- Ødegaard, H. (2016). “A road-map for energy-neutral wastewater treatment plants of the future based on compact technologies (including MBBR).” *Frontiers of Environmental Science & Engineering*, 10(4), 2.
- Ødegaard, H., Cimbritz, M., Christensson, M., and Dahl, C. P. (2010). “Separation of biomass from moving bed biofilm reactors (MBBRs).” *Proceedings of the Water Environment Federation*, 2010(7), 212–233.
- Ødegaard, H., Gisvold, B., and Strickland, J. (2000). “The influence of carrier size and shape in the moving bed biofilm process.” *Water Science and Technology*, 41(4–5), 383–391.
- Ødegaard, H. (2004). “Sludge minimization technologies - An overview.” *Water Science and Technology*, 49(10), 31–40.
- Piculell, M., Suarez, C., Li, C., Christensson, M., Persson, F., Wagner, M., Hermansson, M., Jönsson, K., and Welander, T. (2016a). “The inhibitory effects of reject water on nitrifying populations grown at different biofilm thickness.” *Water Research*, 104, 292–302.
- Piculell, M., Welander, P., Jönsson, K., and Welander, T. (2016b). “Evaluating the effect of biofilm thickness on nitrification in moving bed biofilm reactors.” *Environmental Technology*, 37(6), 732–743.
- Plana, Q., Carpentier, J., Tardif, F., Pauléat, A., Gadbois, A., Lessard, P., and Vanrolleghem, P.

- A. (2018). “Grit particle characterization: Influence of sample pretreatment and sieving method.” *Water Science and Technology*, 78(6), 1400–1406.
- Plana, Q., Pauléat, A., Gadbois, A., Lessard, P., and Vanrolleghem, P. A. (2020). “Characterizing the settleability of grit particles.” *Water Environment Research*, 92(5), 731–739.
- Schindelin, J., Arganda-Carreras, I., Frise, E., Kaynig, V., Longair, M., Pietzsch, T., Preibisch, S., Rueden, C., Saalfeld, S., Schmid, B., Tinevez, J.-Y., White, D. J., Hartenstein, V., Eliceiri, K., Tomancak, P., and Cardona, A. (2012). “Fiji: an open-source platform for biological-image analysis.” *Nature Methods*, 9(7), 676–682.
- Tijhuis, L., Huisman, J. L., Hekkelman, H. D., van Loosdrecht, M. C. M., and Heijnen, J. J. (1995). “Formation of nitrifying biofilms on small suspended particles in airlift reactors.” *Biotechnology and Bioengineering*, 47(5), 585–595.
- Torfs, E., Nopens, I., Winkler, M., Vanrolleghem, P., Balemans, S., and Smets, I. (2016). “Settling Tests.” *Experimental Methods In Wastewater Treatment*, IWA Publishing, London, UK, 235–262.
- Vallet, B., Muschalla, D., Lessard, P., and Vanrolleghem, P. A. (2014). “A new dynamic water quality model for stormwater basins as a tool for urban runoff management: Concept and validation.” *Urban Water Journal*, 11(3), 211–220.
- Vanrolleghem, P. A., Tik, S., and Lessard, P. (2019). “Advances in modelling particle transport in urban storm- and wastewater systems.” *International Conference on Urban Drainage Modelling*, Green Energy and Technology, (G. Mannina, ed.), Springer International Publishing, Cham, 907–914.
- Vieira, M. J., Melo, L. F., and Pinheiro, M. M. (1993). “Biofilm formation: Hydrodynamic effects on internal diffusion and structure.” *Biofouling*, 7(1), 67–80.
- WEF. (2011). *Moving Bed Biofilm Reactors. WEF Manual of Practice No. 35*, McGraw Hill, Alexandria, Virginia, USA.
- Yadu, A., Sahariah, B. P., and Anandkumar, J. (2018). “Influence of COD/ammonia ratio on simultaneous removal of  $\text{NH}_4^+ - \text{N}$  and COD in surface water using moving bed batch reactor.” *Journal of Water Process Engineering*, 22, 66–72.

- Young, B. (2017). “Nitrifying MBBR performance optimization in temperate climates through understanding biofilm morphology and microbiome.” Ph.D. thesis, University of Ottawa, ON, Canada.
- Young, B., Banihashemi, B., Forrest, D., Kennedy, K., Stintzi, A., and Delatolla, R. (2016a). “Meso and micro-scale response of post carbon removal nitrifying MBBR biofilm across carrier type and loading.” *Water Research*, 91, 235–243.
- Young, B., Delatolla, R., Abujamel, T., Kennedy, K., Laflamme, E., and Stintzi, A. (2017). “Rapid start-up of nitrifying MBBRs at low temperatures: nitrification, biofilm response and microbiome analysis.” *Bioprocess and Biosystems Engineering*, 40(5), 731–739.
- Young, B., Delatolla, R., Ren, B., Kennedy, K., Laflamme, E., and Stintzi, A. (2016b). “Pilot-scale tertiary MBBR nitrification at 1°C: Characterization of ammonia removal rate, solids settleability and biofilm characteristics.” *Environmental Technology*, 37(16), 2124–2132.

# **Chapter 5 – Particle Characteristics and Settling Behaviour of MBBR Produced Solids along with Removal Performance and Biofilm Responses to Various Carbonaceous Loading Rates**

## **5.1 Context**

Chapter 5 presents a version of the article prepared for submission to the Journal of Environmental Sciences and titled: “*Particle Characteristics and Settling Behaviour of MBBR Produced Solids along with Removal Performance and Biofilm Responses to Various Carbonaceous Loading Rates*”. This research describes the MBBR effluent solids characteristics, settling behaviour and the biofilm responses to the various loading rates in addition to the reactor removal performance. This study is the first study using the ViCAs method combined with microscopy imaging to investigate the settling behaviour of MBBR produced particles.

## **5.2 Abstract**

Particles in moving bed biofilm reactor (MBBR) effluents are mostly fragments of biofilm that are detached from the substratum. They are considerably influenced by the reactor’s operational conditions. This study investigates the effect of various loading rates on reactor kinetics, biofilm characteristics, particle characteristics and settling behaviour. The BOD loading rate was increased from 1.5 to 2.5 and 6.0 g-sBOD/m<sup>2</sup>·d (equal to 4.2, 6.5 and 14.9 g-sCOD/m<sup>2</sup>·d, respectively) by decreasing the available surface area provided in the reactor. The ViCAs method is combined with microscopy imaging to analyze particle settling velocity distribution (PSVD) and particle size distribution (PSD). The results obtained indicate a positive correlation between loading rate and removal rate, with the lowest removal rate of  $3.8 \pm 0.3$  g-sBOD/m<sup>2</sup>·d

(corresponding to  $59.9 \pm 3.0\%$  sBOD removal) for the highest loading rate. However, the biofilm response, solid characteristics and settling behaviour were significantly different at the loading rate of  $2.5 \text{ g-sBOD/m}^2\cdot\text{d}$  with no evident trend across the loading rates. The SRT significantly decreases by increasing the SALR, and this worsens the settling characteristics. Moreover, as the study was performed on-site, at a full-scale WRRF, the significant variation of biofilm characteristics might be due to the transition of cold to warm weather that coincidentally occurred during this loading rate variation. The thickest biofilm ( $369.1 \pm 25.5 \mu\text{m}$ ) was shown to occur with the lowest percent coverage of viable cells in the biofilm, the highest solids production and detachment rates ( $2.4 \pm 0.9 \text{ g-TSS/m}^2\cdot\text{d}$ ) and also the largest effluent particles size and fastest particle settling.

### **5.3 Introduction**

Biological wastewater treatment processes are implemented in wastewater treatment technology to remove pollutants through biologically mediated microbial activity. The separation of the solids produced during the biological processes is a critical step to achieving complete biological treatment, as the produced solids have a significant impact on effluent quality (WEF, 2009; Wang, 2012; Metcalf & Eddy, 2014). Over the past decades, the moving bed biofilm reactor (MBBR) has received considerable attention as an add-on and standalone technology to upgrade or replace ageing and existing wastewater treatment infrastructure (Aygun et al., 2008; Delatolla et al., 2010; Young et al., 2016b, 2017a; Ødegaard, 2016; Ahmed et al., 2019). However, the relatively low solids concentrations in MBBR systems do not allow efficient bio-flocculation to occur, as is common in suspended growth treatment systems. The MBBR effluent solids concentration is approximately ten to twenty times lower than that observed in activated sludge systems (Ødegaard, 2006; Ødegaard et al., 2010; Ivanovic and Leiknes, 2012; Metcalf & Eddy,

2014), which leads to a significantly lower settling potential (Melin et al., 2005; Karizmeh et al., 2014). Therefore, it is reported that the MBBR effluents require intense solids separation methods such as filtration, lamella settling, and enhanced sedimentation with pre-coagulation (Ødegaard et al., 2010; Ivanovic and Leiknes, 2012; Bassin and Dezotti, 2018). Few studies have focused on the effluent particle characteristics of biofilm reactors in general, despite the fact that a weak settling potential of MBBR effluent suspended solids have been reported (Ødegaard et al., 2010; Karizmeh, 2012; Ivanovic and Leiknes, 2012; Bassin and Dezotti, 2018). As such, a comprehensive understanding of MBBR-produced solids characteristics and the potential factors that influence their settling behaviour is yet to be achieved.

MBBR-produced solids are mostly fragments of biofilm detached from the substratum due to erosion, abrasion, and sometimes sloughing due to various factors, including predator grazing. These detachment processes considerably depend on the operational conditions of the reactors (Wuertz et al., 2003; Metcalf & Eddy, 2014). Furthermore, the detachment of the biofilm is an important factor that affects the thickness of biofilm in the reactor, the quantity of biomass, the solids retention time in the reactor and the suspended solids concentration of the bulk liquid (Rittmann, 2007). Therefore, it is hypothesized that the MBBR effluent solid characteristics are interconnected with the biofilm characteristics and subsequently with anything that influences the biofilm characteristics (such as operational conditions). The substrate loading rate has been shown to be one of the important operational parameters that can affect the reactor performance (Aygün et al., 2008; Javid et al., 2013). Where increasing the substrate loading rate has demonstrated increases in the production of solids with undesirable floc structures in the effluent, negatively affecting settling performance (Ødegaard, 2000; Ivanovic et al., 2006; Aygün et al., 2008; Javid et al., 2013; Karizmeh et al., 2014). Despite the importance of particle characteristics in solid-liquid

separation, there is still a fundamental lack of understanding of MBBR effluent particle characteristics with respect to the reactor loading rate.

The particle settling velocity distribution (PSVD) and the particle size distribution (PSD) are two parameters conventionally used to understand the particle settling behaviour of wastewater treatment systems (Maruėjouls et al., 2014; Bachis et al., 2015; Torfs et al., 2017; Plana et al., 2020). However, previous studies have largely focused on PSD analysis to quantify the particle characteristics under different operational conditions (Melin et al., 2005; Åhl et al., 2006; Ødegaard et al., 2010; Karizmeh et al., 2014; Young et al., 2016a; Forrest et al., 2016). It has been demonstrated that the PSD correlates well with hydraulic retention time (HRT) and surface area loading rate (SALR). Larger particles were observed at higher HRT (hence, lower SALR) (Ødegaard et al., 2000, 2010; Melin et al., 2005; Åhl et al., 2006). Increasing SALR was reported to decrease solids settleability for both nitrifying and carbon removal MBBR systems (Karizmeh et al., 2014; Young et al., 2016b). In these studies, the settleability of solids was estimated by comparing the PSD before and after a short settling time of 30 minutes. However, no research on the PSVD for MBBR systems currently exists. Thus, the effect of various loading rates on particle settling behaviour has not been studied in sufficient detail, leaving a fundamental gap of knowledge on the topic.

Several methods were developed to measure the PSVD in wastewater systems (Aiguier et al., 1996; Hasler, 2007; Berrouard, 2010), with "Vitesse de Chute en Assainissement" (ViCAs), which has shown good repeatability, becoming a reference method among them (Chebbo and Gromaire, 2009; Vallet et al., 2014). The studies to date have measured the PSVD for different wastewaters and stormwaters using ViCAs (Hasler, 2007; Maruėjouls et al., 2013; Bachis et al., 2015; Vanrolleghem et al., 2019; Plana et al., 2020). However, no study has yet used PSVD analysis

applying ViCAs to investigate the biologically produced MBBR solids with a comprehensive observation of settling behaviour, which will help advance the design of downstream clarifiers for MBBR technology, and ultimately result in enhanced effluent water quality.

The main objective of this research is to extend the current knowledge concerning the settleability of MBBR-produced particles by studying detailed particle characteristics and settling behaviour in an MBBR reactor treating real wastewater. Therefore, the impact of various SALRs on system performance, biofilm characteristics, particle characteristics and their settleability are pursued in this research. Coincidentally, because the experiments were conducted during a seasonal transition period, the effect of temperature along with the SALR is also monitored and discussed in this paper. In particular, the effect of three different SALRs (1.5, 2.5 and 6.0 g-sBOD/m<sup>2</sup>·d) was studied on reactor kinetics, biofilm characteristics and biomass cell viability. Moreover, the relation between biofilm characteristics and particle characteristics, and subsequently, with particle settling behaviour is studied by investigation of biofilm morphology, biofilm thickness, biofilm density, biofilm mass, solids production, detachment rate, PSD and PSVD. Furthermore, this study combines the settling velocity characterization method, ViCAs, along with particle size distribution analysis to comprehensively characterize MBBR effluent solids, which has not previously been performed.

## **5.4 Materials and methods**

### **5.4.1 Experimental setup and reactor operation**

This study was conducted at the Gatineau water resource recovery facility (WRRF), Quebec, Canada. The experimental setup comprised one four-litre reactor housing the AnoxK<sup>TM</sup> K5 carriers (AnoxKaldnes, Lund, Sweden). The K5 carrier, which is commonly used in full-scale applications (Barwal and Chaudhary, 2014), is a flat cylindrical-shaped carrier with a projected diameter of 25

mm, a height of 3.5 mm and an available surface area of 2420 mm<sup>2</sup> per carrier (Piculell, 2016; Bassin and Dezotti, 2018). The reactor was fed with primary clarified wastewater at a constant flow rate of 3.7 ± 0.1 L/h and an HRT of 1.1 hours throughout the experiment. The number of carriers (filling percentage of the carriers) in the reactor was adjusted throughout the experiment to achieve three different loading rates. The steady-state was confirmed at loading rates of 1.5, 2.5 and 6.0 g-sBOD/m<sup>2</sup>·d (equal to 4.2, 6.5 and 14.9 g-sCOD/m<sup>2</sup>·d) by changing the carriers' surface area in the reactor (Table 5-1). Based on the research objectives, these operational conditions were selected in the range of low to normally loaded MBBR systems (Ødegaard et al., 2010; WEF, 2011) to minimize the potential impacts of high loaded operational conditions on MBBR system performance, biofilm and solids characteristics. Since the reactor was operated at a full-scale WRRF and fed with real wastewater, seasonal temperature changes were inevitable. The temperature of the influent wastewater increased from 9 to 13 to 18 °C, respectively, for SALR of 1.5, 2.5 and 6.0 g-sBOD/m<sup>2</sup>·d, which the effects of these two parameters are confounded as will be discussed in the results and discussion section.

**Table 5-1:** Reactor properties for different experimental loading rates

<b>SALR (g-sBOD/m<sup>2</sup>·d)</b>	<b>No. of carriers</b>	<b>Reactor surface area (m<sup>2</sup>/reactor)</b>	<b>Carrier type</b>	<b>Reactor volume (L)</b>	<b>Carrier surface area (mm<sup>2</sup>/carrier)*</b>
<b>1.5</b>	500	1.2	AnoxK <sup>TM</sup> K5	4	2420
<b>2.5</b>	320	0.8			
<b>6.0</b>	160	0.4			

#### 5.4.2 Constituent analysis

To determine the MBBR system performance, wastewater samples were taken from the influent and effluent of the reactor two to three times a week. The samples were analyzed and tested in triplicate within 4 hours of collection. Throughout the study, total and soluble biochemical oxygen demand (BOD and sBOD), total suspended solids (TSS), volatile suspended solids (VSS),

total ammonia nitrogen (TAN), nitrite, and nitrate were analyzed in accordance with Standard Methods (APHA, 2005): methods 5210B-5 day BOD, 2540 D-TSS (TSS dried at 103–105°C) and 2540 E-VSS (fixed and volatile solids ignited at 550°C), 4500-NH<sub>3</sub>, 4500-NO<sub>3</sub><sup>-</sup>, and 4500-NO<sub>2</sub><sup>-</sup>, respectively. Total and soluble chemical oxygen demand (COD and sCOD) concentrations were determined using HACH method 8000 with a HACH DR 5000 Spectrophotometer (HACH, Loveland, CO, USA). Dissolved oxygen (DO), pH and temperature were measured using an HQ40d portable PH/DO meter (HACH, USA).

### **5.4.3 Biofilm characteristics**

A total of nine different carriers were randomly harvested during steady-state from each reactor to characterize the biofilm at the three different loading rates investigated in this study. The biofilm characteristics, including biofilm morphology (using three random carriers), biofilm thickness (using another three random carriers), and biofilm mass (using another three random carriers), were analyzed without any sample preparation to minimize sample destruction prior to analysis (Delatolla et al., 2009; Young, 2017). The biofilm density and age were then calculated using the obtained data to better understand the biofilm characteristics.

To visualize biofilm morphology, a Vega II-XMU variable pressure scanning electron microscopy (VPSEM) (Tescan USA Inc., US, PA) was used to acquire images from the attached biofilm on carriers. At each SALR, a total of 15 VPSEM images were acquired from triplicate carriers with magnifications ranging from 60× to 600× to analyze the biofilm morphology (Karizmeh et al., 2014; Young et al., 2016a). Zeiss Stemi 305 stereoscope (Toronto, Canada) was used to acquire images to determine biofilm thickness. The acquired images were analyzed on Fiji/ImageJ software (Schindelin et al., 2012). All the voids of the triplicate carriers were imaged and analyzed for thickness measurements per condition (Arabgol et al., 2020). The protocol

modified from Delatolla et al. (2008) was used to quantify the attached biofilm mass on triplicate carriers. Briefly, the amount of biofilm mass attached to each carrier is calculated as the difference between the mass of dried carrier with attached biofilm at 105°C and the mass of dried clean carrier at 105°C when the biofilm is washed off (Delatolla et al., 2009; Young et al., 2017a).

Biofilm density is expressed as the dry weight of biofilm per unit volume. Therefore, the density was calculated using the biofilm thickness and mass data by considering the carriers' surface area (density = Biofilm mass/(Biofilm thickness × Surface area)). As a good indicator of biofilm age, solids retention time (SRT) was calculated as the biofilm mass in the reactor (attached biofilm) divided by solids mass flow rate that leaves the reactor (Karizmeh, 2012). The average of triplicate biofilm thickness, mass and density were reported as the mean value at each experimental condition.

#### **5.4.4 Cell viability and microbial activity**

Cell viability (live/dead analysis) was assessed by confocal laser scanning microscopy (CLSM) using a Zeiss LSM 510 AxioImager confocal microscope (Zeiss, US, VA). A FilmTracer™ LIVE/DEAD Biofilm viability kit (Life Technologies, US, CA) was used to prepare the samples for imaging. This kit comprised two stains: the green stain, SYTO9, to identify the live cells and the red stain, propidium iodide (PI), to identify dead cells.

For analyzing cell viability, three replicate carriers were harvested randomly during steady-state operation at each of the three different loading rates investigated in this study and prepared for CLSM images immediately after. Each carrier was imaged at five randomly selected locations. At each location, a stack of at least five CLSM images was acquired with a 63× water immersion objective (providing at least 75 images per experimental condition). The analytical quantification of viable cells was performed using Nikon NI Vision Assistant Software (National Instruments,

LabView 14, TX, US). The fraction of viable cells in the biofilm is defined as the quantified viable cells divided by the total number of cells (viable and non-viable) (Delatolla et al., 2009; Young et al., 2017b).

The carbonaceous biofilm volume removal rate (BVRR) across loading conditions was evaluated by normalizing the BOD removal rate per biofilm volume. The BVRR was determined by dividing the surface area removal rate (SARR) by the biofilm thickness. Moreover, the viable cell removal rate (VCRR) is defined as BVRR divided by the viable cell coverage of the biofilm in order to evaluate the microbial activity across loading conditions (Hoang et al., 2014; Young et al., 2016a; Almomani and Khraisheh, 2016).

#### **5.4.5 Solids analysis**

Solids analysis was performed to quantify the solids production and the solids detachment rate based on TSS and VSS concentration measurements (explained in the constituent analysis section). Since all experimental conditions were performed at a short HRT (1.1 h), the effects of hydrolysis of the particles in the reactor were assumed negligible (Ivanovic and Leiknes, 2012). Moreover, to ease the interpretation of the results, all the influent particles are assumed to leave the reactor unchanged, with no attachment to the biofilm. Therefore, the solids production and likewise the biofilm detachment rate is determined by knowing the influent and the effluent TSS mass flow rate (g/d) and TSS mass fluxes (g/m<sup>2</sup>·d) (Arabgol et al., 2020).

#### **5.4.6 Particle settling velocity distribution (PSVD)**

The ViCAs protocol, developed by Chebbo and Gromaire (2009), was used in this study to directly measure the distribution of particle settling velocity in wastewater samples. ViCAs is a French acronym for "Vitesse de Chute en Assainissement", meaning settling velocity in

wastewater. The ViCAs setup comprises a settling column (height of 70 cm and 7cm inner diameter) and replaceable cups located underneath the column. To allow assuming that the solids are uniformly distributed over the ViCAs column at the beginning of the test, the wastewater sample should be gently mixed and homogenized right before pumping it into the column and held in a vacuum pressure state for the rest of the test in a quiescent condition (Figure 5-1). The solids settled at different time intervals ( $t = 2, 6, 14, 30, 60, 120,$  and  $240$  min) are collected in the cups at the bottom of the column, dried at  $105^{\circ}\text{C}$  overnight and weighed (SM 2540 D-TSS) (APHA, 2005; Chebbo and Gromaire, 2009; Torfs et al., 2016). The evolution of the cumulative mass settled over time,  $M(t)$ , allows generating the PSVD curve,  $F(V_s)$ , indicating the percentage of the cumulated fraction of particle mass having a settling velocity lower than  $V_s$ . The calculation was implemented employing a small Excel solver macro using the following equations (Bertrand-Krajewski, 2001; Chebbo and Gromaire, 2009; Torfs et al., 2016).

$$F(V_s) = 100\left(1 - \frac{S(t)}{M_d + M_f}\right) \quad \text{Equation 5-1}$$

$$S(t) = M(t) - t \frac{dM(t)}{dt} \quad \text{Equation 5-2}$$

Where  $F(V_s)$  is the cumulative percentage of total particle mass with a settling velocity lower than  $V_s$ ;  $M_d$  is the total settled mass over time;  $M_f$  is the mass of particles remaining in the column at the end of the test;  $S(t)$  is the mass of particles that have a settling velocity larger than  $V_s$ ;  $M(t)$  is the cumulated mass of particles settled to the bottom of the column between  $t = 0$  and  $t$ ;  $t \frac{dM(t)}{dt}$  is the mass of particles that have a settling velocity less than  $V_s$ ; and  $V_s$  is the settling velocity equal to  $H/t$ , with  $H$  the water height in the column.

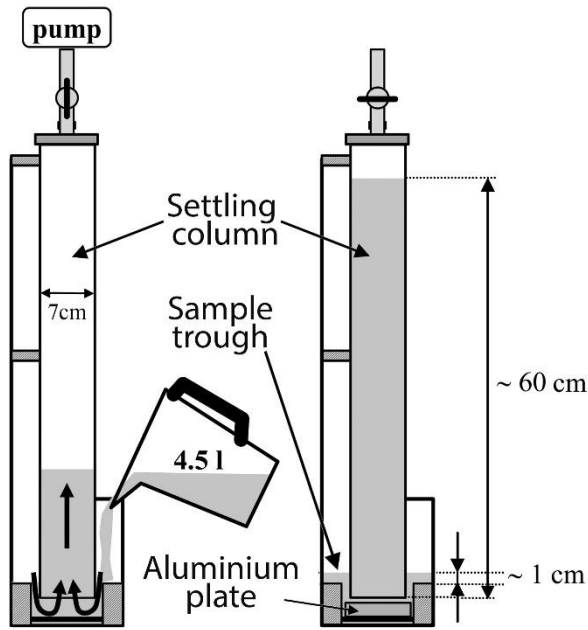


**Figure 5-1:** ViCAs experimental setup

During each of the three steady-state experimental conditions, the reactor's influent and effluent were collected and analyzed immediately after sampling to minimize the particles' flocculation in the sample. The samples were well mixed before starting the ViCAs test, and the test was considered valid if the mass balance error was less than  $\pm 15\%$  (Chebbo and Gromaire, 2009; Maruejols et al., 2011; Torfs et al., 2016).

#### 5.4.7 Particle size distribution (PSD)

Microscopy imaging was combined with the ViCAs test to analyze the settled particle characteristics over time. A bright-field moving stage microscope, Carl Zeiss Axio Examiner.Z1 (Carl Zeiss Canada Ltd., Toronto, Canada) with A-plan 2.5x/0.06 objective, was used to determine the particle size distribution. The collected samples in ViCAs cups at times 2, 30 and 240 minutes were prepared for microscope imaging. These samples contain the settled particles between 0 to 2 minutes, 15 to 30 minutes, and 120 to 240 minutes, separately. 5 ml of well-mixed and

homogenized samples were poured into a glass petri dish for visualization and image acquisition immediately after preparation. A total of 16 images per sample were acquired; each image covers an area of  $2580\ \mu\text{m} \times 2680\ \mu\text{m}$  at a resolution of  $1388 \times 1040$  pixels. Therefore, a total area of  $14320\ \mu\text{m} \times 10720\ \mu\text{m}$  was imaged and analyzed. The acquired images were analyzed on Fiji/ImageJ software to quantify the number of particles, particle size, equivalent circular diameter (ECD), area, perimeter and shape factor (Schindelin et al., 2012). The diameter of a circle with an equivalent area of the irregular-shaped particle was called ECD and is calculated as  $2 \times (\text{Area}/\pi)^{0.5}$ .

#### **5.4.8 Statistical analyses**

Statistical significance of all wastewater constituents, removal rates, all solids analysis, solids production and detachment rates, biofilm thickness, biofilm mass, biofilm density and PSVD curves was determined using two-tailed student t-tests with a *p*-value less than 0.05 to designate significance. To this end, three sets of t-test were performed to determine the significance of the differences between all aforementioned parameters at SALR 1.5, 2.5 and 6.0 g-sBOD/m<sup>2</sup>·d (to compare SALR 1.5 with 2.5, SALR 1.5 with 6.0, and SALR 2.5 with 6.0, see Appendix A). The average and 95% confidence intervals, shown as error bars, are displayed in all figures throughout the study. The significance level could not be assessed for PSD due to a lack of replicate data.

### **5.5 Results and discussion**

#### **5.5.1 Reactor kinetics**

Carbonaceous removal (sBOD and sCOD) and TAN removal rates were investigated across three experimental loading rates during steady-state conditions to determine the effects of varying SALR on MBBR kinetics (Figure 5-2). The sBOD removal rate was investigated for low to moderate SALRs, 1.5, 2.5 and 6.0 g-sBOD/m<sup>2</sup>·d (corresponding to COD SALRs of 4.2, 6.5 and

14.9 g-sCOD/m<sup>2</sup>·d). Since the flow rate and HRT were constant throughout the study, the SALR was simply increased by decreasing the available surface area in the reactor (Table 5-1).

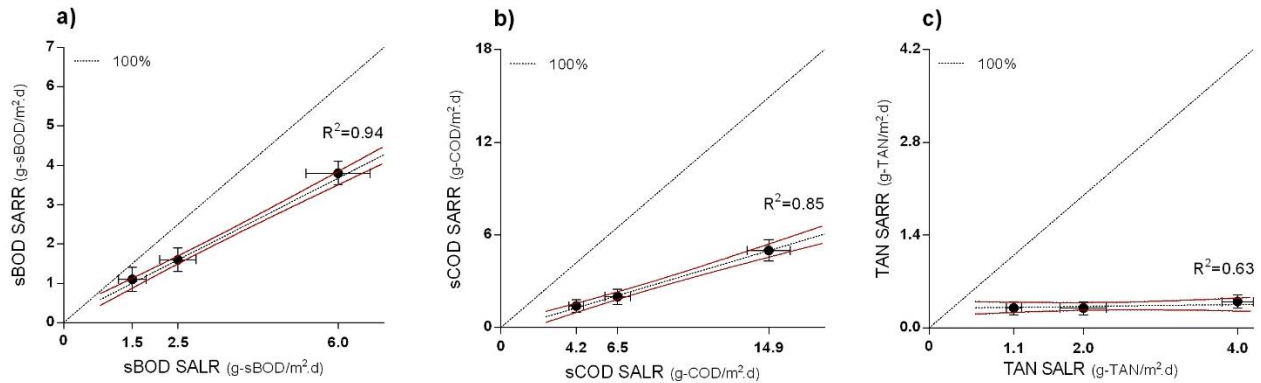


**Figure 5-2:** SARRs across three different experimental SALRs with respect to (a) sBOD (b) sCOD, and (c) TAN removal, with 95% confidence band of the best-fit regression line

The reactor was fed with primary clarified wastewater of the Gatineau WRRF with a constant flow rate of  $3.7 \pm 0.1$  L/h and operated with a constant HRT of 1.1 h (Table 5-2) throughout the study. The average total carbonaceous substrate concentration in the influent was  $53.6 \pm 4.4$  mg-BOD/L and  $118.8 \pm 6.8$  mg-COD/L, with a COD to BOD ratio of  $2.3 \pm 0.1$ . Note that due to the lack of a settling unit in this study, the carbonaceous material is tracked in the soluble phase. The average concentration of sBOD and sCOD in the effluent was  $23.0 \pm 2.4$  mg-sBOD/L and  $58.7 \pm 4.5$  mg-sCOD/L, respectively, with a sCOD to sBOD ratio of  $2.7 \pm 0.2$ . The TAN concentration was  $16.0 \pm 0.9$  mg-TAN/L. The influent characteristics might seem slightly dilute but are in the range of typical strength raw wastewater for Canadian WRRFs (Table 5-2).

**Table 5-2:** Experimental conditions, Influent and effluent wastewater characteristics at the three tested experimental loading rates

<b>Constituent</b> (Average $\pm$ 95 % CI)	<b>Influent<sup>a</sup></b>	<b>SALR 1.5<sup>b</sup></b>	<b>SALR 2.5<sup>b</sup></b>	<b>SALR 6.0<sup>b</sup></b>
TSS (mg/L)	49.3 $\pm$ 4.2	57.9 $\pm$ 8.5	66.7 $\pm$ 15.4	53.4 $\pm$ 8.5
VSS (mg/L)	38.1 $\pm$ 2.4	45.9 $\pm$ 6.5	46.2 $\pm$ 8.6	42.2 $\pm$ 2.3
COD (mg/L)	118.8 $\pm$ 6.8	111.0 $\pm$ 12.3	112.3 $\pm$ 15.3	104.7 $\pm$ 10.9
BOD (mg/L)	53.6 $\pm$ 4.4	73.0 $\pm$ 6.6	75.0 $\pm$ 7.2	55.1 $\pm$ 6.1
sCOD (mg/L)	58.7 $\pm$ 4.5	40.2 $\pm$ 3.5	38.4 $\pm$ 3.2	41.5 $\pm$ 5.8
sBOD (mg/L)	23.0 $\pm$ 2.4	6.1 $\pm$ 0.7	7.2 $\pm$ 1.8	9.6 $\pm$ 2.4
TAN,( NH <sub>3</sub> /NH <sub>4</sub> <sup>+</sup> -N mg/L)	16.0 $\pm$ 0.9	11.0 $\pm$ 2.4	12.4 $\pm$ 1.6	15.2 $\pm$ 1.6
Nitrite, (NO <sub>2</sub> <sup>-</sup> -N mg/L)	0.0 $\pm$ 0.0	0.4 $\pm$ 0.2	0.3 $\pm$ 0.1	0.2 $\pm$ 0.1
Nitrate, (NO <sub>3</sub> <sup>-</sup> -N mg/L)	2.7 $\pm$ 0.1	3.8 $\pm$ 1.4	2.7 $\pm$ 0.3	2.4 $\pm$ 0.2
VSS/TSS ratio (%)	79.3 $\pm$ 2.7	76.6 $\pm$ 3.6	72.1 $\pm$ 7.6	82.0 $\pm$ 4.4
COD/BOD	2.3 $\pm$ 0.1	1.5 $\pm$ 0.2	1.5 $\pm$ 0.1	1.8 $\pm$ 0.1
sCOD/sBOD	2.7 $\pm$ 0.2	6.0 $\pm$ 0.8	4.5 $\pm$ 0.4	4.4 $\pm$ 0.5
sBOD SARR (g-sBOD/ m <sup>2</sup> ·d)	-	1.1 $\pm$ 0.3	1.6 $\pm$ 0.3	3.8 $\pm$ 0.3
sBOD Removal efficiency (%)	-	68.9 $\pm$ 5.3	63.1 $\pm$ 6.9	59.9 $\pm$ 3.0
sCOD SARR (g-sCOD/ m <sup>2</sup> ·d)	-	1.4 $\pm$ 0.4	2.0 $\pm$ 0.5	5.0 $\pm$ 0.7
sCOD Removal efficiency (%)	-	31.8 $\pm$ 7.4	31.1 $\pm$ 4.2	31.5 $\pm$ 4.0
TAN SARR (g-TAN/ m <sup>2</sup> ·d)	-	0.3 $\pm$ 0.1	0.3 $\pm$ 0.1	0.4 $\pm$ 0.1
Removal efficiency (%)	-	29.9 $\pm$ 12.8	18.1 $\pm$ 4.0	9.1 $\pm$ 2.6
<b>Experimental conditions:</b>		<b>SALR 1.5</b>	<b>SALR 2.5</b>	<b>SALR 6.0</b>
SALR (g-sBOD/ m <sup>2</sup> ·d)		1.5 $\pm$ 0.3	2.5 $\pm$ 0.4	6.0 $\pm$ 0.7
SALR (g-sCOD/ m <sup>2</sup> ·d)		4.2 $\pm$ 0.4	6.5 $\pm$ 0.7	14.9 $\pm$ 1.6
SALR (g-TAN/ m <sup>2</sup> ·d)		1.1 $\pm$ 0.1	2.0 $\pm$ 0.3	4.0 $\pm$ 0.2
Temperature (°C)		9.0 $\pm$ 1.0	13.0 $\pm$ 1.0	18.0 $\pm$ 1.0
DO (mg/L)		7.1 $\pm$ 0.6	7.2 $\pm$ 0.4	6.5 $\pm$ 0.5
pH		7.8 $\pm$ 0.1	7.8 $\pm$ 0.1	7.8 $\pm$ 0.1

<sup>a</sup> Average and 95% confidence interval (95% CI) across the study (n  $\approx$  50)

<sup>b</sup> Average and 95% confidence across each experimental condition (n  $\approx$  10).

A strong linear correlation was observed between the measured sBOD (sCOD) loading rate and the removal rate (Figure 5-2a and b). As such, the reactors demonstrated first-order sBOD (sCOD) kinetics. The first-order kinetics or linear correlation between the substrate removal rate

and loading rate indicates that the substrate is mass transfer rate-limited in this study, likely due to the low loading rate of the substrate (WEF, 2011).

In attached growth wastewater systems, including the MBBR technology, the substrate removal performance is mediated by the mass transfer of the substrate (carbonaceous matter or nutrients) or the electron acceptor (DO) from the bulk liquid to the biofilm surface and subsequently through the biofilm itself. Therefore, the removal reaction order shifts from first-order relation (substrate mass transfer-dependent) at low substrate loading rates to zero-order relation (DO mass transfer-dependent) at high substrate loading rates (WEF, 2011; Qiqi et al., 2012; Barwal and Chaudhary, 2014). Transitioning from a low loaded operation (SALR of 1.5 g-sBOD/m<sup>2</sup>·d) to a higher loaded operation of 6.0 g-sBOD/m<sup>2</sup>·d corresponds to a statistically significant decrease in sBOD removal efficiency (Table 5-2). This decrease in removal efficiency expectedly increases the effluent carbonaceous matter concentrations. The significantly highest sBOD removal efficiency of  $68.9 \pm 5.3\%$  is observed at the lowest loading rate of  $1.5 \pm 0.3$  g-sBOD/m<sup>2</sup>·d with a corresponding SARR of  $1.1 \pm 0.3$ . Therefore, the concentration of sBOD in the effluent significantly increased at a SALR of 6.0 g-sBOD/m<sup>2</sup>·d with a corresponding SARR of  $3.8 \pm 0.3$  g-sBOD/m<sup>2</sup>·d. It should be noted that the confounding effects of temperature is not affecting the interpretation. Although the effluent sBOD concentration increased by increasing the SALR, the removal rate and efficiency were not statistically different between SALR of 1.5 and 2.5 g-sBOD/m<sup>2</sup>·d, most likely due to the relatively small increase in SALR between these two conditions. Also, the effects of increasing temperature might partly compensate the negative effects of increasing loading rates on system performance. Therefore, the effects of increasing loading rate would have been more evident if the temperature had been kept constant.

Although the nitrification kinetics was not included in the scope of this study, TAN removal rate and efficiency were monitored during the three experimental conditions (Figure 5-2c). Since the influent wastewater quality was relatively stable and the HRT of all the reactors were constant throughout the experiments, the TAN SALR values increased from 1.1 to 4.0 g-TAN/m<sup>2</sup>·d as the sBOD SALR increased from 1.5, 2.5 and 6.0 g-sBOD/m<sup>2</sup>·d by adjusting the number of carriers. Throughout different experimental loading rates, TAN SARRs were similar and did not change significantly. Influent sBOD concentrations larger than 12 mg/L, organic loads above 5 g-sBOD/m<sup>2</sup>·d, and C/N ratios (BOD to total Kjeldahl nitrogen (TKN)) larger than 1.0 are known to limit the TAN removal in MBBR reactors (Hem et al., 1994; WEF, 2009). Therefore, the observed relatively low TAN removal at an SALR of 6.0 g-sBOD/m<sup>2</sup>·d was likely only due to nitrogen assimilation by heterotrophic microorganisms. The faster-growing heterotrophic community likely outcompetes the nitrifying autotrophic community in this study's biofilm, hence preventing nitrification. However, the highest TAN removal efficiency (29.9 ± 12.8% N-removal) and the lowest effluent TAN concentration (11.0 ± 2.4 mg-TAN/L) were observed at lower sBOD loaded conditions (SALR of 1.5 g-sBOD/m<sup>2</sup>·d). These observations in addition to the observed changes in NO<sub>x</sub> concentrations between influent and effluent at the lower sBOD loaded conditions (SALR of 1.5 g-sBOD/m<sup>2</sup>·d) and higher TAN:sBOD removal ratio, indicates that nitrification might be occurring at the lower sBOD loaded conditions, in addition to the assimilation of TAN.

### **5.5.2 Biofilm characteristics (thickness, mass, density)**

The biofilm responses to varying loading conditions were investigated by evaluating the changes in biofilm thickness, mass, density and the biofilm age at three different SALRs during steady-state conditions. The initial biofilm thickness was measured at a SALR of 1.5 g-sBOD/m<sup>2</sup>·d, the lowest SALR and coincidentally the lowest temperature studied in this research.

The biofilm thickness increased from  $316.2 \pm 11.1$  to  $369.1 \pm 25.5$   $\mu\text{m}$  when the SALR rose from  $1.5$   $\text{g-sBOD/m}^2\cdot\text{d}$  to  $2.5$   $\text{g-sBOD/m}^2\cdot\text{d}$ , and then decreased by approximately 25%, down to  $281.1 \pm 8.7$   $\mu\text{m}$ , at the SALR of  $6.0$   $\text{g-sBOD/m}^2\cdot\text{d}$ . Although the difference between the biofilm thickness at SALR of  $1.5$  and  $2.5$   $\text{g-sBOD/m}^2\cdot\text{d}$  was not statistically different at the 95 % confidence level, it still could be considered that the biofilm thickness is almost significantly different ( $p$ -value =  $0.06$ ). Meanwhile, it should be noted that, since the reactor was operated with real wastewater, the biofilm thickness might also be affected by the seasonal temperature changes. The average temperature was recorded at  $9.0 \pm 1.0$ ,  $13.0 \pm 1.0$  and  $18.0 \pm 1.0$   $^{\circ}\text{C}$  during SALR of  $1.5$ ,  $2.5$  and  $6.0$   $\text{g-sBOD/m}^2\cdot\text{d}$ , respectively. Similar to the biofilm thickness, the biofilm mass was also statistically significantly higher at a SALR of  $2.5$  compared to the SALR of  $6.0$   $\text{g-sBOD/m}^2\cdot\text{d}$  (Figure 5-3). Therefore, the results demonstrated a significant decline in biofilm thickness, biofilm mass, and biofilm density when the SALR increases ( $p$ -value  $< 0.05$ ). The biofilm mass increased from  $54.7 \pm 1.4$  to  $62.7 \pm 2.4$   $\text{mg}$  per carrier and then decreased by approximately 25%, reaching to  $43.9 \pm 1.0$   $\text{mg}/\text{carrier}$ , at a SALR of  $6.0$   $\text{g-sBOD/m}^2\cdot\text{d}$ . Overall, the findings of this study did not indicate statistically significant changes in biofilm responses at low loaded conditions (between loading rates of  $1.5$  and  $2.5$ ). However, statistically significant changes in biofilm responses were observed at the highest SALR ( $6.0$   $\text{g-sBOD/m}^2\cdot\text{d}$ ), where the thinnest biofilm with the lowest density was found (Figure 5-3).

The authors believe that these significant changes in biofilm responses are more affected by the temperature than the SALR, as it is consistent with previous studies. Previous studies indicated a significant increase of nitrifying biofilm thickness along with decreases in biofilm densities when decreasing temperature (Hoang et al., 2014; Young et al., 2017b; Ahmed et al., 2019). Moreover, a thicker biofilm has been reported at higher substrate concentrations (Peyton, 1996; Wijeyekoon

et al., 2004; Forrest et al., 2016), which is in contrast with the findings of this study. This is probably due to the confounding effects of increasing temperature. Sometimes, no apparent correlation between biofilm thickness and loading rates was observed (Karizmeh et al., 2014). Therefore, it should be considered that the biofilm response to an operational condition is a complex phenomenon that can be affected by the combination of many factors such as hydrodynamics, nutrient loading, DO concentration, carrier type, SALR, HRT and temperature.

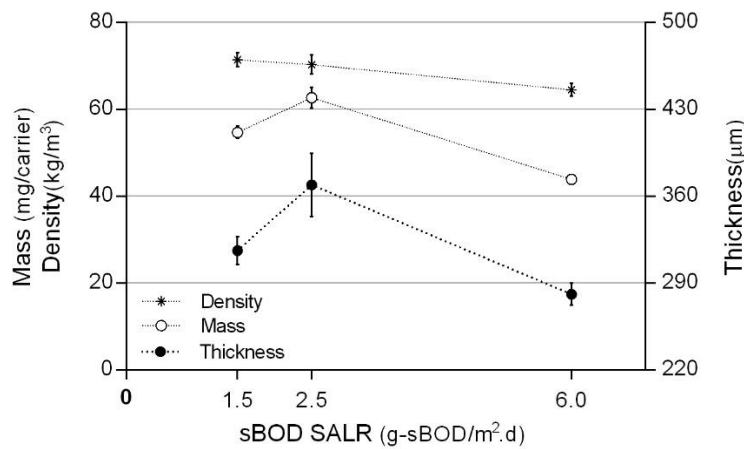


**Figure 5-3:** Biofilm thickness, density and biomass in the reactors for different experimental phases

As a good indication of biofilm age, solids retention time (SRT) was calculated at three SALRs. The results indicated a decrease in biofilm age as the SALR increases. The SRT decreased from  $5.6 \pm 0.8$  to  $1.7 \pm 0.1$  days when the SALR increased from 1.5 to 6.0 g-sBOD/m<sup>2</sup>.d. The longer SRT at SALR 1.5 well explains the significantly better TAN removal efficiency, as it allows accumulation of slow-growing nitrifiers in the reactor (Rittmann and McCarty, 2001).

### 5.5.3 Biofilm morphology

VPSEM images were acquired at a magnification of 60× and 600× to demonstrate the changes in biofilm morphology and microorganism communities with respect to SALR (Figure 5-4). No evident differences in biofilm morphology were observed at different SALRs. Previous studies on high-loaded carbon removal MBBR systems observed distinct differences in the biofilm morphology between different loading conditions; however, the changes were less detectable at short HRTs (Karizmeh et al., 2014). Protozoans are significant predators of bacteria and were observed at all studied conditions. The protozoans obtain their energy for cell synthesis by consuming biodegradable nutrients. The presence of such organisms in a system indicates healthy conditions in wastewater treatment systems (Wang, 2012). The higher organisms observed in the biofilm at all SALRs investigated in this study were mostly nematodes, rotifers and ciliates (including free-swimming ciliates and stalked ciliates). Ciliates appeared to be the most abundant protozoans in all loading conditions. Although nematodes and rotifers were seen in the biofilm, they were not dominant. Nematodes were captured more frequently at SALR of 2.5 g-sBOD/m<sup>2</sup>·d than other SALRs, which could signify that more of them might exist at this SALR. Nematodes are complex animals that consume large numbers of bacteria. These motile worms can break up flocs with their rapid thrashing motion (Wang, 2012), which might explain why the higher biofilm detachment rate observed at SALR of 2.5 g-sBOD/m<sup>2</sup>·d and will be discussed further in the solids analyses section. Moreover, rotifers can consume small floc particles and the bacteria on the surface of particles. The presence of rotifers indicates that the effluent contains few soluble, biodegradable organic compounds and a good DO concentration level (Wang, 2012).

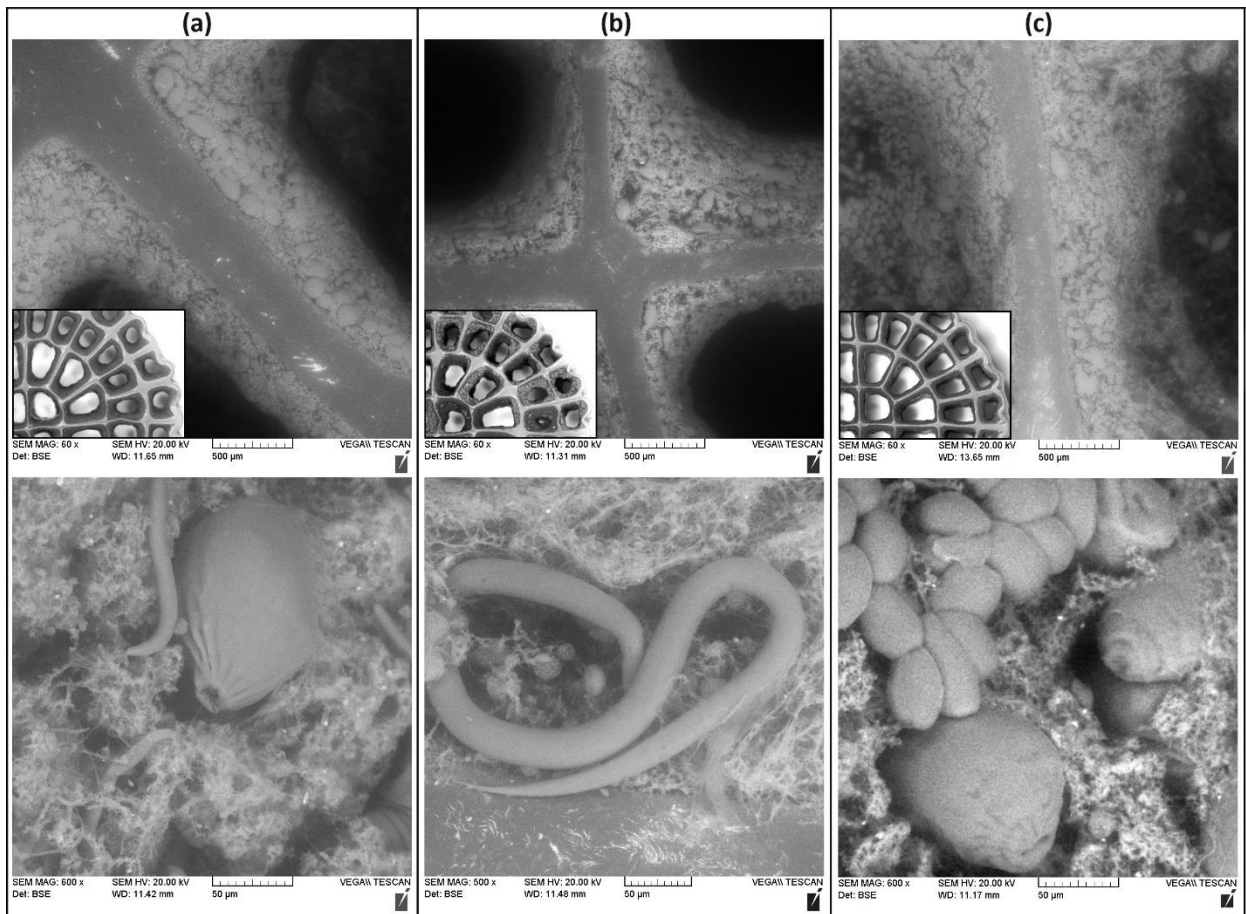


**Figure 5-4:** VPSEM images acquired for assessment of biofilm morphology at (a) SALR of 1.5 g-sBOD/m<sup>2</sup>·d, (b) SALR of 2.5 g-sBOD/m<sup>2</sup>·d and (c) SALR of 6.0 g-sBOD/m<sup>2</sup>·d (the small middle left images are stereoscope images that illustrate a quarter of carrier at each condition)

#### 5.5.4 Biomass characteristics - Cell Viability

The biomass viability is defined as the live fraction of total cells in the biofilm. Viability was assessed at three different loading rates during steady-state conditions. Analyzing the cell viability indicated a significant change in percent coverage of viable cells (live fraction of total cells) with respect to the applied loading rate (Table 5-3). The biomass viability was measured to be  $74.0 \pm 1.9\%$  at a SALR of 1.5 g-sBOD/m<sup>2</sup>·d and increased to  $81.8 \pm 1.7\%$  at a SALR of 6.0 g-sBOD/m<sup>2</sup>·d. As such, a statistically largest live fraction of total cells was observed for the highest SALR of 6.0

g-sBOD/m<sup>2</sup>·d, with the thinnest and youngest biofilm occurring when the substrate mass transfer might be less restricted due to the lower density. A drop in percent coverage of viable cells was observed from SALR of 1.5 to 2.5 g-sBOD/m<sup>2</sup>·d when a significant change in biofilm thickness occurred. The significantly lowest cell viability is related to the thickest biofilm at a SALR of 2.5 sBOD/m<sup>2</sup>·d (Figure 5-3). Therefore, the difference in cell viability might be due to the biofilm age or the biofilm thickness changes during the transition of cold to warm temperature at low loaded (SALR 1.5) to high loaded (SALR 6.0) conditions. At the SALR of 6.0 g-sBOD/m<sup>2</sup>·d with the lowest thickness, the sloughing of the biofilm may have initiated the growth of newly formed biofilm (younger biofilm) and, therefore, a higher percentage of viable cells. In contrast, the thickest biofilm demonstrated a less viable biofilm (more dead cells), probably due to the restrictive mass transfer of substrates and nutrients during the overgrowth observed at SALR of 2.5 g-sBOD/m<sup>2</sup>·d in this study (Tijhuis et al., 1995).

**Table 5-3:** Average and 95% confidence interval values of the percentage of cell viability in the biofilm, biofilm volume (BVRR) and the viable cell sBOD removal rate (VCRR)

SALR (g-sBOD/m <sup>2</sup> ·d)	Cell viability (%)	BVRR×10 <sup>3</sup> (g-sBOD/m <sup>3</sup> ·d)	VCRR×10 <sup>3</sup> (g-sBOD/m <sup>3</sup> ·d)
<b>1.5</b>	74.0 ± 1.9	3.1 ± 1.0	4.2 ± 1.4
<b>2.5</b>	68.2 ± 1.2	4.6 ± 1.3	6.4 ± 1.6
<b>6.0</b>	81.8 ± 1.7	13.3 ± 1.1	16.3 ± 1.3

Both BVRR and VCRR did not differ significantly at low SALRs of 1.5 and 2.5 g-sBOD/m<sup>2</sup>·d, while the calculated values of BVRR and VCRR indicate that more viable and active cells exist at the high loading rate, SALR of 6.0 g-sBOD/m<sup>2</sup>·d (Figure 5-5). Therefore, the cellular activity of embedded cells in the carriers at high loaded condition is approximately four times larger than at the low loaded condition (SALR 1.5), probably due to the thinner biofilm, the higher

mass transfer and substrate availability at higher SALRs (Herrling et al., 2015; Young et al., 2016a).

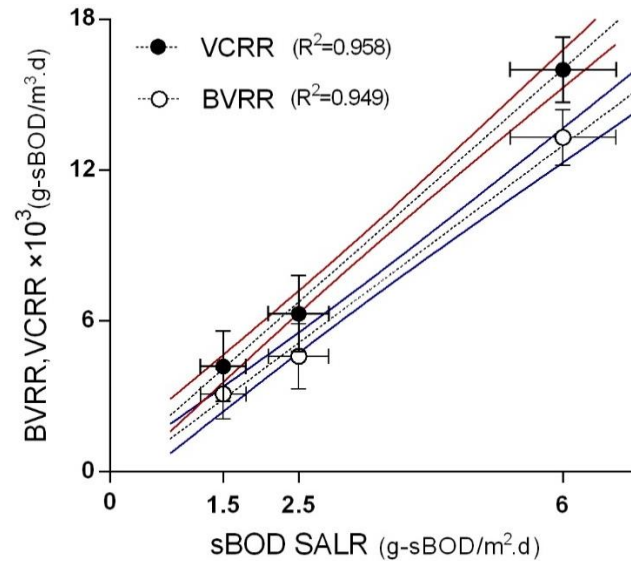


**Figure 5-5:** Biofilm volume and viable cell removal rates across the three different loading rates with 95% confidence band of the best-fit regression line (showing a linear correlation between SALR and RR)

### 5.5.5 Solids analysis

The TSS concentration, solids production and detachment rate in the reactor were analyzed to investigate the effect of increasing loading rate on solids characteristics (Figure 5-6). According to the constituents analyses of the effluent wastewater at the three different tested loading rates (Table 5-2), the TSS, VSS, and the VSS:TSS ratio did not demonstrate a significant difference with respect to the loading rate due to the high fluctuations in the TSS concentration inherent to the full-scale wastewater variability. The effluent TSS concentration comprises influent suspended solids plus biologically produced solids, which are detached biofilm from the carriers. Although the influent particles' fate might be affected by the collision with other particles and the carriers inside the reactor, it is assumed that the influent suspended solids remain unchanged in high rate

MBBR systems with HRTs lower than 2 hours (Ivanovic and Leiknes, 2012) and leave the reactor, to simplify the interpretation of the result.

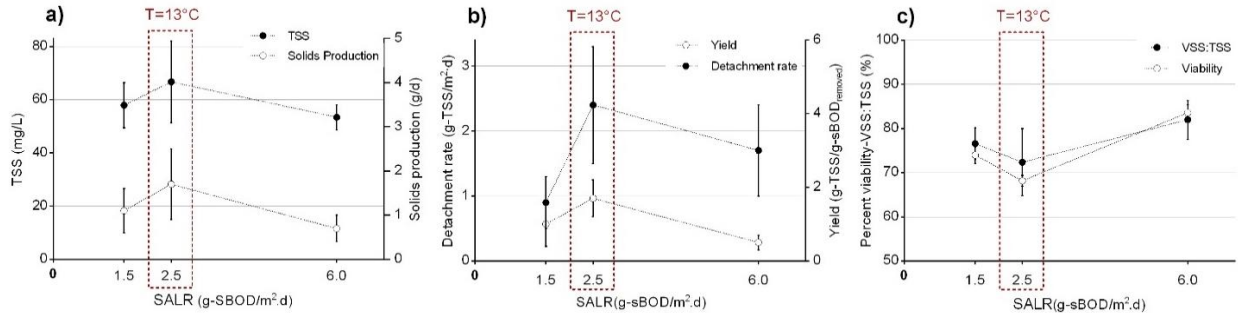


**Figure 5-6:** (a) TSS, and solids production, (b) yield and detachment rate, and (c) VSS:TSS ratio of the effluent solids and percent coverage of viable cells in the biofilm at three different SALRs

Although no significant changes were observed in TSS concentration and solids production among the three SALRs (Figure 5-6 a), the solids characteristics showed a statistically significant difference in detachment rate ( $2.4 \pm 0.9$  g-TSS/m<sup>2</sup>·d) and observed yield ( $1.7 \pm 0.5$  mg-TSS<sub>produced</sub>/g-SBOD<sub>removed</sub>) at a SALR 2.5 with a temperature of  $13.0 \pm 1.0$  °C (Figure 5-6 b). The lowest effluent VSS:TSS ratio at SALR 2.5 indicated more inert solids in the effluent and could be well connected to the significantly less viable cells in the biofilm (Figure 5-6 c). Therefore, a direct correlation is observed between the VSS:TSS ratio of the suspended solids and the cell viability of attached biofilm on the carriers, which expectedly supports the hypothesis that says a portion of effluent TSS is biologically produced solids detached from the biofilm.

Because the experiment was performed at a full-scale WRRF, seasonal temperature changes should also be considered when interpreting the results. In this study, no clear trend was found for the solids characteristics with respect to the SALR, probably due to the confounding effects of temperature, previous studies have indicated an increasing trend for solids concentration, detachment and production when SALR increases (Karizmeh et al., 2014; Forrest et al., 2016).

Therefore, the authors hypothesize that the transition from cold ( $9.0 \pm 1.0$  °C) to warm ( $18.0 \pm 1.0$  °C) condition, after the period of snow melting, caused the thicker biofilm, higher biofilm mass (Figure 5-3), higher solids detachment, yield and, in general, is causing noticeable changes in biofilm and solid characteristics.

### **5.5.6 Solids characteristics and settleability**

Following solids analysis, the ViCAs test was used to obtain a better understanding of the solids characteristics and their settling behaviour with respect to different SALR. The ViCAs test was performed on influent and effluent of the reactor at SALR of 1.5, 2.5 and 6.0 g-sBOD/m<sup>2</sup>·d during steady-state conditions. The ViCAs test gives the PSVD curve, which is the cumulative mass percentage of particles (y-axis) with settling velocities ( $V_s$ ) below  $V_s$  on the x-axis (Chebbo and Gromaire, 2009). Therefore, the PSVD curves for samples that contain particles with faster-settling velocities will be located below the samples with a higher fraction of particles with slow-settling velocities.

According to the PSVD curves (Figure 5-7), the significant difference between the influent and effluents PSVD curves at three studied SALRs, simply indicates a significant change in particle settling properties ( $p$ -value < 0.05). The curves clearly illustrated that the influent particles settle statistically significantly slower than the effluent particles. This could be explained by the fact that all fast settleable particles have already settled in the primary clarifier as primary clarified wastewater was used in this study and that the solids detached from the biofilm settle faster.

As mentioned above, the effluent particles are a mixture of influent particles, which are assumed to remain unchanged during the process due to the short HRT and detached particles from the biofilm. The latter is highly affected by operational conditions such as SALR and temperature. The worst settling behaviour is observed at the highest SALR (SALR of 6.0 g BOD/m<sup>2</sup>·d), which

is consistent with previous studies that showed a negative impact of higher organic load on settling properties of effluent particles in biofilm reactors (Ødegaard et al., 1994; Ivanovic and Leiknes, 2012; Karizmeh et al., 2014).

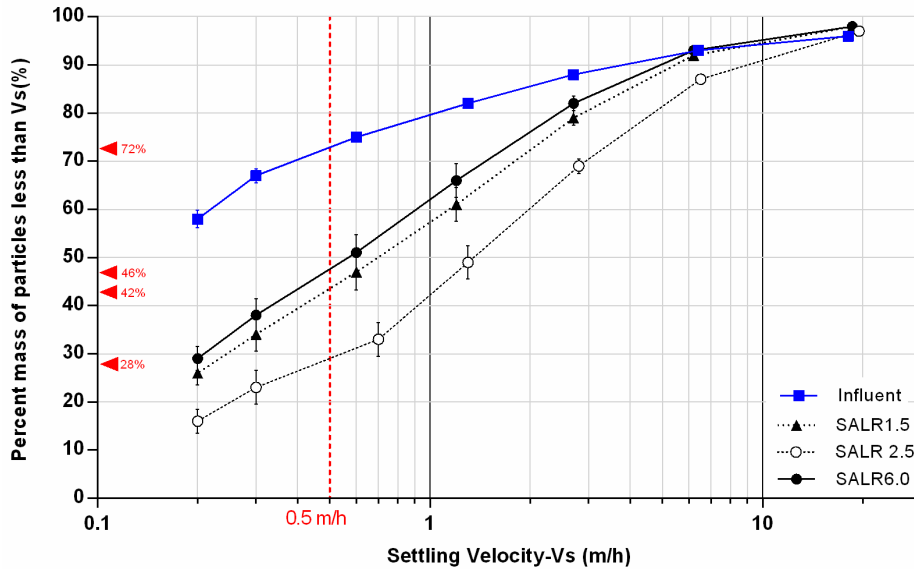


**Figure 5-7:** Particle settling velocity distribution curves for influent and effluent at three different experimental SALRs

Furthermore, a low SRT (less than 2 to 3 days) creates poorly stabilized particles with poor settling characteristics (Smeraldi, 2012; Mancell-Egala et al., 2016), which can well explain the significantly worst settling characteristics of the effluent particles at SALR 6.0 with the lowest SRT. However, a significantly better settling behaviour was observed at SALR 2.5, where different solids characteristics were observed (see the "solids analysis" section). The PSVD curve obtained under a SALR 2.5 is located significantly lower among the other curves ( $p$ -value < 0.05). That means the effluent suspended solids at SALR 2.5 contain a higher fraction of rapidly settling particles than the effluent at SALR 1.5 and 6.0. The longer SRT at this SALR might be another reason for the observed particles with improved settling characteristics (Smeraldi, 2012).

The typical design overflow rate of settling tanks for primary clarified wastewater at normally loaded MBBR ( $< 8 \text{ g BOD/m}^2\cdot\text{d}$ ) is defined as  $0.5 \text{ m/h}$  (Ødegaard et al., 2010). With this, the cumulative mass percentage of particles with settling velocities below  $0.5 \text{ m/h}$  could be calculated to be 42%, 28% and 46% for SALR 1.5, 2.5 and 6.0, respectively. In other words, the results illustrated that 72% of the total particle mass in the effluent of MBBR operated at SALR 2.5 would settle in such a clarifier (Figure 5-8).

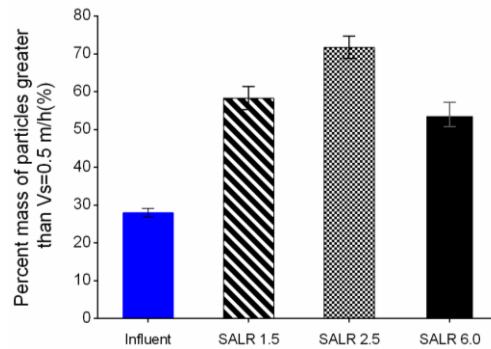


**Figure 5-8:** Percent mass of particles with a velocity greater than  $0.5 \text{ m/hr}$

A positive correlation is reported between the PSVD and TSS concentration for a wide range of TSS concentrations in different types of wastewater (Maruéjols et al., 2013; Bachis et al., 2015), the higher TSS concentration corresponds with a higher fraction of fast settling particles and hence better settleability (Maruéjols et al., 2013; Bachis et al., 2015). Subsequently, in this study, the higher TSS concentration of the effluent at the SALR 2.5 could be a reason for having a better settleability of particles. Significantly better settling behaviour of the solids, observed at this SALR, can also be linked to the effect of temperature on settling behaviour, where the reactor was operated at a temperature of  $13.0 \pm 1.0 \text{ }^\circ\text{C}$ . Previous studies illustrated a decline in the fraction of large particles with increasing temperature (Patry et al., 2018). They identified that the operating temperature significantly affects the settling performance in bioreactors, and the best settling performance is observed at temperatures around  $10^\circ\text{C}$  (Patry et al., 2018).

In addition to investigating the PSD of the MBBR effluent at different loading rates, a PSD study was combined with the ViCAs test. To this end, the collected particles in the ViCAs cups after 2, 30 and 240 minutes of settling were imaged and analyzed for PSD to investigate the effect of SALR on particle size over time (Figure 5-9). The particle size is an important factor in settling processes. Since the particles in wastewater are not uniformly circular and spherical, the size of irregular particles is simplified, and the equivalent circular diameter (ECD) is defined, assuming the particles as a circle. Therefore, the accumulative percent volume of particles across the ECD is graphed to investigate the effluent PSD at each SALR. The results indicated that the settled particles became smaller over time. In other words, the larger particles have settled faster, and the majority of particles with larger ECD settled within the first 30 minutes of the study. Looking at the first 30 minutes of settling (Figure 5-9 a, b), the graph illustrates larger particles in the effluent at SALR 2.5. For this loading rate, the effluent has also demonstrated higher TSS with better settleability, and the biofilm was older with higher non-viable cells and a higher detachment rate.

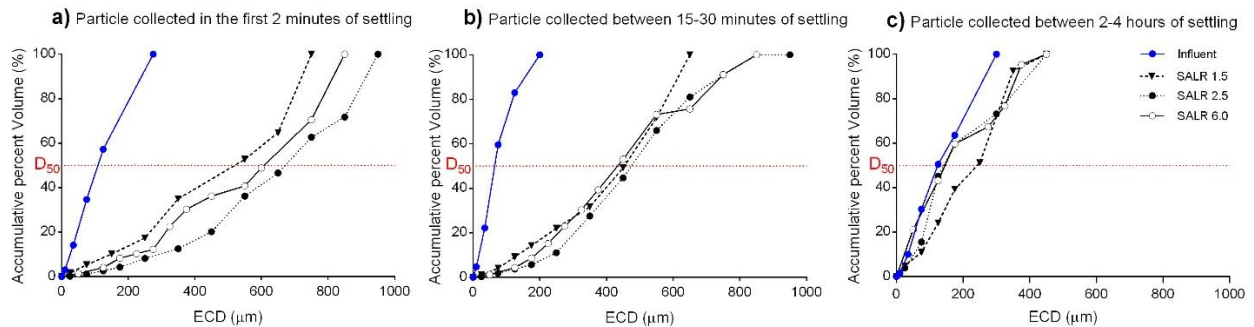


**Figure 5-9:** Accumulative particle size distribution at different settling intervals related to ViCAs column (a) settled particle between time 0 to 2 minutes, (b) settled particle between time 15 to 30 minutes, and (c) settled particle between time 120 to 240 minutes.

## 5.6 Conclusion

This study has investigated the characteristics and settling behaviour of MBBR effluent particles along with the biofilm characteristics and pollutant removal at different SALRs. A new analytical method, ViCAs, which has not been used before to characterize MBBR-produced solids, was used to quantify the PSVD of the MBBR effluent solids and the settling behaviour of the particles. This method was combined with microscopy imaging to analyze the PSD. Expectedly, a positive correlation was observed between the loading rate and removal rate. However, the evaluation of biofilm characteristics and particle characteristics have clarified that in addition to the loading rate, the operational temperature may also affect the obtained data in this study because the experiment was conducted during the seasonal transition period, from cold to warm conditions. The SALR will directly affect the SRT in the reactor, with a lower SRT at the higher SALR deteriorating the settling characteristics, as the worst settling was observed for SALR  $6.0 \text{ g-sBOD/m}^2 \cdot \text{d}$ . Moreover, the intermediate SALR of  $2.5 \text{ g-sBOD/m}^2 \cdot \text{d}$  at a temperature of  $13.0 \pm 1.0 \text{ }^\circ\text{C}$  resulted in the thickest biofilm, lowest percent coverage of viable cells, highest solids production, highest detachment rate, highest yield, larger particle size and significantly better settling behaviour.

## 5.7 References

- Åhl, R. M., Leiknes, T., and Ødegaard, H. (2006). "Tracking particle size distributions in a moving bed biofilm membrane reactor for treatment of municipal wastewater." *Water Science and Technology*, 53(7), 33–42.
- Ahmed, W., Tian, X., and Delatolla, R. (2019). "Nitrifying moving bed biofilm reactor: Performance at low temperatures and response to cold-shock." *Chemosphere*, 229, 295–302.
- Aiguier, E., Chebbo, G., Bertrand-Krajewski, J.-L., Hedges, P., and Tyack, N. (1996). "Methods for determining the settling velocity profiles of solids in storm sewage." *Water Science and*

*Technology*, 33(9), 117–125.

Almomani, F. A., and Khraisheh, M. A. M. (2016). “Treatment of septic tank effluent using moving-bed biological reactor: kinetic and biofilm morphology.” *International Journal of Environmental Science and Technology*, 13(8), 1917–1932.

APHA, A. (2005). “Standard Methods for the Examination of Water and Wastewater.” USA: Washington DC, USA.

Arabgol, R., Vanrolleghem, P. A., Piculell, M., and Delatolla, R. (2020). “The impact of biofilm thickness-restraint and carrier type on attached growth system performance, solids characteristics and settleability.” *Environmental Science: Water Research & Technology*, 6(10), 2843–2855.

Aygun, A., Nas, B., and Berktaş, A. (2008). “Influence of high organic loading rates on COD removal and sludge production in moving bed biofilm reactor.” *Environmental Engineering Science*, 25(9), 1311–1316.

Bachis, G., Maruéjols, T., Tik, S., Amerlinck, Y., Melcer, H., Nopens, I., Lessard, P., and Vanrolleghem, P. A. (2015). “Modelling and characterization of primary settlers in view of whole plant and resource recovery modelling.” *Water Science and Technology*, 72(12), 2251–2261.

Barwal, A., and Chaudhary, R. (2014). “To study the performance of biocarriers in moving bed biofilm reactor (MBBR) technology and kinetics of biofilm for retrofitting the existing aerobic treatment systems: a review.” *Reviews in Environmental Science and Bio/Technology*, 13(3), 285–299.

Bassin, J. P., and Dezotti, M. (2018). “Moving Bed Biofilm Reactor (MBBR).” *Advanced Biological Processes for Wastewater Treatment*, Springer, Cham, 37–75.

Berrouard, E. (2010). “Caractérisation de la décantabilité des eaux pluviales.” M.Sc. thesis, Université Laval, QC, Canada.

Bertrand-Krajewski, J. L. (2001). “Détermination des vitesses de chute des polluants en phase particulaire des rejets urbains par ajustement numérique de la courbe M(t) pour le protocole VICTOR.” *Villeurbanne (France): INSA de Lyon-Laboratoire URGC Hydrologie Urbaine*,

*rapport de recherche.*

- Chebbo, G., and Gromaire, M.-C. (2009). "VICAS—An operating protocol to measure the distributions of suspended solid settling velocities within urban drainage samples." *Journal of Environmental Engineering*, 135(9), 768–775.
- Delatolla, R., Berk, D., and Tufenkji, N. (2008). "Rapid and reliable quantification of biofilm weight and nitrogen content of biofilm attached to polystyrene beads." *Water Research*, 42(12), 3082–3088.
- Delatolla, R., Tufenkji, N., Comeau, Y., Gadbois, A., Lamarre, D., and Berk, D. (2010). "Investigation of laboratory-scale and pilot-scale attached growth ammonia removal kinetics at cold temperature and low influent carbon." *Water Quality Research Journal of Canada*, 45(4), 427–436.
- Delatolla, R., Tufenkji, N., Comeau, Y., Lamarre, D., Gadbois, A., and Berk, D. (2009). "In situ characterization of nitrifying biofilm: Minimizing biomass loss and preserving perspective." *Water Research*, 43(6), 1775–1787.
- Forrest, D., Delatolla, R., and Kennedy, K. (2016). "Carrier effects on tertiary nitrifying moving bed biofilm reactor: An examination of performance, biofilm and biologically produced solids." *Environmental Technology*, 37(6), 662–671.
- Hasler, M. (2007). "Field and laboratory experiments on settling process in stormwater storage tanks." Graz University of Technology, Austria.
- Hem, L., Rusten, B., and Ødegaard, H. (1994). "Nitrification in a moving bed biofilm reactor." *Water Research*, 28(6), 1425–1433.
- Herrling, M. P., Guthausen, G., Wagner, M., Lackner, S., and Horn, H. (2015). "Determining the flow regime in a biofilm carrier by means of magnetic resonance imaging." *Biotechnology and Bioengineering*, 112(5), 1023–1032.
- Hoang, V., Delatolla, R., Abujamel, T., Mottawea, W., Gadbois, A., Laflamme, E., and Stintzi, A. (2014). "Nitrifying moving bed biofilm reactor (MBBR) biofilm and biomass response to long term exposure to 1 °C." *Water Research*, 49, 215–224.

- Ivanovic, I., and Leiknes, T. O. (2012). "Particle separation in moving bed biofilm reactor: Applications and opportunities." *Separation Science and Technology*, 47(5), 647–653.
- Ivanovic, I., Leiknes, T., and Ødegaard, H. (2006). "Influence of loading rates on production and characteristics of retentate from a biofilm membrane bioreactor (BF-MBR)." *Desalination*, 199(1–3), 490–492.
- Javid, A. H., Hassani, A. H., Ghanbari, B., and Yaghmaeian, K. (2013). "Feasibility of utilizing moving bed biofilm reactor to upgrade and retrofit municipal wastewater treatment plants." *International Journal of Environmental Research*, 7(4), 963–972.
- Karizme, M. S. (2012). "Investigation of biologically-produced solids in moving bed bioreactor (MBBR) treatment systems." M.Sc. thesis, University of Ottawa, Canada.
- Karizme, M. S., Delatolla, R., and Narbaitz, R. M. (2014). "Investigation of settleability of biologically produced solids and biofilm morphology in moving bed bioreactors (MBBRs)." *Bioprocess and Biosystems Engineering*, 37(9), 1839–1848.
- Mancell-Egala, W. A. S. K., Kinnear, D. J., Jones, K. L., De Clippeleir, H., Takács, I., and Murthy, S. N. (2016). "Limit of stokesian settling concentration characterizes sludge settling velocity." *Water Research*, 90, 100–110.
- Maruéjols, T., Lessard, P., and Vanrolleghem, P. A. (2014). "Impact of particle property distribution on hydrolysis rates in integrated wastewater modelling." *13th International Conference on Urban Drainage, Sarawak, Malaysia*.
- Maruejols, T., Lessard, P., Wipliez, B., Pelletier, G., and Vanrolleghem, P. A. (2011). "Characterization of the potential impact of retention tank emptying on wastewater primary treatment: A new element for CSO management." *Water Science and Technology*, 64(9), 1898–1905.
- Maruéjols, T., Vanrolleghem, P. A., Pelletier, G., and Lessard, P. (2013). "Characterisation of retention tank water quality: particle settling velocity distribution and retention time." *Water Quality Research Journal*, 48(4), 321–332.
- Melin, E., Leiknes, T., Helness, H., Rasmussen, V., and Ødegaard, H. (2005). "Effect of organic loading rate on a wastewater treatment process combining moving bed biofilm and membrane

- reactors.” *Water Science and Technology*, 51(6–7), 421–430.
- Metcalf & Eddy. (2014). *Wastewater Engineering: Treatment and Resource Recovery*. McGraw-Hill, New York.
- Ødegaard, H. (2000). “Advanced compact wastewater treatment based on coagulation and moving bed biofilm processes.” *Water Science and Technology*, 42(12), 33–48.
- Ødegaard, H. (2006). “Innovations in wastewater treatment: The moving bed biofilm process.” *Water Science and Technology*, 53(9), 17–33.
- Ødegaard, H. (2016). “A road-map for energy-neutral wastewater treatment plants of the future based on compact technologies (including MBBR).” *Frontiers of Environmental Science & Engineering*, 10(4), 2.
- Ødegaard, H., Cimbritz, M., Christensson, M., and Dahl, C. P. (2010). “Separation of biomass from moving bed biofilm reactors (MBBRs).” *Proceedings of the Water Environment Federation*, 2010(7), 212–233.
- Ødegaard, H., Gisvold, B., and Strickland, J. (2000). “The influence of carrier size and shape in the moving bed biofilm process.” *Water Science and Technology*, 41(4–5), 383–391.
- Ødegaard, H., Rusten, B., and Westrum, T. (1994). “A new moving bed biofilm reactor: applications and results.” *Water Science and Technology*, 29(10–11), 157–165.
- Patry, B., Boutet, É., Baillargeon, S., and Lessard, P. (2018). “Solid-liquid separation of an effluent produced by a fixed media biofilm reactor.” *Water Science and Technology*, 77(3), 589–596.
- Peyton, B. M. (1996). “Effects of shear stress and substrate loading rate on *Pseudomonas aeruginosa* biofilm thickness and density.” *Water Research*, 30(1), 29–36.
- Piculell, M. (2016). “New dimensions of moving bed biofilm carriers influence of biofilm thickness and control possibilities.” Ph.D. thesis, Lund University, Sweden.
- Plana, Q., Pauléat, A., Gadbois, A., Lessard, P., and Vanrolleghem, P. A. (2020). “Characterizing the settleability of grit particles.” *Water Environment Research*, 92(5), 731–739.
- Qiqi, Y., Qiang, H., and T. Ibrahim, H. (2012). “Review on moving bed biofilm processes.” *Pakistan Journal of Nutrition*, 11(9), 804–811.

- Rittmann, B. E. (2007). “Where are we with biofilms now? Where are we going?” *Water Science and Technology*, 55(8–9), 1–7.
- Rittmann, B. E., and McCarty, P. L. (2001). *Environmental Biotechnology: Principles and Applications*. McGraw-Hill, New York.
- Schindelin, J., Arganda-Carreras, I., Frise, E., Kaynig, V., Longair, M., Pietzsch, T., Preibisch, S., Rueden, C., Saalfeld, S., and Schmid, B. (2012). “Fiji: an open-source platform for biological-image analysis.” *Nature Methods*, 9(7), 676.
- Smeraldi, J. D. (2012). “Occurrence and fate of nanoscale particles in water reclamation Processes.” Ph.D. thesis, University of California, Irvine.
- Tijhuis, L., Huisman, J. L., Hekkelman, H. D., van Loosdrecht, M. C. M., and Heijnen, J. J. (1995). “Formation of nitrifying biofilms on small suspended particles in airlift reactors.” *Biotechnology and Bioengineering*, 47(5), 585–595.
- Torfs, E., Martí, M. C., Locatelli, F., Balemans, S., Bürger, R., Diehl, S., Laurent, J., Vanrolleghem, P. A., François, P., and Nopens, I. (2017). “Concentration-driven models revisited: Towards a unified framework to model settling tanks in water resource recovery facilities.” *Water Science and Technology*, 75(3), 539–551.
- Torfs, E., Nopens, I., Winkler, M., Vanrolleghem, P., Balemans, S., and Smets, I. (2016). “Settling Tests.” *Experimental Methods In Wastewater Treatment*, IWA Publishing, London, UK, 235–262.
- Vallet, B., Muschalla, D., Lessard, P., and Vanrolleghem, P. A. (2014). “A new dynamic water quality model for stormwater basins as a tool for urban runoff management: Concept and validation.” *Urban Water Journal*, 11(3), 211–220.
- Vanrolleghem, P. A., Tik, S., and Lessard, P. (2019). “Advances in modelling particle transport in urban storm- and wastewater systems.” *International Conference on Urban Drainage Modelling*, Green Energy and Technology, (G. Mannina, ed.), Springer International Publishing, Cham, 907–914.
- Wang, J. (2012). “Fundamentals of biological processes for wastewater treatment.” *Biological Sludge Minimization and Biomaterials/Bioenergy Recovery Technologies*, John Wiley &

- Sons, Inc., Hoboken, NJ, USA, 1–80.
- WEF. (2009). *Design of Municipal Wastewater Treatment Plants: WEF Manual of Practice No. 8*. McGraw-Hill, New York.
- WEF. (2011). *Moving Bed Biofilm Reactors. WEF Manual of Practice No. 35*, McGraw Hill, Alexandria, Virginia, USA.
- Wijeyekoon, S., Mino, T., Satoh, H., and Matsuo, T. (2004). “Effects of substrate loading rate on biofilm structure.” *Water Research*, 38(10), 2479–2488.
- Wuertz, S., Bishop, P. L., and Wilderer, P. A. (2003). *Biofilms in Wastewater Treatment: An Interdisciplinary Approach*. IWA publishing.
- Young, B. (2017). “Nitrifying MBBR performance optimization in temperate climates through understanding biofilm morphology and microbiome.” Ph.D. thesis, University of Ottawa, ON, Canada.
- Young, B., Banihashemi, B., Forrest, D., Kennedy, K., Stintzi, A., and Delatolla, R. (2016a). “Meso and micro-scale response of post carbon removal nitrifying MBBR biofilm across carrier type and loading.” *Water Research*, Elsevier Ltd, 91, 235–243.
- Young, B., Delatolla, R., Abujamel, T., Kennedy, K., Laflamme, E., and Stintzi, A. (2017a). “Rapid start-up of nitrifying MBBRs at low temperatures: nitrification, biofilm response and microbiome analysis.” *Bioprocess and Biosystems Engineering*, 40(5), 731–739.
- Young, B., Delatolla, R., Kennedy, K., Laflamme, E., and Stintzi, A. (2017b). “Low temperature MBBR nitrification: Microbiome analysis.” *Water Research*, 111, 224–233.
- Young, B., Delatolla, R., Ren, B., Kennedy, K., Laflamme, E., and Stintzi, A. (2016b). “Pilot-scale tertiary MBBR nitrification at 1°C: Characterization of ammonia removal rate, solids settleability and biofilm characteristics.” *Environmental Technology*, 37(16), 2124–2132.

## Chapter 6 – Discussion and Conclusion

This Ph.D. study was performed to enhance the current knowledge of the MBBR produced solids characteristics and their settling behaviour. A comprehensive study was conducted at the macro, meso, and micro scales to investigate the potential interdependence between operational conditions of the MBBR reactor and system performance, biofilm characteristics, particle characteristics, and biomass activity. In particular, the research investigated the impact of carrier types, limited biofilm thickness and varying carbonaceous surface area loading rate (SALR) on the removal kinetics, on biofilm responses (morphology, thickness, mass, density, detachment rate), on solids production, particle size distribution and particle settling velocity distribution. In addition, the analytical method of ViCAs, combined with particle size distribution analyses, was applied to contribute to a better evaluation of particle characteristics and settling behaviour, which would lead to a better assessment of the performance of subsequent downstream solids separation units.

### 6.1 The impacts of Carrier types

Chapters 3 and 4 provide the findings of the possible impacts of different carrier types on the MBBR system performance, biofilm characteristics, MBBR produced solids characteristics and their settleability. This portion of the research was conducted under the same operational conditions (identical reactors with a moderate SALR of  $6.0 \pm 0.8$  g-sBOD/m<sup>2</sup>·d equal to  $14.9 \pm 1.6$  g-sCOD/m<sup>2</sup>·d, an HRT of 1.1 hours along with consistent DO, pH, and temperatures) to isolate the effects of carrier type. To this end, the conventional AnoxK™ K5 carrier was compared to two newly designed AnoxK™ Z-carriers. The shape and the geometric configuration of these two types of carriers are significantly different; as the AnoxK™ K5 carrier is a porous, cylindrical, flat carrier with the biofilm growth inside the protected voids, while the AnoxK™ Z-carriers are three-

dimensional, saddle-shaped carriers where the biofilm grows on the exposed surface area, outside of the carriers.

At the macro-scale, the K5 carrier demonstrated a statistically significantly higher carbon removal rate and efficiency as compared to the Z-carriers. The K5 carrier with a SARR of  $3.8 \pm 0.3$  g-sBOD/m<sup>2</sup>·d (or  $5.0 \pm 0.7$  g-sCOD/m<sup>2</sup>·d) and  $59.9 \pm 3.0\%$  sBOD removal efficiency (or  $31.5 \pm 4.0\%$  sCOD removal efficiency) showed 45 to 80% better removal efficiency as compared to Z-carriers, which implies a significant effect of carrier type on carbonaceous removal kinetics at the studied operational conditions.

At the meso and micro-scales, the results indicated that the carrier type significantly affects the biofilm characteristics such as biofilm morphology, thickness, mass and density. The acquired variable pressure scanning electron microscope (VPSEM) images highlighted a more filamentous morphology on the biofilm surface formed on Z-carriers compared to K5. In addition, the obtained results indicated that the meso-scale environments developed on each carrier type could differ and hence might result in the proliferation of different biota. Moreover, the statistically significant thickest biofilm was observed on the K5 carrier. The biofilm grown on the K5 carrier with an average thickness of  $281.1 \pm 8.7$  μm was 60–150% thicker than the biofilm grown outside the saddle-shaped Z-carrier. This finding showed that the protected surface area inside the voids of the K5 carrier allowed a non-restraint biofilm growth as opposed to the exposed surface area of the Z-carriers. Moreover, a significantly higher biofilm mass was measured per K5 carrier ( $43.9 \pm 1.0$  mg) because the K5 carrier had thicker biofilm and higher surface area (2420 mm<sup>2</sup>/carrier) than the Z-carriers with a surface area of 1280 mm<sup>2</sup> per carrier. Statistical analysis also confirmed that the biofilm densities differ between the carrier types. The biofilm density for the K5 carrier was calculated as  $65 \pm 1.5$  kg/m<sup>3</sup>, significantly lower than the density of biofilm formed on the Z-

carriers. The denser biofilm on Z-carriers could be indicative of the higher shear stress in the Z-carriers reactor, as the Z-carriers with three-dimensional shape might lead to different hydraulic characteristics and higher shear forces in the reactor.

Furthermore, the carrier type significantly impacted solids characteristics such as solids production, biofilm detachment rate, particle size distribution, and particle settling velocity distribution. The lowest TSS concentration ( $53.4 \pm 8.5$  mg/L), the lowest solids production ( $0.7 \pm 0.3$  g-TSS/d, which is 53–65% lower than Z-carriers), as well as the lowest biofilm detachment rate ( $1.7 \pm 0.7$  g-TSS/m<sup>2</sup>·d) were observed in the K5 carrier MBBR effluent. Statistical analysis confirms that the K5 carrier has produced significantly lower solids than the Z-carriers, as the Z-carriers showed three times higher yields than the K5 carrier at the studied operational conditions. According to the solids characteristics analyses, the K5 carrier indicated a statistically significantly lower percent volume of particles, between 2-400  $\mu$ m ( $38.4 \pm 2.3\%$ ), compared to Z-carriers. Moreover, the K5 carrier contained a higher TSS fraction of large particles with higher settling velocity leading to a better settling behaviour as compared to the Z-carriers effluent solids. The findings of this research indicated that the carrier design could affect the quantity of particles detached from the carriers and their size and settleability.

Overall, the investigation of the impacts of carrier types on MBBR performance in a normally loaded reactor demonstrated a statistically significant difference between the two types of carriers, studied in this research, in system performance, biofilm characteristics, solids characteristics and settling behaviour of the effluent particles.

## 6.2 The impacts of biofilm thickness-restraint

Chapters 3 and 4 also provide the findings on biofilm thickness-restraint effects on the MBBR system performance, biofilm characteristics, MBBR produced solids characteristics and their settleability. Two identical reactors housed with two different newly designed AnoxK™ Z-carriers, Z-200 and Z-400, were performed under similar normally loaded operational conditions (a SALR of  $6.0 \pm 0.8$  g-sBOD/m<sup>2</sup>·d equal to  $14.9 \pm 1.6$  g-sCOD/m<sup>2</sup>·d, an HRT of 1.1 hours along with consistent DO, pH, and temperatures) to isolate the effects of biofilm thickness-restraint. Z-carriers are saddle-shaped, three-dimensional carriers with an exposed gridded surface area. These external grids on the Z-carriers' surface are designed with different wall heights to limit the maximum thickness of the biofilm growth to the predefined wall height. The maximum allowed biofilm thickness on Z-200 and Z-400 carriers used in this study is 200 μm and 400 μm, respectively.

At the macro-scale, the comparison of the Z-200 carrier's system performance with that of the Z-400 carrier demonstrated that restraining the biofilm thickness did not affect the overall removal rates or efficiencies of the systems. Therefore, the Z-200 carriers did not demonstrate statistically significant difference in carbon removal performance compared to the Z-400 carriers; a SARR of  $2.9 \pm 0.4$  g-sBOD/m<sup>2</sup>·d (or  $3.4 \pm 0.7$  g-sCOD/m<sup>2</sup>·d) and  $2.6 \pm 0.5$  g-sBOD/m<sup>2</sup>·d (or  $2.8 \pm 0.8$  g-sCOD/m<sup>2</sup>·d) was observed for Z-200 and Z-400, respectively.

At the meso and micro-scales, comparing the thickness-restraint Z-200 carrier to the Z-400 carrier did not significantly affect biofilm morphology nor biofilm density. The acquired VPSEM images did not show significant changes in biofilm structure, morphology or even the micro animals between the two Z-carriers. The overall average biofilm thickness on the Z-carriers was approximately  $111.6 \pm 11.3$  μm, and  $174.3 \pm 11.1$  μm for Z-200 and Z-400, respectively, which

successfully was maintained below the predefined maximum allowed biofilm thickness. Since the Z-carriers have a similar surface area of 1280 mm<sup>2</sup> per carrier, the dry biofilm mass per carrier increased with biofilm thickness, as a higher biofilm mass of 24.0 ± 2.1 mg was measured on the Z-400 carrier as compared to a biofilm mass of 16.5 ± 0.7 mg per Z-200 carrier. Moreover, the biofilm densities were not statistically significantly different between the two levels of thickness restraint biofilm (116 ± 5.3 and 108 ± 4.3 kg/m<sup>3</sup> for Z-200 and Z-400, respectively).

On the other hand, the particle characteristics analyses indicated that the biofilm thickness restraint of the Z-200 carrier compared to the Z-400 carrier did not significantly affect the solids production, biofilm detachment rate, particle size distribution and particle settling velocity distribution. A solids production of 1.7 ± 0.7 g-TSS/d (or biofilm detachment rate of 5.0 ± 2.0 g-TSS/m<sup>2</sup>·d) for Z-200 and 1.3 ± 0.4 g-TSS/d (or biofilm detachment rate of 3.7 ± 1.0 g-TSS/ m<sup>2</sup>·d) for Z-400 was observed. Moreover, 1.9 ± 0.7 g-TSS was produced per g-sBOD removed in the Z-200 MBBR reactor, which was not statistically significantly different from the Z-400 with an observed yield of 1.6 ± 0.5 g-TSS/g-sBOD<sub>removed</sub>. The particle size distribution and the particle settling velocity distribution did not illustrate significant differences in the settling behaviour of the particles for these two biofilm thickness-restraint carriers. The percent volume of particles for Z-200 and Z-400, either for particles between 2-400 µm or for particles larger than 400 µm, did not differ significantly, although the Z-400 carriers contain a higher percentage volume of particles smaller than 150 µm that remained unsettled. As the particle settling velocity distribution illustrated, the settling behaviour of the two Z-carriers is considerably similar, with only 44% and 42% of the total particle mass settling in a clarifier with a typical overflow rate of 0.5 m/h. Hence, the results indicated that the MBBR system performance, biofilm characteristics, MBBR produced

solids characteristics, and settleability were not affected by the biofilm thickness-restraint at normally loaded conditions and for the specific thickness restraint levels studied in this research.

### **6.3 The impacts of varying SALR**

Chapter 5 provides the findings of the possible impacts of various SALRs on the MBBR system performance, biofilm characteristics, MBBR produced solids characteristics and their settleability. To this end, a study was conducted under three different loading rates but constant HRT, DO and pH using conventional AnoxK™ K5 carriers. The SALR was kept in the range of low to moderately loaded systems and increased from 1.5 to 2.5 and 6.0 g-sBOD/m<sup>2</sup>·d (corresponding to 4.2, 6.5 and 14.9 g-sCOD/m<sup>2</sup>·d) by decreasing the available surface area provided in the reactor. As the reactor was operated at a full-scale wastewater treatment plant using real wastewater, temperature variation occurred coincidentally with the variation of the loading rates due to the transition of cold to warm weather.

At the macro-scale, the carbonaceous removal rate across the surface area loading rates demonstrated a strong linear correlation between the measured sBOD loading rate and the removal rate ( $R^2=0.94$ ). It demonstrated that the sBOD removal rate is first order and mass-transfer limited, likely due to the low loading rate of the substrate. Moreover, increasing the SALR led to a decrease in surface area removal rate (SARR) and an expected increase in effluent carbonaceous material concentration. As such, transitioning from a lower SALR (1.5 g-sBOD/m<sup>2</sup>·d) to the higher SALR (6.0 g-sBOD/m<sup>2</sup>·d) corresponded to a statistically significant decrease in sBOD removal efficiency from  $68.9 \pm 5.3$  to  $59.9 \pm 3.0\%$  sBOD removal.

At the meso and micro-scales, the acquired VPSEM images did not show a significant difference in biofilm morphology and structure at the three different SALRs. Ciliates appeared to

be the most abundant protozoans in the biofilm at all studied loading conditions. However, nematodes and rotifers were also observed. The biofilm thickness decreased from  $316.2 \pm 11.1 \mu\text{m}$  to  $281.1 \pm 8.7 \mu\text{m}$  when the SALR increased from  $1.5 \text{ g-sBOD/m}^2\cdot\text{d}$  to  $6.0 \text{ g-sBOD/m}^2\cdot\text{d}$ . However, a peak in biofilm thickness was observed at the intermediate SALR, which might be because of the biofilm response to the temperature transition (from cold to warm weather). Similar to the biofilm thickness, the significantly highest biofilm mass ( $62.7 \pm 2.4 \text{ mg per carrier}$ ) was observed at SALR 2.5 with an operational temperature of  $13.0 \pm 1.0 \text{ }^\circ\text{C}$ ; and the lowest biofilm mass ( $43.9 \pm 1.0 \text{ mg/carrier}$ ) was related to the highest SALR (SALR of  $6.0 \text{ g-sBOD/m}^2\cdot\text{d}$ ). Moreover, the biofilm density decreased when the SALR was increased, as the statistically significant lowest density of  $65 \pm 1.5 \text{ kg/m}^3$  was calculated at SALR  $6.0 \text{ g-sBOD/m}^2\cdot\text{d}$ . The results indicated that the solids retention time (or the biofilm age) decreases from  $5.6 \pm 0.8$  to  $1.7 \pm 0.1$  days, when the SALR increases from 1.5 to  $6.0 \text{ g-sBOD/m}^2\cdot\text{d}$ . Therefore, the highest cell viability ( $81.8 \pm 1.7\%$ ) at SALR of  $6.0 \text{ g-sBOD/m}^2\cdot\text{d}$  might also be an initiation of newly formed biofilm (younger biofilm) with a higher percentage of viable cells. In contrast, the older biofilm and the thickest biofilm demonstrated less viable biofilm (more dead cells), probably due to the restrictive mass transfer of substrates and nutrients during the overgrowth observed at SALR of  $2.5 \text{ g-sBOD/m}^2\cdot\text{d}$  in this study. The solids characteristics analyses at three different SALRs illustrated no significant changes in TSS concentration and TSS production. However, a statistically significant difference was observed in detachment rate ( $2.4 \pm 0.9 \text{ g-TSS/m}^2\cdot\text{d}$ ) and observed yield ( $1.7 \pm 0.5 \text{ mg-TSS}_{\text{produced}}/\text{sBOD}_{\text{removed}}$ ) at SALR 2.5 with a temperature of  $13.0 \pm 1.0 \text{ }^\circ\text{C}$ , where the thickest biofilm and more dead cells were observed. Consequently, a higher fraction of larger particles and rapidly settling particles was observed at SALR  $2.5 \text{ g-sBOD/m}^2\cdot\text{d}$ , which led to a significantly better settling behaviour of the MBBR effluent solids.

## **6.4 Novel contribution, practical implication, and future direction**

This research is a comprehensive study on MBBR-produced solids characteristics, which, in addition to the MBBR system performance, investigated biofilm characteristics, biofilm morphology and detachment, solids production, and settling behaviour of the produced suspended solids. It is also the first long-term investigation of thickness-restraint Z-carriers in a carbon removal MBBR system using real wastewater to compare these carriers with conventional K5 carriers. It provides new information on the biofilm characteristics, solids characteristics and settling behaviour of thickness-restraint Z-carriers. The settling behaviour of MBBR-produced solids was also investigated for the first time using the ViCAs analytical method. Moreover, the benefits of combining the ViCAs method with microscopy imaging were assessed and allowed relating particle size distribution to the settling behaviour of MBBR produced particles.

This study provides comprehensive information at the macro, meso, and micro-scale and develops new fundamental knowledge of carrier design impacts on MBBR technology performance. Additional knowledge on biofilm characteristics, the characteristics of the MBBR-produced solids and the potential interdependence of the impacts of carrier types and operational conditions on the settleability of the particles are provided and will contribute to the optimized design of MBBR systems and the subsequent downstream solids separation units. This study shows that the MBBR system performance is affected by single important design selections and how biofilm characteristics, solids characteristics, and settling behaviour are interconnected at the macro, meso and micro-scale. As such, simply choosing a proper carrier type or limiting the biofilm growth via the carrier selection or an optimum loading rate might lead to significant changes in performance, solids characteristics, and hence the settling behaviour.

Since a specific range of loading rates and thickness restraint levels were studied based on the objectives of this research, further studies can be useful to generalize these findings to high-loaded systems under other operational conditions. Also, studying the vast Z-carrier's family (in particular, all Z-carriers that are able to restrain the biofilm thickness from 50  $\mu\text{m}$  to 1000  $\mu\text{m}$ ) would provide improved understanding over a wide range of thickness restraint levels and would be useful to assess how far the findings of this research can be generalized.

Finally, more recommendations arising from the findings of this research are herein provided for consideration in future research. A better understanding of the biofilm system and control of the biofilm growth that affects solids characteristics will require both engineers and microbiologists to evaluate biofilm characteristics and to assess heterotrophic and autotrophic bacterial communities using DNA sequencing and other molecular techniques, eventually leading to outstanding results linking the various parameters and identification causation at different scales. To provide additional information, it would be interesting to evaluate and quantify filaments in the particles (or even identify the predominant filamentous species), which are highly affected by the operational conditions and influence particle settling behaviour. Moreover, exploiting mathematical modelling and computational methods to simulate biofilm evolution in combination with analytical methods is promising in view of developing additional knowledge on biofilm behaviour and its potential impacts on solids characteristics. The fate of influent particles and their potential influence on the characteristics of the MBBR effluent particles is required to be studied in detail or to be simulated to demonstrate the role of primary solids in biofilm development, detachment and the subsequent particle characteristics. Last but not least, it would be relevant to monitor the system performance, biofilm characteristics and settling performance within a larger scale system to validate the results obtained in this study.

## Appendix A- Statistical analysis

Along with the correlation analysis of the measured data, the residual sum of squares is plotted, and an analysis of variance (ANOVA) is performed to test the significance of the regression line with 95% confidence. The result of the ANOVA test for linear regression was summarized in the following tables. The  $df$  is the number of independent observations to compile each sum of squares,  $SS$  is the sum of squares, and  $MS$  is the mean square (variance). Larger *significance F* than  $F$  values indicates that the model's variation is significantly larger than the variation due to random error, which means the regression is statistically significant and the variables are correlated.

**Table 7-1:** ANOVA for linear regression between sBOD removal rate and loading rate

Carriers		$df$	$SS$	$MS$	$F$	<i>Significance F</i>	<i>Significant?</i> ( $\alpha=0.05$ )
<b>K5</b> $R^2=0.94$	Regression	1	58.7218	58.7218	1052.87	2.28E-31	Yes
	Residual	42	2.34246	0.05577			
	Total	43	61.0643				
<b>Z-200</b> $R^2=0.83$	Regression	1	47.18875	47.18875	209.1167	6.55E-18	Yes
	Residual	42	9.477615	0.225658			
	Total	43	56.66636				
<b>Z-400</b> $R^2=0.79$	Regression	1	52.3227	52.3227	165.6936	3.6E-16	Yes
	Residual	42	13.26276	0.31578			
	Total	43	65.58545				

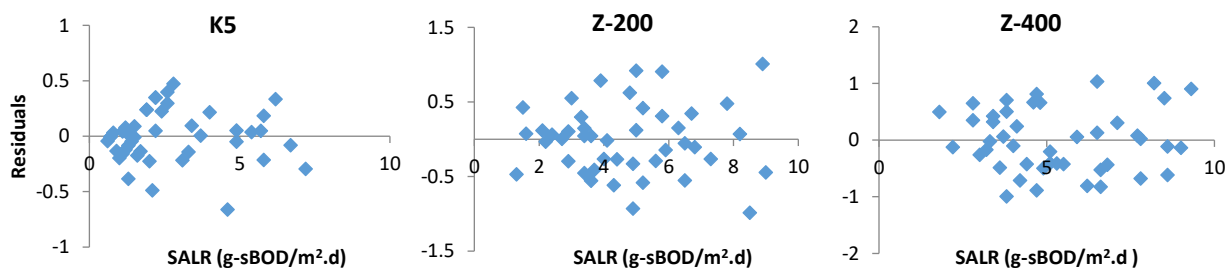


**Figure 7-1:** Residual Plot for sBOD SARR for different carrier types across SALR.

**Table 7-2:** ANOVA for linear regression between TAN removal rate and loading rate

Carriers		<i>df</i>	<i>SS</i>	<i>MS</i>	<i>F</i>	<i>Significance F</i>	<i>Significant?</i> ( $\alpha=0.05$ )
<b>K5</b> $R^2=0.63$	Regression	1	0.001434	0.001434	0.042328	0.83799	No
	Residual	42	1.422884	0.033878			
	Total	43	1.424318				
<b>Z-200</b> $R^2=0.31$	Regression	1	0.000859	0.000859	0.008889	0.925335	No
	Residual	42	4.059141	0.096646			
	Total	43	4.06				
<b>Z-400</b> $R^2=0.28$	Regression	1	1.73E-05	1.73E-05	0.000228	0.988033	No
	Residual	42	3.187937	0.075903			
	Total	43	3.187955				

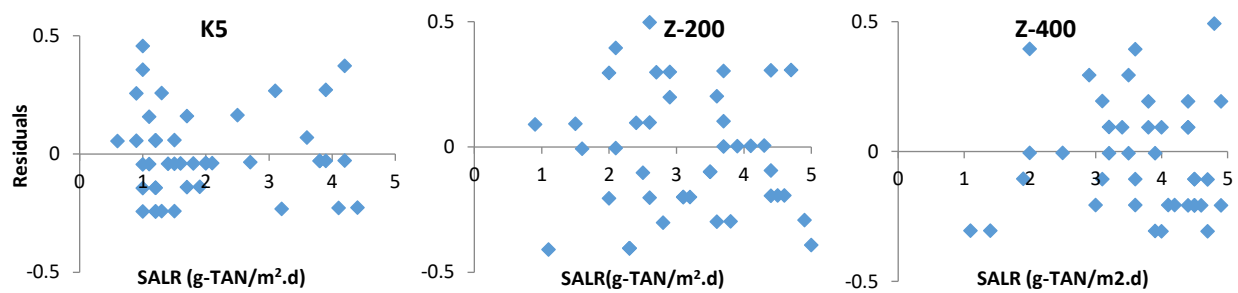


**Figure 7-2:** Residual Plot for TAN SARR for different carrier types across SALR.

**Table 7-3:** ANOVA results, linear regression analysis of biofilm volume (BVRR) and the viable cell sBOD removal rate (VCRR) across the loading rate

		<i>df</i>	<i>SS</i>	<i>MS</i>	<i>F</i>	<i>Significance F</i>	<i>Significant?</i> <i>(α=0.05)</i>
<b>sBOD BVRR</b> R <sup>2</sup> =0.95	Regression	1	1870.192	1870.192	1682.715	1.49E-26	
	Residual	29	32.23098	1.111413			Yes
	Total	30	1902.423				
<b>sBOD VCRR</b> R <sup>2</sup> =0.96	Regression	1	2946.969	2946.969	2324.856	1.72E-28	
	Residual	29	36.76017	1.267592			Yes
	Total	30	2983.729				

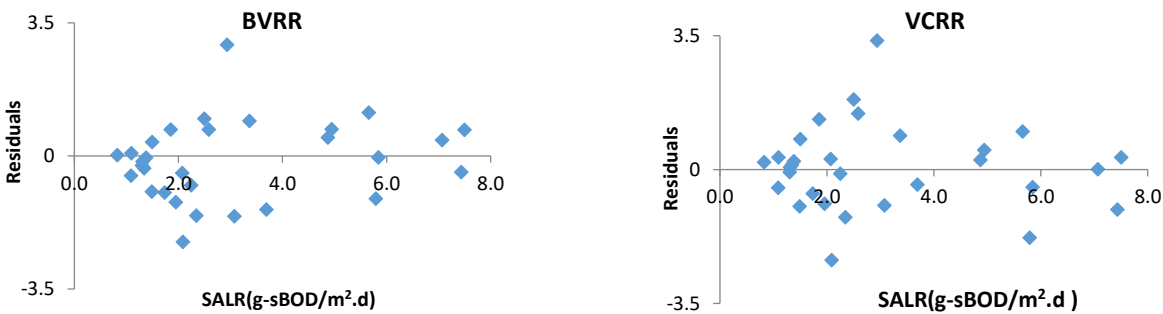


**Figure 7-3:** Residual Plot for sBOD BVRR and VCRR across SALR

Statistical significance of all parameters studied in this research was determined using two-tailed student t-tests (provided in Microsoft Excel) with a *p*-value less than 0.05 to designate significance. The *p*-values were determined between the data set measured for K5, Z-200, and Z-400, as well as SALR 1.5, 2.5 and 6.0 g-sBOD/m<sup>2</sup>.d. The results are summarized in the following tables.

**Table 7-4:** Statistical significance (*p*-values) of measured parameters to designate the difference of system performance, biofilm characteristics and solids characteristics for different carriers

System performance	SARR (g-sBOD/m <sup>2</sup> ·d)	SARR (g-sCOD/m <sup>2</sup> ·d)	SARR (g-TAN/m <sup>2</sup> ·d)		
	<b>K5</b>	3.8 ± 0.3	5.0 ± 0.7	0.4 ± 0.1	
	<b>Z-200</b>	2.9 ± 0.4	3.4 ± 0.7	0.4 ± 0.1	
	<b>Z-400</b>	2.6 ± 0.5	2.8 ± 0.8	0.4 ± 0.1	
<i>p</i> -values (n=10)					
<b>K5 vs Z-200</b>	0.03	0.04	0.66		
<b>K5 vs Z-400</b>	0.04	0.04	0.93		
<b>Z-200 vs Z-400</b>	0.62	0.33	0.60		
Biofilm characteristics	Thickness (µm)	Density (kg/m <sup>3</sup> )	Mass (mg/carrier)		
	<b>K5</b>	281.1 ± 8.7	65 ± 1.5	43.9 ± 1.0	
	<b>Z-200</b>	111.6 ± 11.3	116 ± 5.3	16.5 ± 0.7	
	<b>Z-400</b>	174.3 ± 11.1	108 ± 4.3	24.0 ± 2.1	
	<i>p</i> -values (n=3)				
	<b>K5 vs Z-200</b>	0.00	0.00	0.00	
	<b>K5 vs Z-400</b>	0.00	0.00	0.00	
<b>Z-200 vs Z-400</b>	0.00	0.11	0.02		
Solids characteristics	TSS (mg/L)	Production (g-TSS/d)	Detachment rate (g-TSS/m <sup>2</sup> ·d)	Yield (mg-TSS/sBOD)	
	<b>K5</b>	53.4 ± 8.5	0.7 ± 0.3	1.7 ± 0.7	0.5 ± 0.2
	<b>Z-200</b>	70.4 ± 13.0	1.7 ± 0.7	5.0 ± 2.0	1.9 ± 0.8
	<b>Z-400</b>	65.5 ± 10.5	1.3 ± 0.4	3.7 ± 1.0	1.7 ± 0.5
	<i>p</i> -values (n=10)				
	<b>K5 vs Z-200</b>	0.26	0.02	0.02	0.00
	<b>K5 vs Z-400</b>	0.5	0.02	0.04	0.00
<b>Z-200 vs Z-400</b>	0.52	0.36	0.47	0.61	

**Table 7-5:** Statistical significance (*p*-values) of measured parameters to designate the difference of system performance, biofilm characteristics and solids characteristics at different SALR

System performance	sBOD SARR	sBOD BVRR	sBOD VCRR	sCOD SARR	TAN SARR
	(g/m <sup>2</sup> ·d)	×10 <sup>3</sup> (g/m <sup>3</sup> ·d)	×10 <sup>3</sup> (g/m <sup>3</sup> ·d)	(g/m <sup>2</sup> ·d)	(g/m <sup>2</sup> ·d)
<b>K5 - SALR 1.5</b>	1.1 ± 0.3	3.1 ± 1.0	4.2 ± 1.4	1.4 ± 0.4	0.3 ± 0.1
<b>K5 - SALR 2.5</b>	1.6 ± 0.3	4.6 ± 1.3	6.4 ± 1.6	2.0 ± 0.5	0.3 ± 0.1
<b>K5 - SALR 6.0</b>	3.8 ± 0.3	13.3 ± 1.1	16.3 ± 1.3	5.0 ± 0.7	0.4 ± 0.1
<i>p</i> -values (n=10)					
<b>SALR 1.5 vs 2.5</b>	0.03	0.10	0.06	0.03	0.31
<b>SALR 1.5 vs 6.0</b>	0.00	0.00	0.00	0.00	0.95
<b>SALR 2.5 vs 6.0</b>	0.00	0.00	0.00	0.00	0.42

Biofilm characteristics	Thickness	Density	Mass	Cell viability
	(µm)	(kg/m <sup>3</sup> )	(mg/carrier)	(%)
<b>K5 - SALR 1.5</b>	316.2 ± 11.1	71.4 ± 1.6	54.7 ± 1.4	74.0 ± 1.9
<b>K5 - SALR 2.5</b>	369.1 ± 25.5	70.3 ± 2.2	62.7 ± 2.4	68.2 ± 1.2
<b>K5 - SALR 6.0</b>	281.1 ± 8.7	65 ± 1.5	43.9 ± 1.0	81.8 ± 1.7
<i>p</i> -values (n=3)				
<b>SALR 1.5 vs 2.5</b>	0.06	0.51	0.02	0.77
<b>SALR 1.5 vs 6.0</b>	0.00	0.03	0.00	0.02
<b>SALR 2.5 vs 6.0</b>	0.02	0.00	0.00	0.02

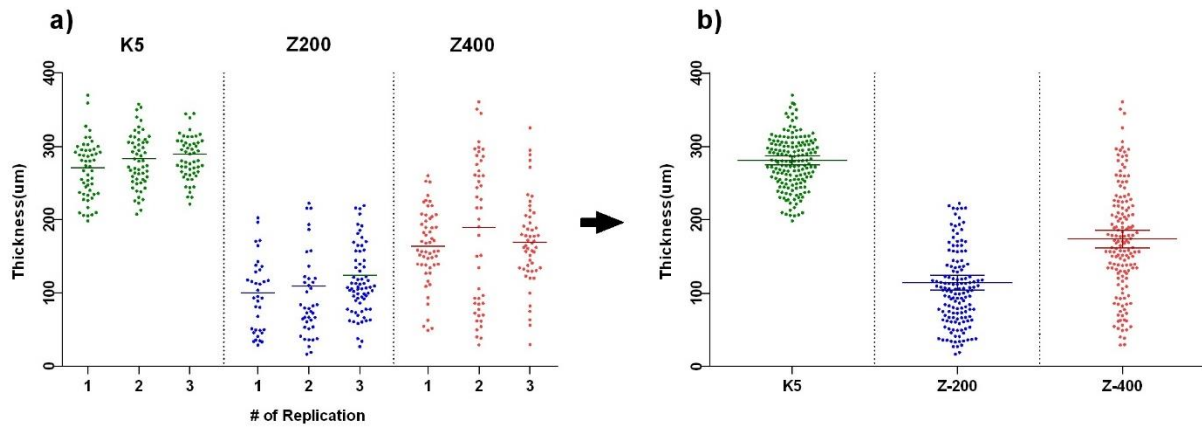
  

Solids characteristics	TSS	Production	Detachment rate	Yield	SRT
	(mg/L)	(g-TSS/d)	(g-TSS/m <sup>2</sup> ·d)	(mg-TSS/sBOD)	(d)
<b>K5 - SALR 1.5</b>	57.9 ± 8.5	1.1 ± 0.5	0.9 ± 0.4	1.0±0.6	5.6 ± 0.8
<b>K5 - SALR 2.5</b>	66.7 ± 15.4	1.7 ± 0.8	2.4 ± 0.9	1.7 ± 0.5	3.6 ± 1.0
<b>K5 - SALR 6.0</b>	53.4 ± 8.5	0.7 ± 0.3	1.7 ± 0.7	0.5 ± 0.2	1.7 ± 0.1
<i>p</i> -values (n=10)					
<b>SALR 1.5 vs 2.5</b>	0.61	0.30	0.03	0.21	0.01
<b>SALR 1.5 vs 6.0</b>	0.26	0.07	0.38	0.03	0.00
<b>SALR 2.5 vs 6.0</b>	0.35	0.19	0.1	0.25	0.00

**Table 7-6:** Statistical significance analysis (*p*-values) for ViCAs tests

Comparison of carrier type	<i>p</i> -value (n=3)	Comparison of SALR	<i>p</i> -value (n=3)
<b>K5 vs Z-200</b>	0.00	<b>SALR 1.5 vs 2.5</b>	0.00
<b>K5 vs Z-400</b>	0.03	<b>SALR 1.5 vs 6.0</b>	0.01
<b>Z-200 vs Z-400</b>	0.56	<b>SALR 2.5 vs 6.0</b>	0.00

## Appendix B – Biofilm thickness measurement



**Figure 8-1:** Thickness measurements for different type of carriers (a) each replication and (b) the average of all three taken carriers with 95% CI

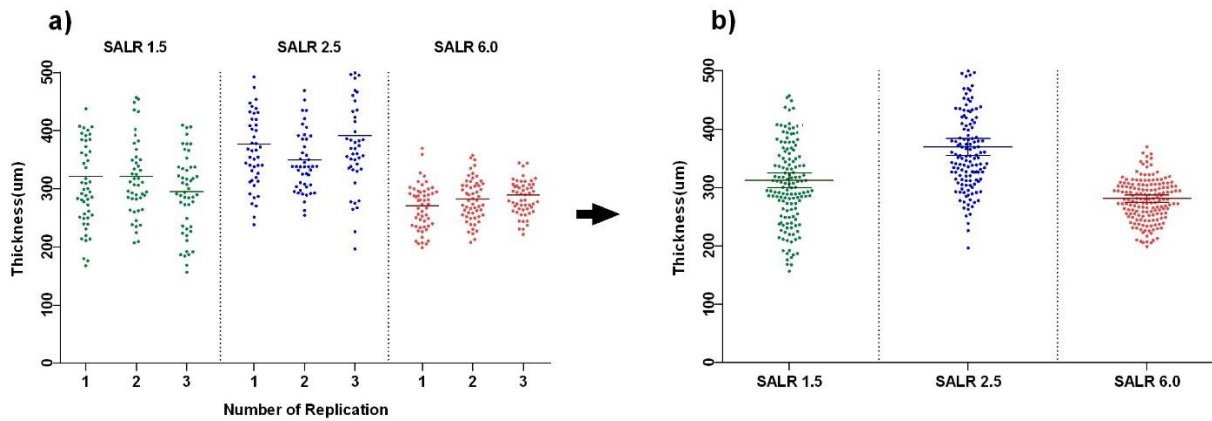


**Figure 8-2:** Thickness measurements for K5 carrier at different SALRs for (a) each replication and (b) the average of all three taken carriers with 95% CI